Life Cycle Assessment of a Steel-Timber Composite Structure and Comparison to an Established Structural System

by

Emma Rohde

A thesis submitted to the Graduate Faculty of
Auburn University
in partial fulfillment of
requirements for the Degree of

Master of Science in Civil Engineering

Auburn, Alabama
May 6, 2023

Keywords: Steel-Timber Composite, Sustainability, Environmental Study, Cross Laminated Timber, CLT, Steel-Concrete Composite

Approved by

Dr. David Roueche, Chair, Assistant Professor of Structural Engineering
Dr. Kadir Sener, Co-Chair, Assistant Professor of Structural Engineering
Dr. Robert Barnes, Brasfield & Gorrie Associate Professor of Structural Engineering

Abstract

The building and construction industry drives global energy use and emissions. With climate change mitigation being a forefront topic of concern, the building and construction industry has a responsibility to alleviate its environmental impact. Therefore, there is a need for more sustainable structural systems that explicitly consider environmental impact. This study examined comparative life cycle assessments on the superstructures of functionally equivalent steel-timber composite and steel-concrete composite office buildings at 7-story (28,800 m^2 nominal floor area) and 18-story (74,000 m^2 nominal floor area) heights. Life cycle assessments were conducted in accordance with *ISO 21931* and outputs quantified environmental impacts associated with each structural systems, creating meaningful and valid comparisons of sustainable merit associated with each structure and the materials within. Results indicate steel framing mass and environmental impacts are comparable between systems of the same height. As a result, environmental benefits attributed to steel-timber composite structures stem primarily from floor assemblages. Overall, the steel-timber composite systems had less severe environmental impacts than the steel-concrete systems, averaging 46% lower global warming potential and 27% lower energy demand.

Acknowledgment

I would like to express gratitude to Dr. Kadir Sener and Dr. David Roueche, Assistant Professors of Structural Engineering at Auburn University, for their pursuit of excellence, advisement, and knowledge throughout my master's degree and this study. I would also like to thank my additional committee member, Dr. Robert Barnes, Brasfield & Gorrie Associate Professor of Structural Engineering, for his guiding role in my advanced education, commitment to mastery, and inspiration in the classroom and beyond.

Furthermore, I would like to acknowledge Dr. Jim Davidson and Dr. Schindler, faculty members within the Auburn University Civil and Environmental Engineering department. I have had the honor of being instructed by the lecturers listed above, and more, who often left me more intrigued at the end of a lecture period than at its launch. Ultimately, I am truly thankful for the privilege I was granted of the role of Graduate Research Assistant by the Auburn University Department of Civil and Environmental Engineering. The financial aid, research experience, and exposure to the structural engineering industry provided through the assistantship have been invaluable to my career development.

Table of Contents

List of Tables

List of Figures

Chapter 1: Introduction

1.1 Background

Roughly 37% of total global energy-related CO_2 emissions are a consequence of the building sector and construction industry, out-emitting the next closest sector by 14 percentage points according to the 2021 Global Status Report for Buildings and Construction by the United Nations (United Nations Environment Programme, 2021). Thus, emission reductions from the building sector are integral in mitigating the effects of climate change and its impact on environmental sustainability (Obafemi 2017). This need has in large part spurred the growing acceptance of mass timber as a sustainable, alternative structural system to traditional steel and concrete building systems. Within this growth, the mass timber market in the U.S. is largely dominated by cross laminated timber products (CLT), with an estimated 71% of square footage and 65% of mass timber building projects in the United States being accounted for by cross laminated timber alone (Atkins et al. 2022).

Beyond mass timber-only structural systems, there is also increased use of hybrid and composite systems that make use of the different strengths of each material to optimize the composite structural system. One such family of promising systems is steel-timber composite structures (Aspila et al. 2022; Hassanieh, Valipour, and Bradford 2017), which utilize lightweight and sustainable mass-timber floor panels compositely working with steel framing, which can more efficiently provide long spans (SOM 2017) and improve structural performance and constructability relative to traditional systems. This relatively new structural system is expected to provide a low-carbon structural solution due to utilizing sustainable construction materials with an efficient and affordable alternative for building structures. Furthermore, the majority of mass timber construction projects are multi-family use (Leafblad, Peters, and Cullen

2021). Hence, steel-timber composite structural systems have the potential to expand the mass timber market into commercial and business occupancy types.

1.2 Scope and Objectives

The relative impact of different structural systems on the environment over the lifespan of the building lacks rigorous quantification; particularly the steel-timber composite system, and its more established counterpart—the steel-concrete composite system. Comparative analyses are often performed using whole building life cycle assessments (WBLCA). The value of WBLCA is largely derived from the comparison of functionally equivalent building assemblages, whereas exclusive studies of materials outside of a functionally equivalent scope may be invalid comparisons. Therefore, WBLCA allows practitioners to make appropriate comparisons, assess environmental impacts associated with design choices, and implement strategies to reduce total environmental impact (Yang 2018).

Several parameters may adversely influence the variability in outcomes and comparative validity of LCAs; some of which are: lack of procedure for system boundaries, inadequate definitions of functional units, contradictory assumptions of life span scenarios and processes, outdated or inapplicable Life Cycle Inventory (LCI), or database quality and subjectivity (Nwodo and Anumba 2019). Consequences of database assumptions may be mitigated by utilizing various databases, conducting uncertainty and sensitivity analyses, and utilizing environmental product declarations (EPDs) in place of commercial databases (Malmqvist et al. 2011; Nwodo and Anumba 2019).

The primary objective of this thesis is to comparatively assess the environmental impacts associated with steel-timber composite and steel-concrete composite structural systems using

whole building life-cycle assessment (WBLCA). A secondary objective is to evaluate the sensitivity of the WBLCA to environmental data sources.

The environmental impacts of steel-timber composite systems were investigated relative to functionally equivalent, conventional steel-concrete composite systems using a whole building life cycle assessment (WBLCA) approach that follows recommended, material-agnostic practice. This study presents the structural analysis and design of two prototype buildings (Figure 1-1) at different heights for each steel-timber and steel-concrete composite system, and then compares the sustainability aspects of each system by providing a comparative WBLCA.

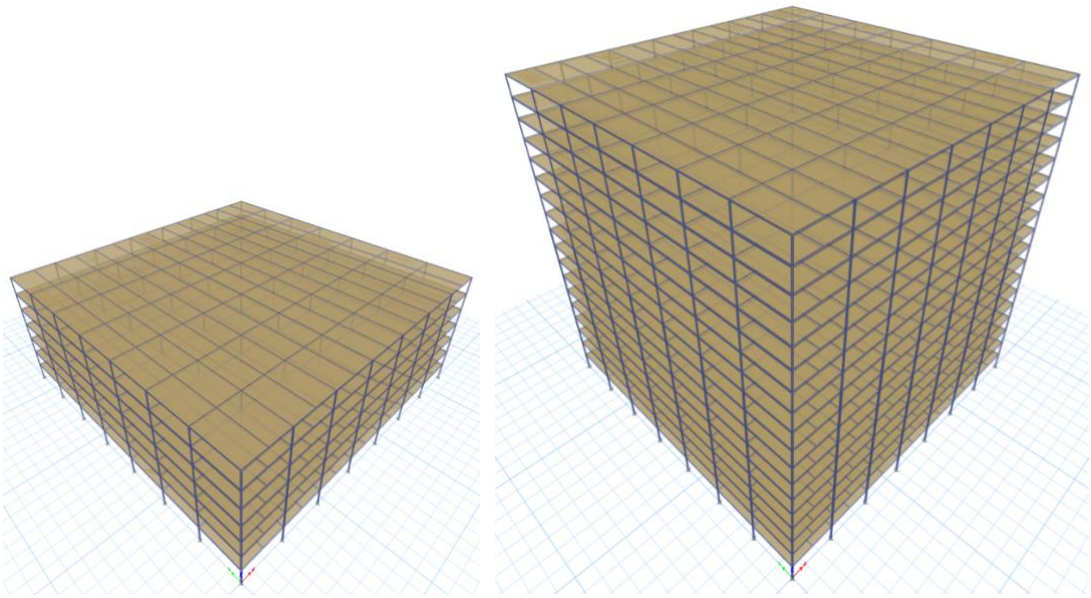

Figure 1-1: Prototype 7-Story and 18-Story Office Buildings

1.3 Organization of Thesis

This thesis consists of five chapters, organized as follows. Following a brief introduction in Chapter 1, a broad review of literature relevant to the topic is presented in Chapter 2. The

review establishes the responsibility of the design and construction industry to alleviate environmental impacts by introducing the topic of sustainability and climate change, as well as providing data points relevant to the argument. Additionally, the literature review explores the viability and advantages of steel timber composite structures and the existing research on the systems. Furthermore, the literature review touches on the vibration analysis of steel-timber floor systems, as it was found to be a critical design parameter.

Chapter 3 presents methodologies utilized in schematic design, material properties, structural analysis, structural design, vibration assessments, life cycle assessments, and life cycle inventory data. Chapter 4 goes on to present the results and discuss the study outputs, resultant of the structural design and life cycle assessments obtained from the discussed methodologies. Explored LCA outputs include total life, cradle to gate, comprehensive life stage, and floor system environmental impacts.

Chapter 5 summarizes the study and presents the primary conclusions, limitations, and recommendations for further research. Appendices contain sample calculations, vibration study outputs, and preliminary designs for various structural elements.

Chapter 2: Literature Review

2.1 Sustainability in Design and Construction

2.1.1 A Brief Introduction to Sustainability and the Anthropocene

Before 1990, the United Nations Brundtland Commission defined sustainability as "meeting the needs of the present without compromising the ability of future generations to meet their own needs" (Imperatives 1987). In addition to this definition, current-day sustainable study programs teach the importance of the Triple Bottom Line (TBL). Often summarized by the phrase "people, planet, profit." Human wellbeing has begun to be coupled with the TBL, as seen in Figure 2-1. The TBL was originally intended as a framework for examining a company's social (people), environmental (planet), and economic (profit) impacts (Elkington 2018). It illustrates that without focusing on all three facets, a business will not succeed long-term, as it does not fully quantify the cost of its operations.

Figure 2-1: Example visualizations of the triple bottom line, including (left) the traditional approach showing the intersection of people, planet, and prosperity (Board of Regents, 2023), and (right) integrating human well-being into the triple bottom line as a sustainability compass (Kensler 2014)

With the rise of this school of thought, it has been found that corporations have been providing greater amounts of information about non-financial aspects of their operations. This is attributed to a growing awareness that humans are consuming natural resources at a rate much faster than can be replenished (Arowoshegbe and Emmanuel 2016). While resource depletion accounts for a portion of the "planet" facet of the triple bottom line, it is only one segment of the environmental equation. Greenhouse gas (carbon dioxide, methane, and nitrous oxide) emissions are widely recognized as the primary driver of global climate change (Ritchie, Roser, and Rosado 2020; Solomon et al. 2007).

Ritchie et al. (2020) found that global emissions of carbon dioxide were relatively slow until the mid-20th century, with only 6 billion tonnes of CO_2 emitted worldwide in 1950. However, global annual CO_2 emissions have continuously grown, with over 34 billion tonnes of CO_2 being emitted annually as of 2020.

In conjunction with this, Lindsey (2022) reports a rise in global atmospheric CO_2 concentrations due to increased emissions. As a result of the increased atmospheric CO_2, the earth's natural greenhouse effect is being amplified. However, this is not a new phenomenon. Earth has periodically undergone natural warming cycles due to increased carbon in the atmosphere, over the past million years or more. These warm periods were mostly due to wobbles in the Earth's axis or the path of its orbit around the sun. However, due to air bubbles in ice cores, up to a mile thick and frozen for thousands of years, it is clear that CO_2 did not exceed 300 ppm during these ice-age cycles (Lindsey 2022; Solomon et al. 2007). The Intergovernmental Panel on Climate Change reported global increases in carbon dioxide concentration are due primarily to fossil fuel use and land-use change, while those of methane and nitrous oxide are primarily due to

agriculture. The report goes on to state that CO_2 is the most important greenhouse gas. It also concludes that the increased atmospheric CO_2 concentration is predominantly a result of fossil fuel use, with land use change providing a significant but smaller contribution (Solomon et al. 2007).

Per Figure 2-2, that before the Industrial Revolution (beginning around 1760), the global average CO_2 concentration in the atmosphere was 280 ppm. However, as of April 2022, the recorded atmospheric concentration was 420 ppm ("Trends in Atmospheric Carbon Dioxide," n.d.). Therefore, armed with Earth's historical CO_2 concentration data, it is logical to conclude that the rise in atmospheric CO_2 concentration is not only due to human activity, but also a disruption to the global environment. This disruption has come to be known as climate change.

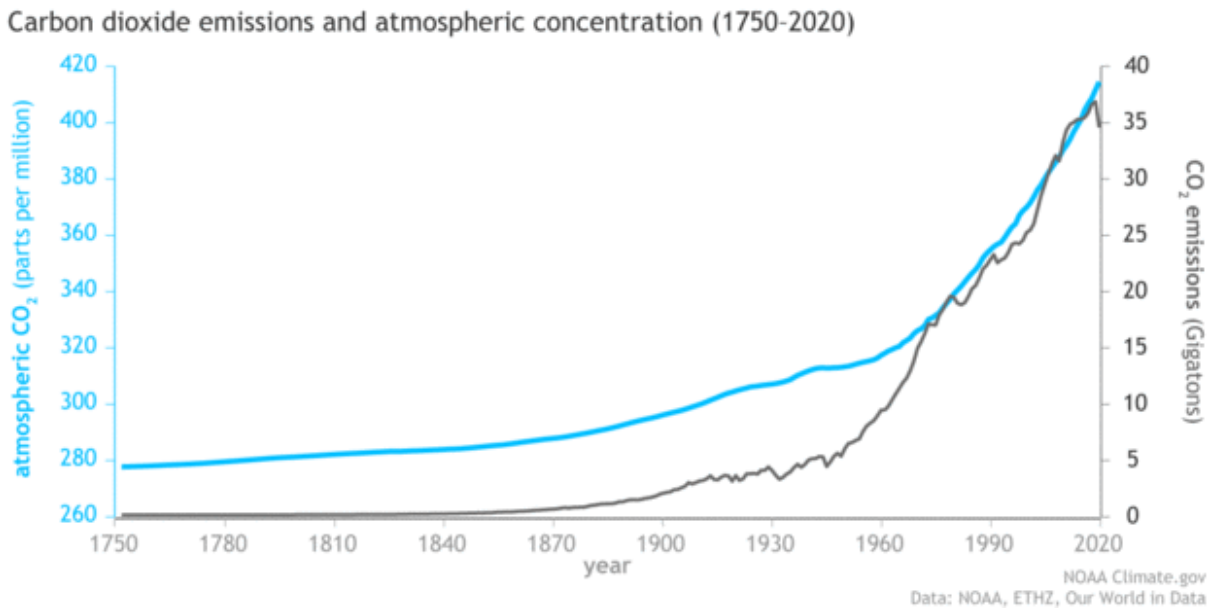

Figure 2-2: Carbon dioxide emissions and atmospheric concentration.Atmospheric CO_2 concentrations (blue) have been following the trend of CO_2 emissions (grey) with the growth of fossil fuel use since the Industrial Revolution (Lindsey 2022).

Human impact on the earth has become substantial enough that it rivals some of the greatest forces of nature in its impact on the earth's ecosystem (Steffen et al. 2011). In recognition of this, the concept of the *Anthropocene* was introduced near the beginning of the 21st century to "capture the quantitative shift in the relationship between humans and the global environment" (Steffen et al. 2011). In geology, time is divided according to shifts in the earth's state. The Anthropocene is believed to be the most current geological epoch, marked by environmental changes indicating that Earth has entered a new human-dominated age (S. L. Lewis and Maslin 2015). Therefore, Earth has a quandary. Do humans have a duty to restore the Earth's environment to its natural state? If so, who will take responsibility for this assignment?

2.1.2 The Building Sector's Environmental Responsibility in the Anthropocene

While there may not be a clear answer to the above quandary, one thing is clear: the building sector and construction industry need to be part of the solution. As of 2020, 37% of total global energy-related CO_2 emissions were a consequence of the building sector and construction industry. The industry out-emitted the next closest sector by 14 percentage points. Figure 2-3 breaks down total global energy consumption and emissions in 2020; all data in green indicate building sector and construction industry contributions. It is important to note, that this data was collected in a year with historically low construction-related emissions due to the COVID-19 pandemic. The drop was a consequence of a decrease in the manufacturing of construction materials as compared to 2019. However, the global CO_2 emissions from the building and construction sector were only 1% lower in 2020 than in 2019 (United Nations Environment Programme, 2021).

Figure 2. Buildings and construction's share of global final energy and energy-related CO_2 emissions, 2020

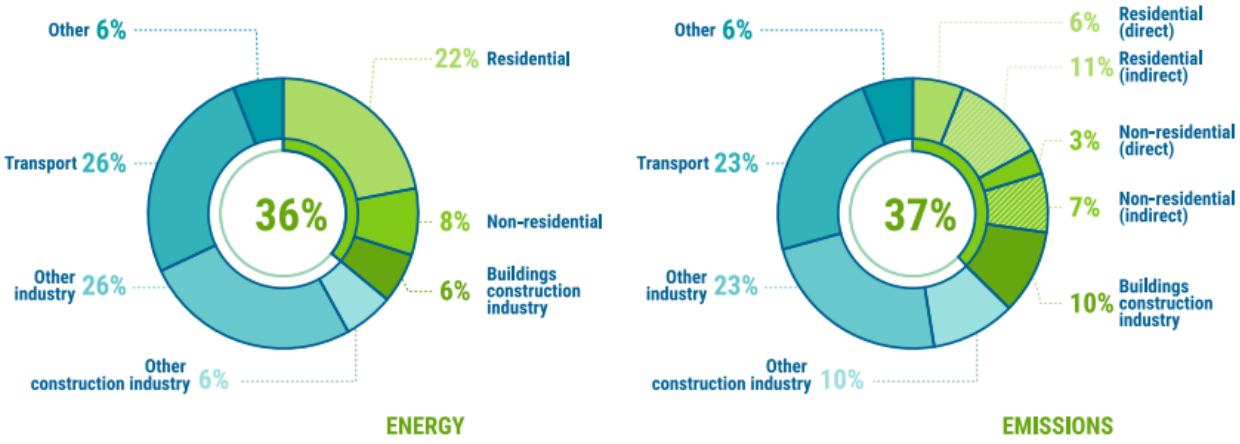

Note: "Buildings construction industry" is the portion (estimated) of overall industry devoted to manufacturing building construction materials such as steel, cement and glass. Indirect emissions are emissions from power generation for electricity and commercial heat.

Source: IEA 2021a. All rights reserved. Adapted from "Tracking Clean Energy Progress"

Figure 2-3: Energy consumption and emissions within the building sector (Global Status Report for Buildings and Construction… 2021).

Table 1 - IEA Buildings operation and construction emissions estimates, 2019

	2019 (MtCO2)	Share
Buildings use phase	**9953**	
Coal	496	9% direct emissions
Oil	939	
Natural gas	1663	
Electricity and heat	6855	19% indirect emissions
Buildings construction	**130**	**10% indirect buildings and construction value chain emissions**
Construction energy use	130	
Material manufacturing	**3430**	
Cement- and steel- manufacturing for construction	2038	
Other	1391	
Buildings and construction value chain	**13512**	**38% of total energy related emissions**

Source:(IEA 2020b). All rights reserved. Adapted from "Energy Technology Perspectives 2020"

Figure 2-4: Building operation and construction emission estimates in 2019

In brief, the building and construction sector is responsible for over 1/3rd of global CO_2 emissions. A correlation between CO_2 emissions and climate impacts has been established (see

2.1.1 A Brief Introduction to Sustainability and the Anthropocene) and current research indicates the sector's emissions are still growing while the annual rate of improvement is decreasing (*2020 Global Status Report for Buildings and Construction…*, 2020). Thus, emission reductions from the building sector are integral in mitigating the effects of climate change and its effects on environmental sustainability (Obafemi 2017).

One may note, from Figure 2-3 and Figure 2-4, that while the largest *single* contributor to building sector emissions is construction, the majority of building sector emissions are a result of the combined effects of direct and indirect energy consumption in both residential and non-residential buildings. Both direct and indirect energy consumption occurs during the building-use life-stage of the building. Direct emissions, during the building-use life-stage, are those emitted directly from the building; resulting from space and water heating, heating and cooling systems, and insulation materials. While indirect emissions, from the building-use life stage, are those emitted from energy consumption of the building; resulting from electric heating and cooling systems, district heating/cooling, artificial lighting, and other building services such as elevators, pumps, and mechanical ventilation systems (GABC and UN Environment 2016).

As a result, the industry could perhaps, most beneficially, focus on the reduction of building-use-related emissions. However, the building and construction sector has been poorly responding to its newfound responsibility of reducing energy use and emissions overall, as seen in Figure 2-5 (*2020 Global Status Report for Buildings and Construction…,* 2020; Obafemi, 2017). Therefore, it is an all-hands-on-deck situation, requiring all contributors to building and construction emissions, large and small alike, to reduce their carbon footprints.

In light of this, a spotlight has been shown on the embodied energy and emissions of a building's materials and construction practices. Embodied energy is the sum of energy consumed

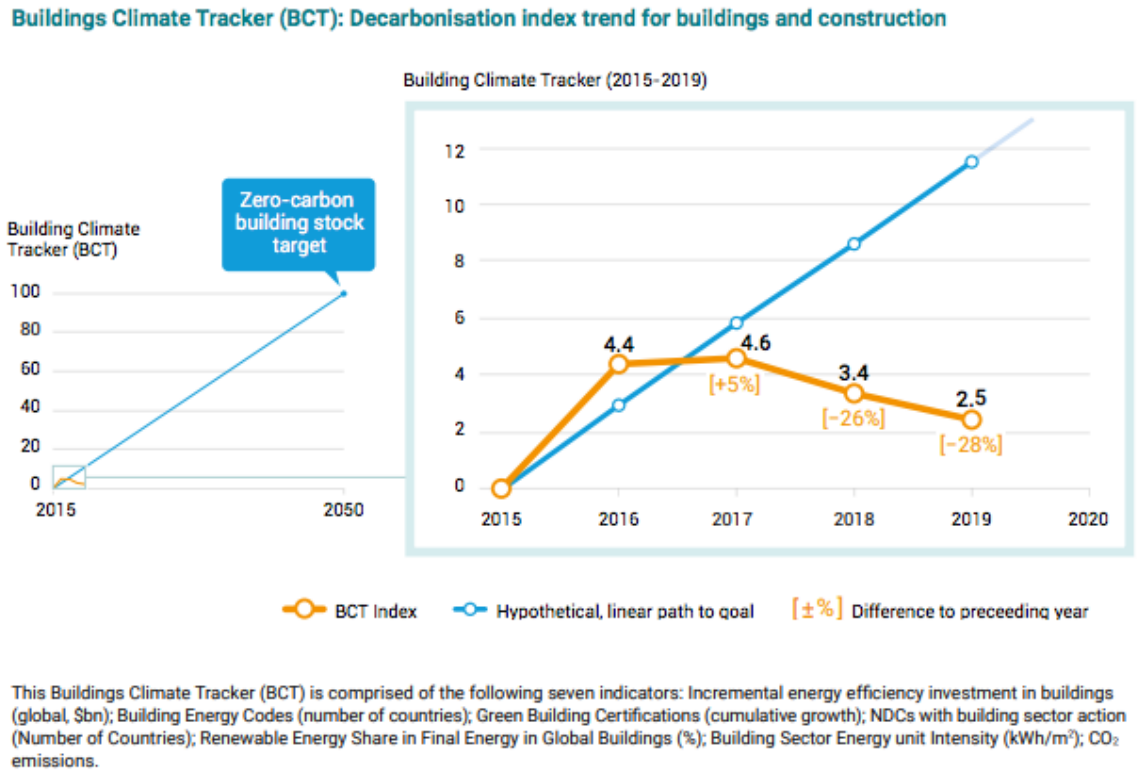

Figure 2-5: BCT decarbonisation index. The Buildings Climate Tracker shows progress on decarbonisation of buildings and construction. The final goal is to reach a decarbonisation index of 100 by 2050. Trends since 2015 are plotted here, against a linear path to 100. Most recent trends resulted in an index of 2.5 in 2019.

in the building's life cycle stages other than the operation of the building itself (Dixit, Culp, and Fernández-Solís 2013). It includes extraction of raw materials, manufacturing of materials and components, transportation, construction, and assembly. Direct energy in this stage is utilized within the bounds of the construction and assembly processes. Whereas, indirect energy, outside of the building-use stage, is associated with the production and transport of materials; it includes the raw material extraction, transportation, and the relevant portions of the energy used in the infrastructure, factories, and machinery of manufacturing (Crowther 1999).

Likewise, embodied carbon is the volume of CO_2 emitted during the same processes. Embodied energy and emissions have received global attention as greenhouse gas reduction has

been identified as a climate change mitigation technique. However, with growing focus on coalitions and energy use standards, evidence of the systematic and coordinated abatement of energy consumption has shown mixed results (Obafemi 2017; United Nations Environment Programme 2021; Hart, D'Amico, and Pomponi 2021) This is concerning, as the consensus projects floor area of the global building sector to double by 2060 at the latest (Dean et al. 2018; United Nations Environment Programme , 2021). Therefore, there is a justifiable need to increase sustainability efforts within the building construction and material manufacturing sectors of construction. This thesis focused specifically on the reduction of embodied energy and carbon in structural design, including the corresponding material manufacturing, transportation, and construction of structures.

2.1.3 Trends and Advancements in Sustainable Design and Construction

In recognition of the Earth's need for action, all United Nations members adopted the 2030 Agenda for Sustainable Development in 2015, which included Seventeen Sustainable Development Goals (*United Nations: DSGS).* The Sustainable Development Goals (SDGs) encompass all aspects of the triple bottom line: environment, society, and economics. As a result, two of the SDGs are directly related to the design and construction industry and four are indirectly related (see Table 2-1). Similarly, initiatives put forth by the World Green Building Council (WGBC) and Structural Engineering Institute (SEI), as well as the growing popularity of lean construction practices are providing sustainable footholds within the design and construction industry (Marhani et al. 2013, *SE2050 2020*, *WGBC*).

In supplement to the SDGs, a worldwide campaign organized by the WGBC is urging all levels of government to implement "bolder, more ambitious regulation, to enable [the building

and construction] industry to scale to solutions." Specifically, the action statement published by the council provides two goals. The first, to be achieved by 2030, requires all new buildings to have net zero operational carbon, as well as 40% less embodied carbon in all new buildings, infrastructure, and renovations. The second, to be achieved by 2050, requires all new buildings to have net zero operational carbon, as well as net zero embodied carbon in all new buildings' infrastructure, and renovations (World Green Building Council 2020). Rising to the WGBC's call, the SEI (a facet of the American Society of Civil Engineers) has developed a comprehensive program to support the professional structural engineering community in the pursuit of net zero carbon structural systems by the year 2050 (SE2050 2020).

Table 2-1: UN's Sustainable Development Goals that pertain to design and construction

SDGs Directly Related to Design and Construction	
Sustainable Development Goal	**Impact**
#9 Industry, Innovation, and Infrastructure	Build resilient infrastructure, promote inclusive and sustainable industrialization, and foster innovation
#11 Sustainable Cities and Communities	Make cities and human settlements inclusive, safe, resilient, and sustainable

SDGs Indirectly Related to Design and Construction	
Sustainable Development Goal	**Impact**
#3 Good Health and Well-Being	Ensure healthy lives and promote well-being for all at all ages
#8 Decent Work and Economic Growth	Make cities and human settlements inclusive, safe, resilient, and sustainable
#12 Responsible Consumption and Production	Ensure sustainable consumption and production patterns
#13 Climate Action	Take urgent action to combat climate change and its impacts
#15 Life on Land	Protect, restore and promote sustainable use of terrestrial ecosystems; sustainably manage forests; halt and reverse land degradation and biodiversity loss

2.1.4 Embodied Energy and Embodied Carbon in Structural Materials

Dixit et al. (2013) defined embodied energy in a building as the energy consumed in the building's life cycle stages other than the operation of the building itself. Embodied carbon is a measure of the emissions consequent of that energy use. The consensus agrees that further research is needed to homogenize the data for embodied energy and embodied carbon in structural building materials. Current inequalities are largely due to variance in the included life-cycle stages, data scarcity and scattering, subjectivity, and bias from proponents of a given material (Cabeza et al. 2021; Purnell 2012; De Wolf et al. 2016). De Wolf et al. (2016) attributed variations between embodied carbon dioxide and embodied energy coefficients to a lack of standardization, largely on the life-cycle stages included. Similarly, Cabeza et al. (2021) referred to the life-cycle boundary system as a crucial parameter (see section *2.2.2 Influence of System Boundaries* for more detail).

De Wolf et al. (2016) went on to write that manufacturers can use different assumptions of life cycle stages to their benefit. Including carbon sequestration may indicate an advantage for timber, whereas accounting for recycled content may be advantageous for steel. Likewise, the exclusion of these elements, when comparing the materials, may result in a skewed reality. Despite inconsistencies, there have been comprehensive efforts to quantify embodied carbon and energy of common structural materials.

One effort, made by Hart et al. (2021) quantified variability within each life stage, and the effects on embodied carbon across all life stages. Results show the main source of embodied carbon variation for steel and reinforced concrete structural frames is in the production stage, accounting for 81% and 65% of variability, respectively. Whereas, the largest source of variation for timber structural frames is in the end-of-life embodied carbon, accounting for 32% of

variability. Additionally, variation in embodied carbon associated with transportation is between 10-20% for all structural materials (see Table 2-2).

Table 2-2: Impact of life stage data variability on total life embodied carbon data (adapted from Hart et al. 2021)

Structural Material	Production	Transportation	Construction and Demolition	Disposal
Steel	0.81	0.11	0.03	0.0
Reinforced Concrete	0.65	0.16	0.11	0.0
Mass Timber	0.46	0.19	0.04	0.32

Beyond determining variability, Hart et al. (2021) used statistical models (Monte Carlo method) to determine the whole-life embodied carbon distribution of 127 structural frames of each steel, reinforced concrete, and mass timber. This resulted in a comprehensive data set, allowing a comparative analysis to be conducted. Resulting median whole-life embodied carbon (WLEC) values for timber, reinforced concrete, and steel frames were 119, 185, and 228 [kg CO_2 eq/m^2] respectively. Embodied carbon from various life-stages are seen in Figure 2-6. Results confirmed the assumption that mass timber frames are likely to have lower embodied carbon than alternative materials. However, the authors indicated that mass timber's upper hand was not as substantial as often assumed, particularly when end-of-life is included—citing literature reviews that resulted in larger reductions for timber when compared to concrete.

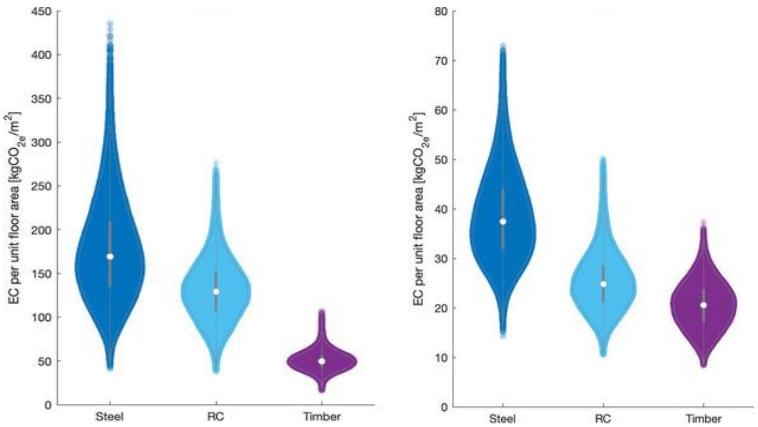

Production (left); Construction Transportation (right)

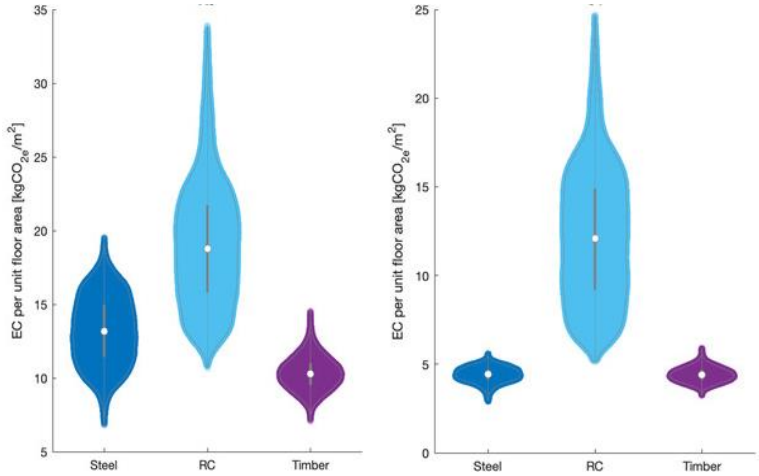

Construction and Installation (left); Deconstruction and Demolition (right)

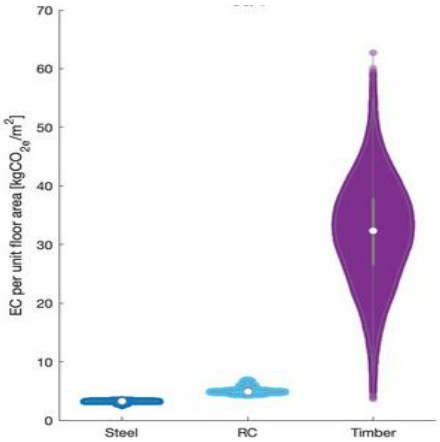

Waste processing and disposal

Figure 2-6: Whole-life embodied carbon, per unit floor area, by life-cycle stage Note scale variation between plots (Hart et al. 2021).

Another effort, made by Cabeza et al. (2021) to summarize the embodied carbon in common structural materials, conducted an international literature study on the topic. Despite citing a worldwide fast-growing interest, their work concluded that there is a shortfall in embodied carbon databases. Concluding that only 70 out of 1003 relevant papers presented values for embodied energy and/or embodied carbon of building materials. Additionally, it was determined there is substantial effort to investigate and compare case studies of whole building or building component environmental impacts. Additionally, a literature trend map revealed not only has the focus been on embodied carbon and embodied energy, but recent research is also driving attention to the concept of a circular economy, centered on reuse and recycling.

In addition to the vast majority of sources excluding embodied energy/carbon data, Cabeza et al. (2021) also found that there were sources which did not specify the crucial parameter of life cycle boundaries. Stating that data sources were scarcely cited, or vaguely referenced as "literature data." Despite this, the authors created a summary of the embodied energy and embodied carbon coefficients which they obtained from the literature. Figure 2-7 and Table 2-3 displays their findings. Note that the boundary is cradle-to-gate and how gradient colors within the bars indicate frequency of reported values in literature—with darker shades being the most commonly reported values. The authors acknowledge diverse numerical results in both embodied energy and embodied carbon—evidence of conflict within associated data sources and boundary definitions.

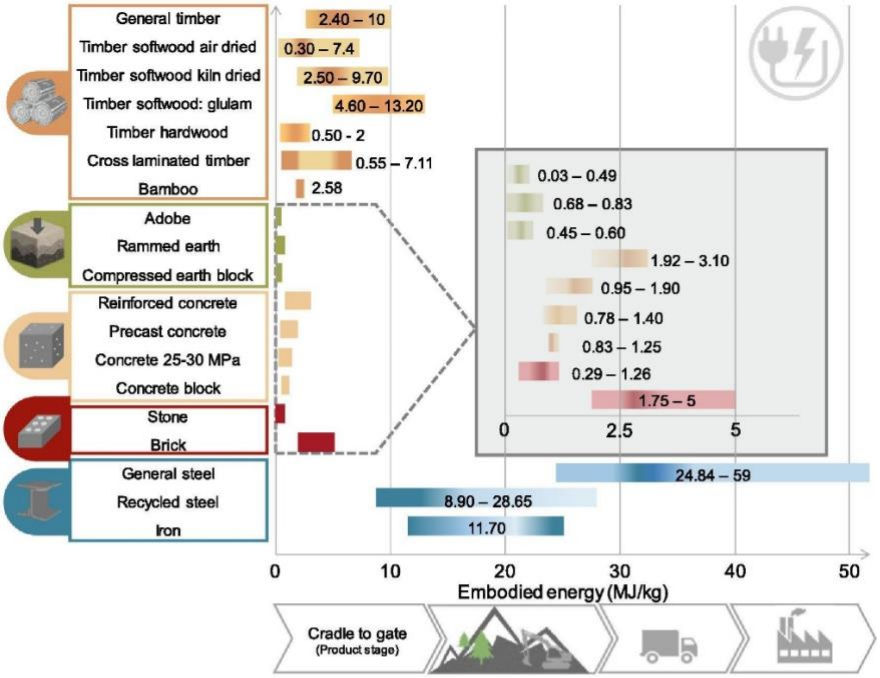

(a)

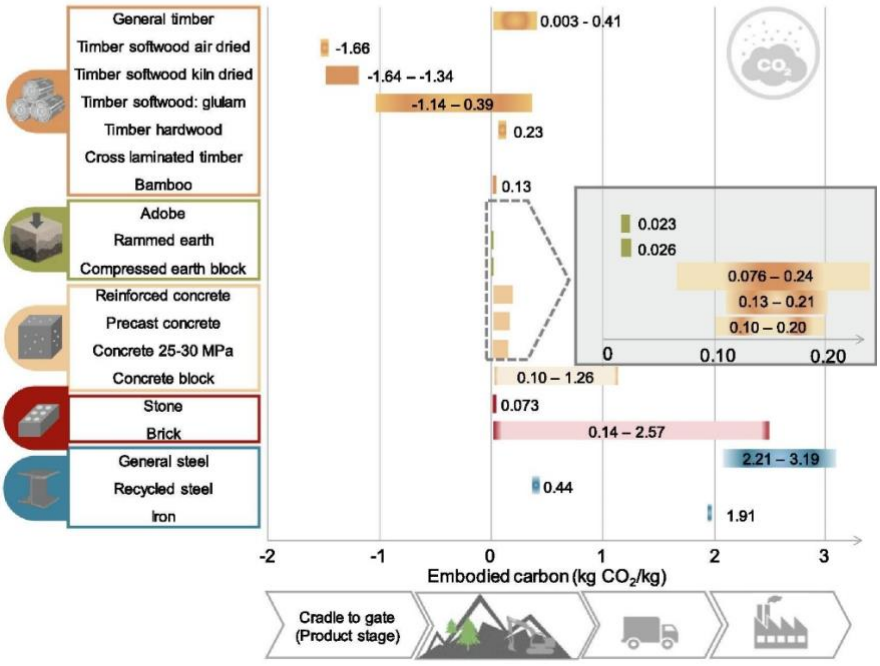

(b)

Figure 2-7: Embodied energy and embodied carbon of structural materials. The embodied carbon coefficients above are attributed to the production life-stage only. (Cabeza et al. 2021)

Table 2-3: Ranges of structural material embodied carbon and embodied energy
Data was interpreted from Figure 2-7, Cabeza et al. (2021)

Structural Material	Embodied Energy [MJ/kg]	Embodied Carbon [kg CO_2/kg]
Steel (General)	24.8 – 59.0	2.21 – 3.19
Steel (100% Recycled)	8.92 – 28.7	0.44
Reinforced Concrete	1.92 – 3.10	0.08 – 0.24
Timber (General)	2.40 – 10.0	0.00 – 0.41
Timber (Glulam)	4.60 – 13.2	-1.14 – 0.39
Timber (CLT)	0.55 – 7.11	No Data

Yet another effort to summarize embodied carbon in structural materials was made by De Wolf et al. (2016) to summarize equivalent CO_2 emissions. This study provided analyses of existing buildings, fully constructed or nearing completion. Their survey revealed the highest material usage and environmental impacts are associated with cultural buildings. In contrast with office buildings, having the lowest material usage and environmental impacts. Additionally, the study determined the highest material weight comes from concrete and steel structures. However, while the amount of material per square meter increased with height and size of the building, the global warming potential did not.

Further study found environmental impacts of steel and concrete composite systems can vary by factors approaching 5. Furthermore, steel had the highest embodied carbon coefficient of the materials examined, resulting in higher global warming potential and embodied carbon for steel structures, despite lower material quantities than concrete structures.

When relating to environmentally conscious buildings, LEED Platinum certified buildings had the highest material usage and the highest environmental impact, while LEED

Certified buildings had the lowest. Leading to the conclusion that higher levels of LEED certification do not correlate with lower environmental embodied impacts. Illustrating how LEED does not currently reward lower embodied impact buildings. Figure 2-8 displays their findings.

Ultimately, the study found that timber and masonry structures have the lowest impacts, however, the authors state that they do not consider timber and masonry practical for all structures. As a result, the suggested method of embodied carbon reduction is to improve material efficiency on a case-by-case basis rather than selecting one particular structural system above another.

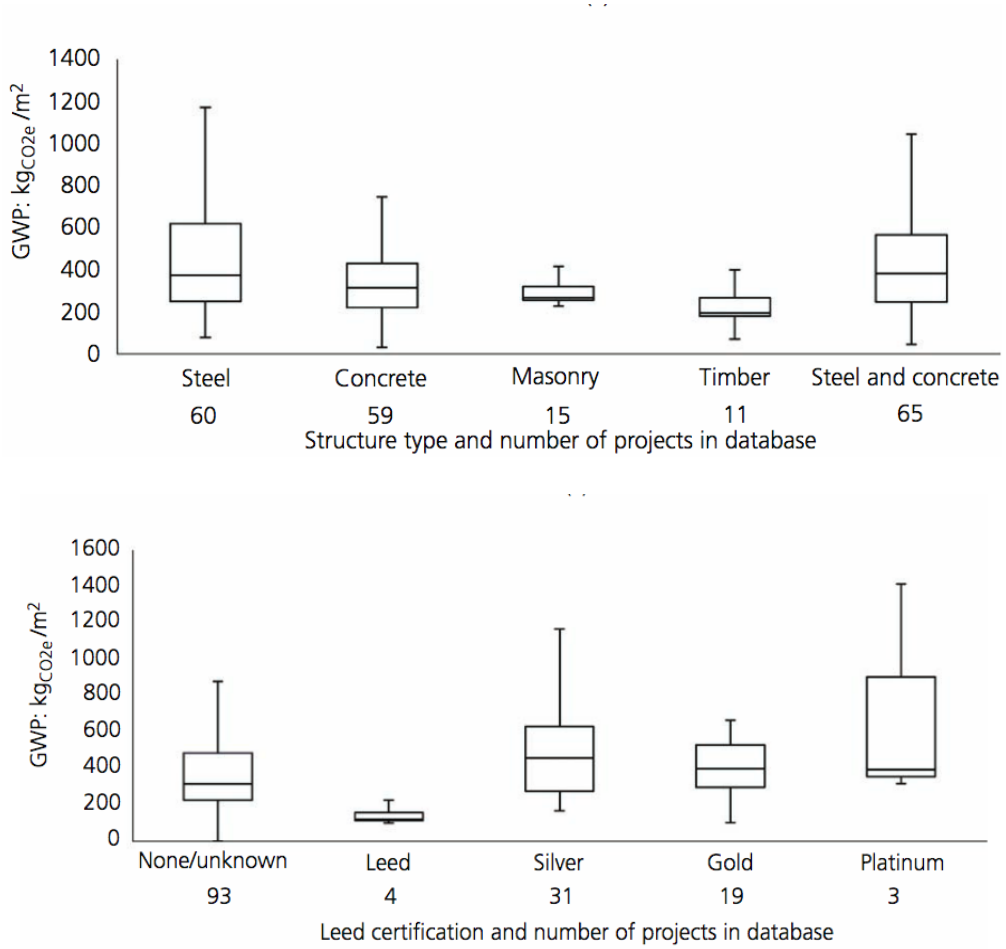

Figure 2-8: Embodied carbon per structural material and LEED certification (De Wolf et al. 2016)

In contrast to the previous studies, Purnell (2012) asserted that green structural materials are mythological. Purnell made cases against each common structural material's sustainability claims. For example, those with a vested interest in timber claim a lower carbon footprint in wood because of its ability to sequester carbon. However, deforestation simultaneously contributes to 17% of global CO_2 emissions and remains a high-profile global environmental concern. Similarly, those with an interest in steel tout its recyclability, resulting in an inherently low-carbon emissive material. For this material, the author claims no account of energy use and CO_2 emissions associated with smelting and refining primary steel, and eventually re-melting the steel for recycle, stating that recycling involves significant energy use (10-20 MJ/kg).
For concrete, Purnell argues that proponents of this material focus on reduced air condition/heating requirements due to its thermal inertia, or focus on the use of waste materials as supplementary cementitious materials, while de-emphasizing that cement production accounts for 5-10% of global carbon emissions.

Purnell (2012) concedes that the Inventory of Carbon and Energy (ICE), despite its various limitations is "the most authoritative single freely available source and has become a de facto standard for many studies." ICE embodied carbon values are reported in Figure 2-9, note that these are consistent with the discoveries of Cabeza et al. (2021), with reasonable variation. Ultimately, the author argues that the functional unit in which embodied carbon is reported is useless, stating that a valid comparison is not made by comparing 1 kg of concrete to 1 kg of steel or 1 kg timber. Purnell suggests compensating for this by normalizing with respect to a mechanical property of interest—such as compressive strength, as seen in Figure 2-9. However, the author concludes these values take no account of variations in cross-sectional geometry; invalidating the approach. Instead, the author calculates embodied carbon as functions of load

capacity and member length. In conclusion, the author claims that structural design parameters such as cross-sectional dimensions and load capacity are equally influential with material choice on embodied carbon per unit load capacity.

The arguments of Purnell (2012) against comparing the embodied carbon per weight of structural material are valid, however, the inequalities of embodied carbon per material weight can be normalized through the process of Whole Building Life Cycle Analysis (WBLCA), which often results in the functional unit of kg CO_2 eq./m^2 (per square meter of building area, see more in section *2.2.3 Influence of Functional Units*); as in the data of De Wolf et al. (2016) and Hart et al. (2021). WBLCA is a comparative method which accounts for the entire building system. Rather than isolating a material to its unit weight, it accounts for the total weight required by design. This normalizes the inequalities between embodied carbon per unit weight of material by accounting for the in-place or design weight. As discussed above, WBLCA often positions timber as the structural material with the lowest embodied energy and embodied carbon (Hart, D'Amico, and Pomponi 2021; De Wolf et al. 2016). As a result, timber—specifically mass timber—has become "a fundamental disruption of conventional concrete-and-steel approaches to building design and construction." Wood is coming into the limelight, not only, as the "only innately renewable structural material with significant market presence" but also as "an advanced structural system that produces communities with greater speed, efficiency, and resilience" (Atkins et al. 2022).

material	EE, MJ/kg	EC, kg-CO_2/kg	EC per unit of compressive strength, (kg-CO_2/kg)/MPa
Steel			
virgin (v)	35	2.8	0.0079
recycled (r)	9.5	0.43	0.0012
typical (60% r, 40% v)*	20	1.4	0.0039
Timber			
sawn softwood	7.4	0.45	~0.02
glulam structural composite*	12	0.7	0.026
Concrete			
low strength (C12)	0.35	0.05	0.0042
medium strength (C50)	0.87	0.15	0.0030
"low-CO_2" (C50, 40% PFA)*	0.56	0.09	0.0018
high strength (C90)*	1.8	0.32	0.0036

Figure 2-9: Embodied CO2 of selected structural materials (Purnell 2012)

2.2 Introduction to Life Cycle Assessment

2.2.1 Whole Building Life Cycle Assessment (WBLCA)

Life Cycle Assessment (LCA) quantifies the environmental impact of a product throughout its entire life. Regarding a building, this process is commonly referred to as Whole Building LCA (WBLCA). It is a procedural attempt to quantify the impacts of raw material extraction, manufacturing, transportation, construction, building operation, and end-of-life demolition/disposal (Chiniforush et al. 2018; Gu et al. 2021; Allan and Phillips 2021). WBLCA typically evaluates the energy consumption or associated carbon emissions due to the above operations. The impact of embodied carbon is typically referred to as Global Warming Potential (GWP) and is measured in carbon dioxide equivalents, quantifying various greenhouse gases emitted throughout a building's life cycle (Budig et al. 2020; De Wolf et al. 2016). Carbon equivalents account for direct emissions of CO_2, NH_4, and N_2O—carbon dioxide, methane, and

nitrous oxide, respectively—normalized, as necessary, to a carbon dioxide equivalent (Ahmad et al., in press). The energy consumption resulting from a building's life cycle is categorized into two broad groups: operational energy and embodied energy (Chiniforush et al. 2018; Allan and Phillips 2021; Gu et al. 2021; Budig et al. 2020). Operational energy is used to fulfill the building's function; whereas embodied energy is used in the building's production, material sourcing, and recycling or disposal. (Gu et al. 2021; Allan and Phillips 2021).

Gu et al. (2021) describe LCA as a computational tool to quantify the environmental impacts of products and processes, as well as a comparative assessment tool. Comparative WBLCAs juxtapose individual LCAs of functionally equivalent buildings. When analyses are high quality, comparative WBLCA allows practitioners to make appropriate comparisons, assess the impacts of a design, and implement strategies to reduce total environmental impact (Allan and Phillips 2021; Gu et al. 2021). However, valid comparisons only occur when best practices are followed and a methodological consensus of goal and scope is completely transparent (Gu et al. 2021; Nwodo and Anumba 2019). Parameters which influence the variability and comparative validity of LCAs are numerous; some of which are: lack of procedure for system boundaries and biogenic carbon consideration, inadequate definitions of functional units, assumptions of life span scenarios and processes, and Life Cycle Inventory (LCI) database quality or subjectivity (Nwodo and Anumba 2019). All of these impair analyses usefulness as assessment tools for sustainable building designs (Chau, Leung, and Ng 2015; Gu et al. 2021)

2.2.2 Influence of System Boundaries

The system boundary of any LCA defines the life cycle stages included in analysis (see Figure 2-10). The various processes that occur during a building's life cycle are classified into

four main life cycle stages: Production, Construction, Use, and End-of-Life (Gu et al. 2021). Embodied energy, or carbon, includes life cycle stages A1-A5, C1-C4, and D—excluding the building use stages. Operational energy, or carbon, includes life cycle stages B1-B7—including only the building use stages.

Common boundaries utilized in life assessments are cradle to gate and cradle to grave (production through the end of life/reuse) (Cabeza et al. 2021). Cradle to gate accounts for the production stage only (A1-A3) and includes all processes and transportation beginning from the extraction (and growth, if applicable) of the raw materials through the manufacturing and processing required to obtain the site-ready structural material. Conversely, cradle to grave encompasses all life stages, beginning with raw material extraction through the structural materials disposal, re-use, or recycling processes.

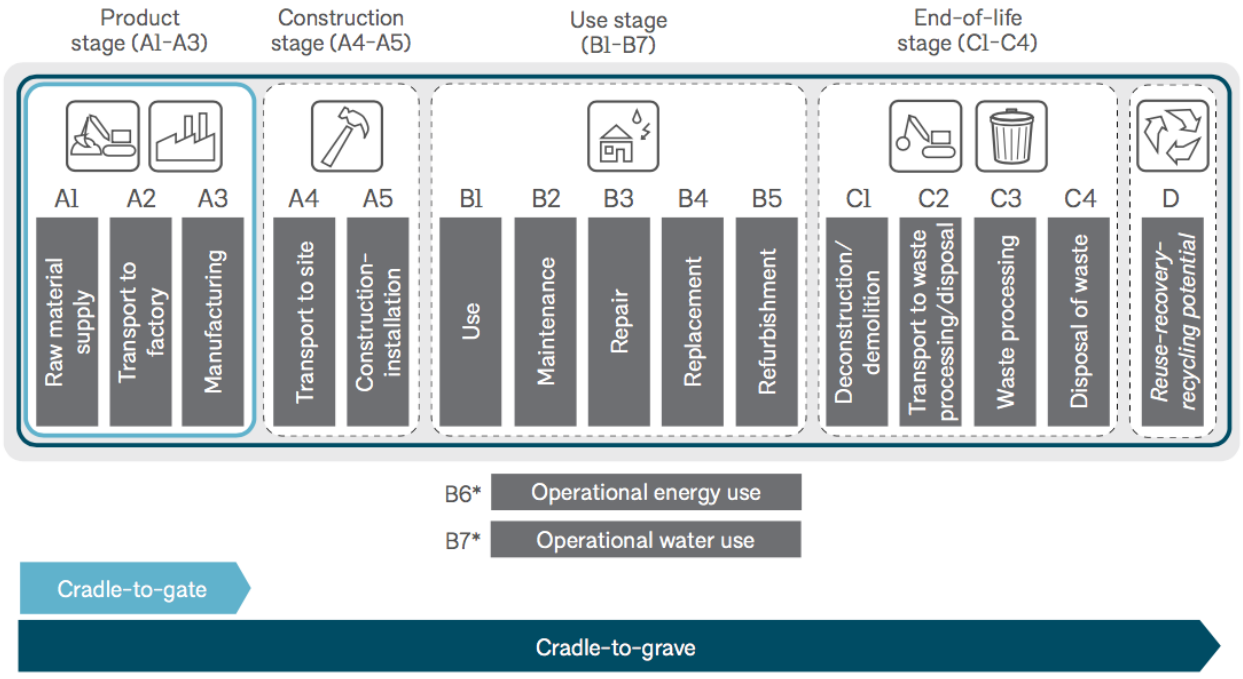

Figure 2-10: Life cycle stages (M. Lewis et al. 2021)

A current challenge facing LCA is the lack of procedure for choosing relevant system boundaries, as they are defined subjectively and on a case-by-case basis (Dixit, Culp, and Fernández-Solís 2013; De Wolf et al. 2016; Nwodo and Anumba 2019). As a result, current embodied energy analyses exhibit gaps—problems of variation, inaccurate evaluations, and incompleteness (De Wolf et al. 2016; Dixit, Culp, and Fernández-Solís 2013). Mitigating these inequalities between analyses requires transparency in all choices, including material choices, upstream production processes, regional production assumptions, system boundaries, biogenic carbon considerations, end-of-life assumptions, scenario predictions, and included buildings components (Dixit, Culp, and Fernández-Solís 2013; Gu, Liang, and Bergman 2020; De Wolf et al. 2016).

2.2.3 Influence of Functional Units

LCA outputs are often normalized against a chosen functional unit to aid in quantified performance comparisons (Nwodo and Anumba 2019; Chau, Leung, and Ng 2015). For example, the total embodied energy of a structure is often reported in (MJ) This may be normalized per net floor area, useable floor area, living area, etc.; all resulting in units of (MJ/m^2). Similarly, total embodied carbon is most often reported in units of (kg CO_2-eq) and may be normalized per any metric of unit area to (kg CO_2-eq/m^2). Other possibilities include functional units of time, volume, unit length, per unit occupant, etc. (Chau, Leung, and Ng 2015; Nwodo and Anumba 2019). Normalizing total quantities by a functional unit facilities comparison between different LCAs (De Wolf et al. 2016; Nwodo and Anumba 2019; Chau, Leung, and Ng 2015)

Inconsistency in use of functional units, varieties in choice of functional units, and the possibility of having several functional units in one building system leads to difficulties in analysis comparison and discrepancies in results (Nwodo and Anumba 2019; Chau, Leung, and

Ng 2015). It is possible, even with clear outlines of methodology, for analyses to be incomparable due to ambiguous units.

There are various proposed methods of rectification for discrepancies in units. One route is standardization of functional units in all LCAs (Feng, Sadiq, and Hewage 2022; Nwodo and Anumba 2019). Another method is extreme transparency in units; perhaps including even building type, technical and functional requirements, pattern of use, and required service life in the unit itself (Nwodo and Anumba 2019; Gu et al. 2021). However, a comprehensive combination of both approaches is likely the most beneficial.

2.2.4 Influence of Life Cycle Inventory

Life Cycle Inventory (LCI) is the compilation of inputs and outputs for the system or product undergoing LCA (Suh and Huppes 2005). It provides quantifiable values, allowing understanding and evaluation of the magnitude of the environmental impacts (Pacheco-Torgal et al. 2014). The inventory data is related to the functional unit of a particular system, element, or product within the system as a whole. Once the amount of commodities fulfilling the element is determined, the functional unit is multiplied by the amount of environmental interventions generated to produce the final product (Suh and Huppes 2005). The LCI phase of an LCA involves the compilation of materials through quantity take off (QTO), defining the processes which the raw materials undergo before installation in the product, developing construction and utilization scenarios, the application of environmental data, and collection of the products of all of these. A simple example calculation is shown in Figure 2-11. Note that there are various functional units, each respective to a unique element or processes in the LCI. In this example, the

life cycle analyst would define the QTO, product use, and service life; a database would likely define the environmental impact of each element and process.

Rigor is essential for an accurate LCA; as a result, LCI can be incredibly data intensive. In effort to grow interest in LCA, despite the existing methodological challenges, BIM-based LCA of buildings has been developed. Reviews indicate that BIM-based analyses enhance data collection and storage, as the required building data can be extracted from the model and applied to LCI databases (Nwodo and Anumba 2019). However, despite growing attentions on environmental impacts and greenhouse gas emissions, one of the main challenges currently facing LCA is variety and inconsistencies in databases and LCI methods (Feng, Sadiq, and Hewage 2022; Suh and Huppes 2005). Suh and Huppes (2005) determined that different methods are available for

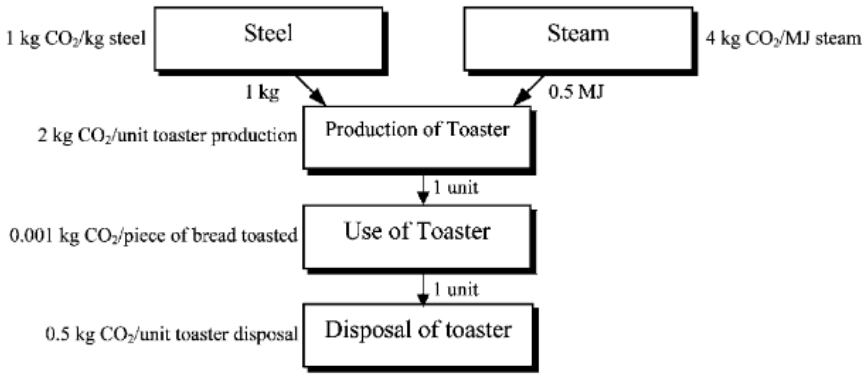

$$\left(\frac{1\text{ kg CO}_2}{\text{kg steel}}\cdot 1\text{ kg steel}\right)+\left(\frac{4\text{ kg CO}_2}{\text{MJ steam}}\cdot 0.5\text{ MJ steam}\right)$$
$$+\left(\frac{2\text{ kg CO}_2}{\text{unit toaster prod.}}\cdot 1\text{ unit toaster prod.}\right)$$
$$+\left(\frac{0.001\text{ kg CO}_2}{\text{piece of toast}}\cdot 1000\text{ pieces of toast}\right)$$
$$+\left(\frac{0.5\text{ kg CO}_2}{\text{unit toaster disposed}}\cdot 1\text{ unit toaster}\right)$$
$$=6.5\text{ kg CO}_2$$

Figure 2-11: Life cycle inventory utilized to calculate the GWP of a toaster (Suh and Huppes 2005)

LCI and each generally creates significantly different results—ultimately resulting in significant differences in environmental impact databases. For example, one study indicated variations over 50% between the Ecoinvent and ICE databases (Feng, Sadiq, and Hewage 2022).

While there are many growing databases, some currently available are Ecoinvent, United States Life Cycle Inventory (USLCI), Inventory of Carbon and Energy (ICE), GaBi, Athena, and European Life Cycle Database (ELCD) (Feng, Sadiq, and Hewage 2022; Nwodo and Anumba 2019). Beyond a variety of methods and uncertainty in environmental impact calculations, many variances between databases are surrounded by assumptions of product involvement. A study by Petersen and Solberg (2002), focused on an LCA of glulam and reported that changes in assumptions arefar more influential than uncertainty in inventory data. Therefore, this is another area in which transparency, in both the scope of the analysis and in the database, are essential. Table 2-4 is an overview of prominent assumptions that may occur in databases and LCA studies.

Scholars have begun to recommend approaches to mitigate the uncertainty and effect of assumptions in databases. Recommendations include utilizing various databases, conducting uncertainty and sensitivity analyses, and utilizing environmental product declarations (EPDs) instead of a commercial database (Gu, Liang, and Bergman 2020; Feng, Sadiq, and Hewage 2022). An EPD is an environmental impact report for a specific product; all EPDs must be developed strictly following the EN 15804 standard. As a result of the strict standards set forth by EN 15804, EPDs have clear and uniform requirements; applying these to LCI dramatically increases the accuracy of an analysis (Feng, Sadiq, and Hewage 2022).

Table 2-4: Partial overview of assumptions in databases which impact LCA (Gu et al. 2021; Petersen and Solberg 2002)

Assumption	Impact Stage
Proportions of utilized renewable and fossil fuel energy	Production, Construction, End of Life
Recycled content in a product (particularly scrap v. ore based steel)	Production, End-of-Life
Waste handling (particularly landfill v. incineration for energy or re-use)	End of Life
Construction and demolition activities	Construction, End-of-Life
Material sourcing	Production
Transportation distances	Production, Construction, End of Life
Construction and installation processes	Construction, End-of-Life
Amount of permanently sequestered carbon in wood biomass	Production, End-of-Life

2.2.5 Influence of Biogenic Carbon Considerations

Biogenic carbon is derived from a material of biological origin (SOM 2022). In the case of lumber, biogenic carbon is the carbon sequestered from the atmosphere during growth and stored within a tree. Because this process removes carbon from the atmosphere, biogenic carbon is typically counted as a negative carbon emission (SOM 2022).

Literature reviews have determined further transparency and conformity of biogenic carbon accounting within LCAs is necessary to improve validity and comparability (Andersen et al. 2021; Allan and Phillips 2021; Gu et al. 2021). LCAs may neglect biogenic carbon in wood products due to uncertainties of proper accounting techniques or uncertainty of sourcing, as a forest must be sustainably managed for biogenic carbon to be characterized as negative. Another common method counts wood products simply as carbon neutral (Andersen et al. 2021). However, based on international standards that govern biogenic carbon accounting practices

(ISO 21930), biogenic carbon consideration is suitable to be characterized as negative within an LCA if there is certainty of sustainable sourcing (SOM 2022).

2.2.6 Current LCA Standards

Beyond standardization of EPDs, general consensus agrees that LCA as a whole requires standardization to allow for meaningful comparisons, eliminate subjectivity, and optimize effort (Feng, Sadiq, and Hewage 2022; Nwodo and Anumba 2019; Gu et al. 2021). As a result, international standards have been developed. Currently, The International Organization of Standardization (ISO 21931) and the European Standard (EN 15978) are guiding uniformity in WBLCA (Gu et al. 2021).

2.3 State of Mass Timber in Design and Construction

2.3.1 Introduction to Mass Timber

Mass Timber is group of engineered wood products (EWPs). Fundamentally different from traditional lumber or timber, EWPs are composite elements. Composite elements are comprised of two separate elements connected to act as one. The connection is integral to the system, unified behavior is only possible when horizontal slippage between the two elements is suppressed. To prevent slip, horizontal shear at the interface must be transferred via a connecting element (Segui 2018). This connection substantially increases the strength and stiffness of the individual elements, creating one stronger and more resilient element.

To achieve composite action, a faction of EWPs are manufactured with adhesives to bind the strands, fibers, veneers, or boards into a composite element. Some of the most prominent glue-laminated products include cross-laminated timber (CLT), mass plywood panels, laminated

veneer lumber, and glulam (Atkins et al., 2022, 1-14). It is important to note that *glue-laminated* and *glulam* are not interchangeable. Glue-laminated products are bonded together with durable, moisture-resistant adhesives. While both CLT and glulam are glue-laminated, the defining factor is the orientation of the dimensioned lumber within the product. CLT is comprised of sawn lumber stacked orthogonally, enabling the element to span in two directions. Whereas glulam is comprised of sawn lumber stacked lumber elements stacked in parallel. resulting one-way spanning capabilities (Atkins et al., 2022, 16-19). In North America, glulam *panels* are often referred to as "glue laminated timber" (GLT) and glulam *beams* or *columns* are referred to as simply "glulam." Figure 2-12 displays the lumber orientations in GLT and CLT panels. Despite the ability to fabricate glulam as a panel, it is typically used as a beam or column (Atkins et al., 2022, 7). Figure 2-13 is exemplary of a typical glulam beam.

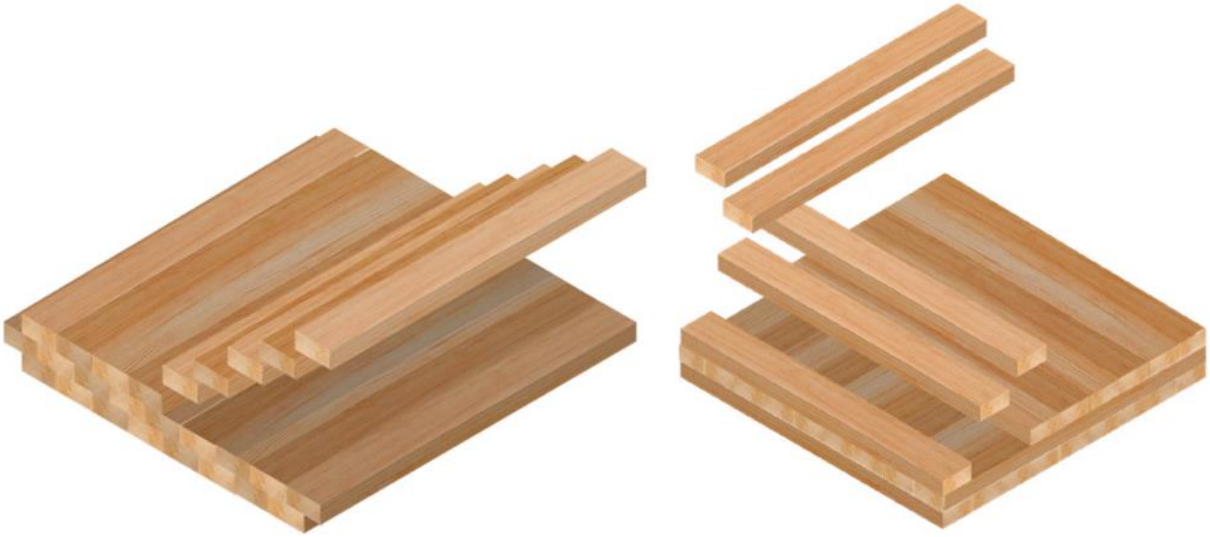

Figure 2-12: Common glue-laminated mass timber panels. The glulam panel, or GLT, (left) has parallel laminations throughout all layers. Whereas, the CLT panel (right) has layers of perpendicular laminations (*The Mass Timber Design Guide* 2022, 16-19).

Figure 2-13: Glulam Beam
A typical glulam is a beam or column composed of lumber stacked with all grains running parallel (StructureCraft Inc 2022)

Other classes of mass timber are connected by means other than adhesives, most commonly nails or dowels. Similar to glue-laminated mass timber, these methods also enable composite action between the sawn lumber components. Nail laminated timber (NLT) is centuries old. This system joins numerous pieces of lumber stacked face to face, fastened together mechanically (Atkins et al., 2022, 3-4). Unique to this type of mass timber, is that it does not require a dedicated fabrication facility. Instead, it can be manufactured on site with readily available lumber and nails or screws (Atkins et al., 2022, 18).

Dowel laminated timber (DLT), on the other hand, uses a process called friction fitting, which requires a controlled environment. To fabricate these elements, hardwood dowels are dried to a very low moisture content and placed in holes drilled perpendicularly into softwood boards. The dowels, then, expand as they gain moisture from the surrounding softwood boards. The result is a tight-fitting connection that holds the boards together. This is the only all-wood mass timber product (Atkins et al. 2022, 4). See figure 2-14 for NLT and DLT configurations.

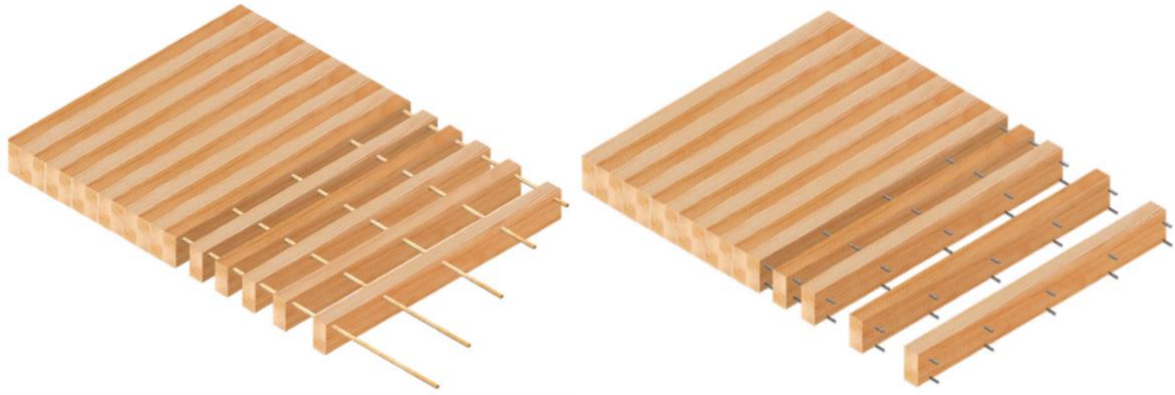

Figure 2-14: Alternative mass timber panels, includingdowel laminated timber, or DLT (left), and nail laminated timber, or NLT (right), (Atkins et al., 2022, 17-18).

2.3.2 Trends and Advancements in Mass Timber Design and Construction

The 2021 World Green Building Trends report, published by Dodge Data and Analytics, announced a 14-point expected growth share in green building engagement. Reportedly, 42% of respondents will build with the intent of registering or certifying more than 60% of their projects green by 2024; up from 28% doing so in 2021. Figure 2-13 expands on the report. It shows expected growth in the fraction of respondents considering green building practices in the majority of their projects; as well as a decline in the fraction of respondents which will consider green building practices less than 15% of their projects.

Between 2013 and June of 2022, the United States' has had 1,502 mass timber projects in the multi-family, commercial, or institutional categories ("U.S. Mass Timber Projects" 2022). While not all of them progressed beyond the design stage, just under half were constructed.

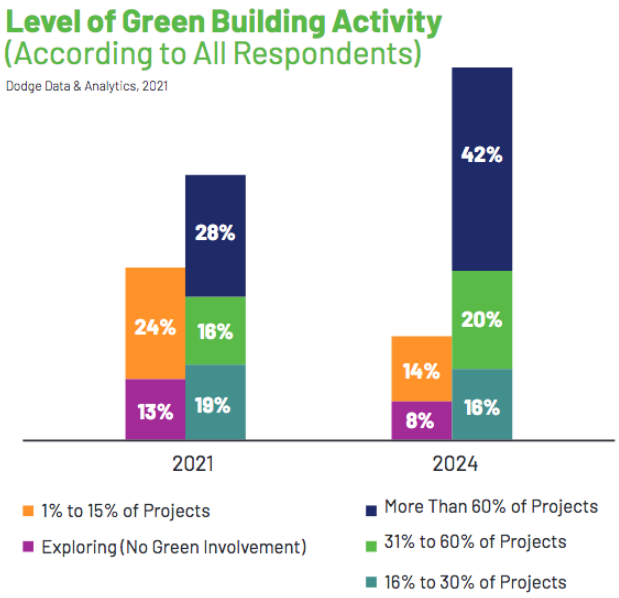

Figure 2-15: Level of green building activity in 2021 and expected growth.Survey respondents were asked about their current overall share of green projects (2021, left) and expected future shares of green projects in 3 years (2024, right). (Dodge Data and Analytics 2021).

Figure 2-16 is a map of all designed and constructed projects. Additionally, not only is there projected to be an increase in green building activity (*Dodge Data and Analytics, 2021*), Atkins et al. (2022) predicted the number of mass timber buildings constructed globally will double every two years between 2020 and 2034.

All projects in Figure 2-16 were mass timber; meaning, no light-frame wood structures contributed to the mass timber construction total. Current wood construction varies greatly between traditional light-frame systems and mass timber systems. Light-frame, consisting of dimensional lumber, is the most familiar timber construction system. It utilizes sawn lumber studs to form vertical wall members; joists and rafters for floor and roof supports, respectively; and plywood or OSB panels to sheath the walls, floors, and roof. The lateral force resisting system (LFRS) in these structures are most commonly light-frame shear walls. Whereas post and beam involves the use of large sawn timber or mass timber beams that frame into sawn timber or

mass timber columns. The LFRS system in mass timber structures may be braced frames, concrete shear walls, or mass timber shear walls. Another wood construction type is mass timber panel systems. This system utilizes large EWP panels for the floor, roof, and walls (Atkins et al. 2022). Figure 2-17 and Figure 2-18 display the construction types.

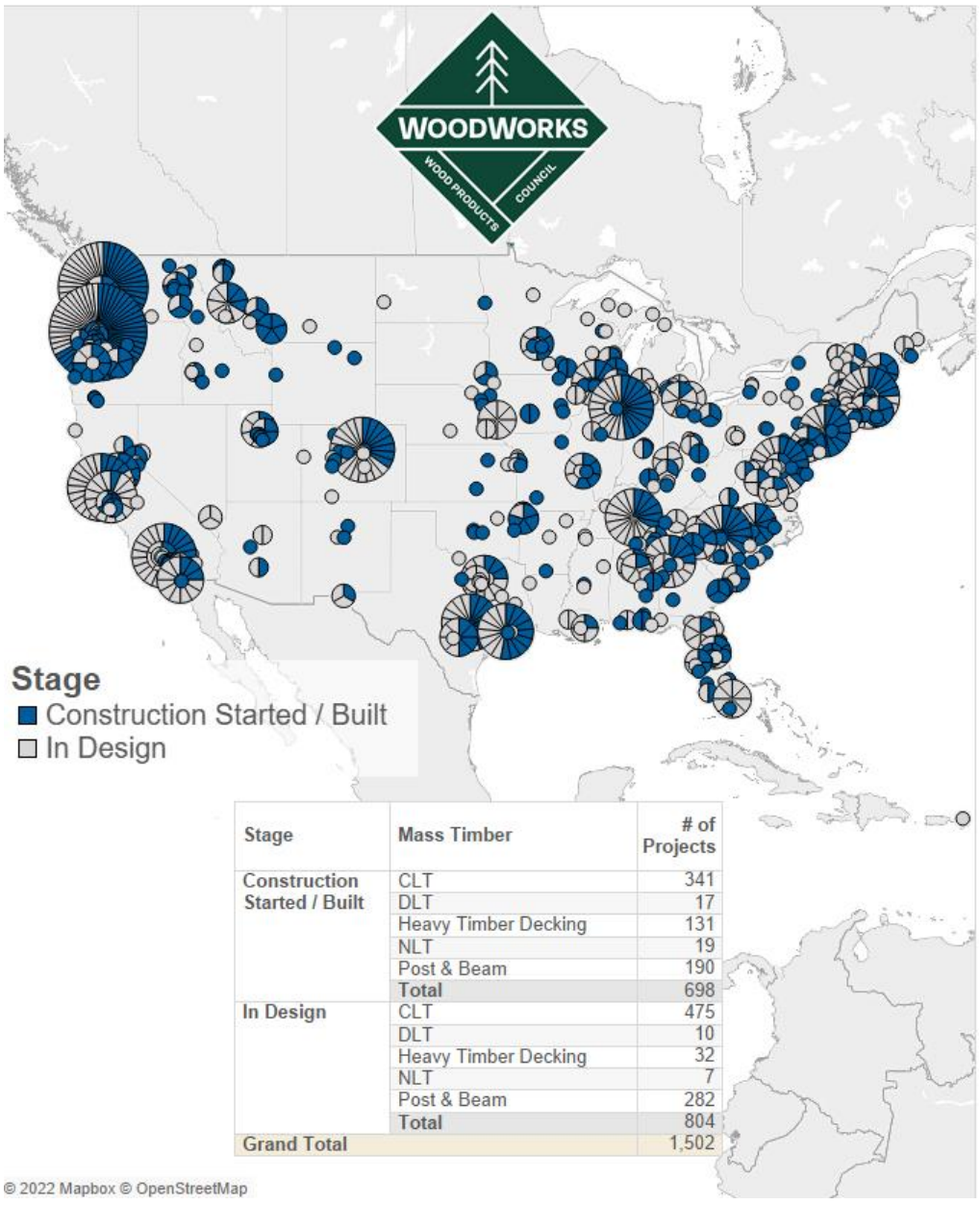

Stage	Mass Timber	# of Projects
Construction Started / Built	CLT	341
	DLT	17
	Heavy Timber Decking	131
	NLT	19
	Post & Beam	190
	Total	698
In Design	CLT	475
	DLT	10
	Heavy Timber Decking	32
	NLT	7
	Post & Beam	282
	Total	804
Grand Total		1,502

Figure 2-16: Map of mass timber design and construction projects in the U.S.

Historically, U.S. construction spending data has indicated a greater market in non-residential construction (Figure 2-19). However, despite significant advancements in the acceptance and recognition of the benefits of mass timber construction, the building industry is still dominated by steel and concrete structural systems for non-residential and multistory residential construction (Figure 2-20). The current majority of timber market share most likely being light-frame, single family homes or multifamily low-rise buildings (Atkins et al. 2022)

There are a few factors likely inhibiting mass timber's evolution as a construction material in the United States. Atkins et al. (2022) writes that at this stage building mass timber building owners are pioneers in adapting new structural technology, financing, and procurement systems. They continue on to expand on the limited experience of contractors, engineers, and

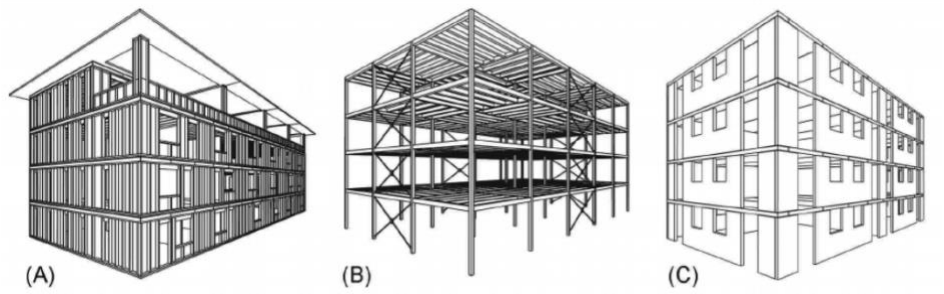

Figure 2-17: Common wood construction systems, including(A) light frame (B) mass timber post and beam (C) mass timber panels (Kuzman and Sandberg 2017).

Figure 2-18: Mass timber construction. Examples of post and beam construction (left) (LWA 2022) and panel construction (right) (WoodWorks 2016).

designers in mass timber construction, which can result in more responsibilities during system implementation for the owner—which can be a deterrent for many.

Another factor inhibiting mass timber's evolution as a construction material in the United States is cost. Ahmed and Arocho (2021) found that the cost competitiveness of mass timber buildings is still under study due to the lack of available cost information. However, preliminary research found that mass timber building designs are estimated have construction costs up to 30% higher than alternative systems (Gu, Liang, and Bergman 2020; Ahmed and Arocho 2022). In a best-value bidding system, like in the construction market, the lowest bid is most often the winner—meaning mass timber systems can be left largely uncompetitive in the mass market (Nguyen et al. 2018).

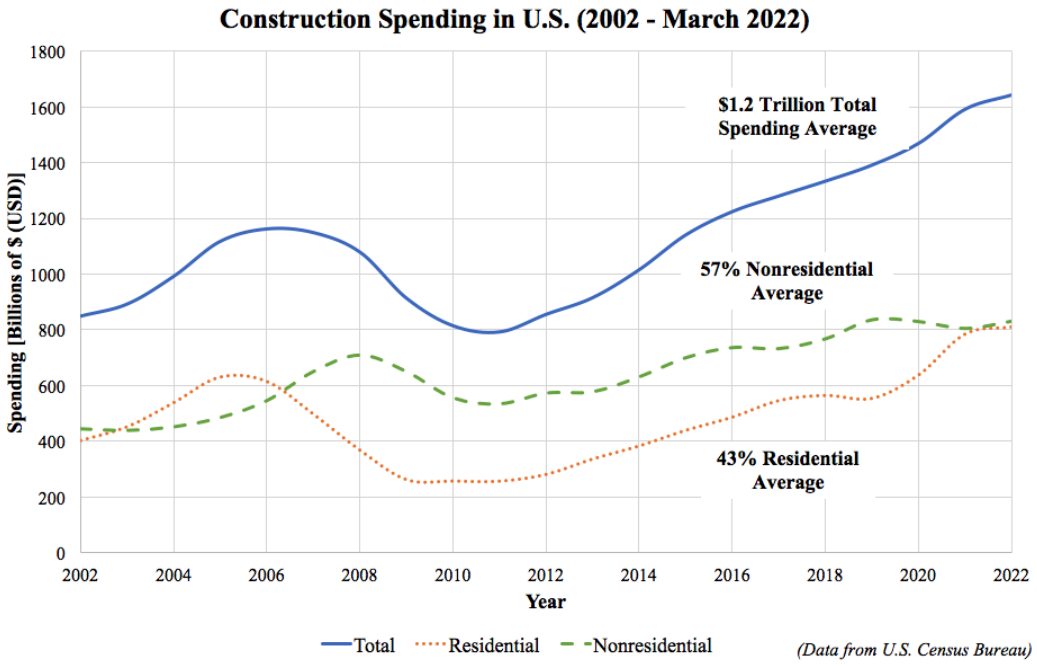

Figure 2-19: Construction spending trends in the United States. Adapted from data published from 2002 through March 2022 (USCS 2022)

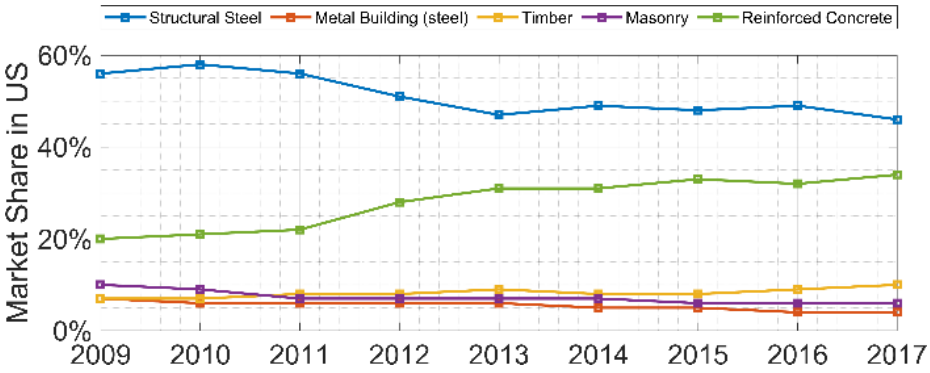

Figure 2-20: Material market shares of construction materials in the U.S. based on building footprint area (Dodge Data & Analytics 2018)

2.3.3 Financial Implications of Mass Timber in Construction Projects

Being one of the most resource-intensive industry sectors in the global economy, cost is an important parameter of all construction projects. However, cost competitiveness of timber structures is still under study due to the lack of available cost information. Cost of a product not only indicates its market potential, it also is a critical parameter in construction which has significant impacts on the overall quality of the project. Unfortunately, there is a significant gap in the availability of cost information of mass timber buildings. (Ahmed and Arocho 2022; 2021). Gu et al. (2020) determined that despite attention from both academia and the construction industry, very little transparent data or cost analyses are available, which has created a hazy debate between the cost differential of mass timber and other traditional structural materials.

Similar to the inconsistencies in embodied energy data, the consideration or neglect of life cycle stages greatly influences the economy of mass timber (see *2.1.4 Embodied Energy and Embodied Carbon in Structural Materials* and *2.2.2 Influence of System Boundaries*). Therefore, a functional method of comparing structural costs is Life Cycle Cost Analysis (LCCA). LCCA can be useful to quantify cost effectiveness of various buildings designs or in exploration of

trade-offs between initial and long-term costs (Gu, Liang, and Bergman 2020). Other studies, such as those conducted by Ahmed and Arocho (2021) note that total life cycle costs could have potential to offset mass timber's high construction costs. For example, the schedule of a mass timber project can be 18-30% faster than a more established structural system, and should be included in cost considerations (Burback and Pei 2017; Crespell and Gagnon 2010).

One example of LCCA, conducted by Gu et al. (2020), compared a 12-story mass timber (glulam + CLT) building design to a functionally equivalent reinforced concrete building design. The study included permit, design, material, construction, replacement, end-of-life, deconstruction, demolition, and salvage costs. Using a bill of materials from architectural drawings and cost data from RSMeans, a construction cost estimate was created; it included material, labor, and overhead costs. The operational energy and water use were determined via energy simulation software and plumbing design systems; these values were then multiplied by current utility rates. Maintenance and repair costs were estimated from frequencies in research studies, as most mass timber buildings in North America have been built within the last 10 years and do not have maintenance/repair data at this time.

Comparing the mass timber and concrete buildings, Gu et al. (2020) found the operational energies were functionally equivalent, and thus operational costs were considered equal between the buildings. Thus, variations were due to front-end and end-of-life costs. Figure 2-21 displays the calculated cost variances between the mass timber and reinforced concrete buildings due to material, labor, and overhead costs. In conclusion, the team found that front-end costs were 26% higher for the mass timber building while the building value at year 60 was 153% higher than the concrete alternative. Therefore, LCCA revealed a 2.4 – 4.6% decrease in

total life cycle cost for the mass timber building when compared to the concrete. The authors go on to note that high mass timber recycling rates would further improve the cost benefits of mass timber buildings.

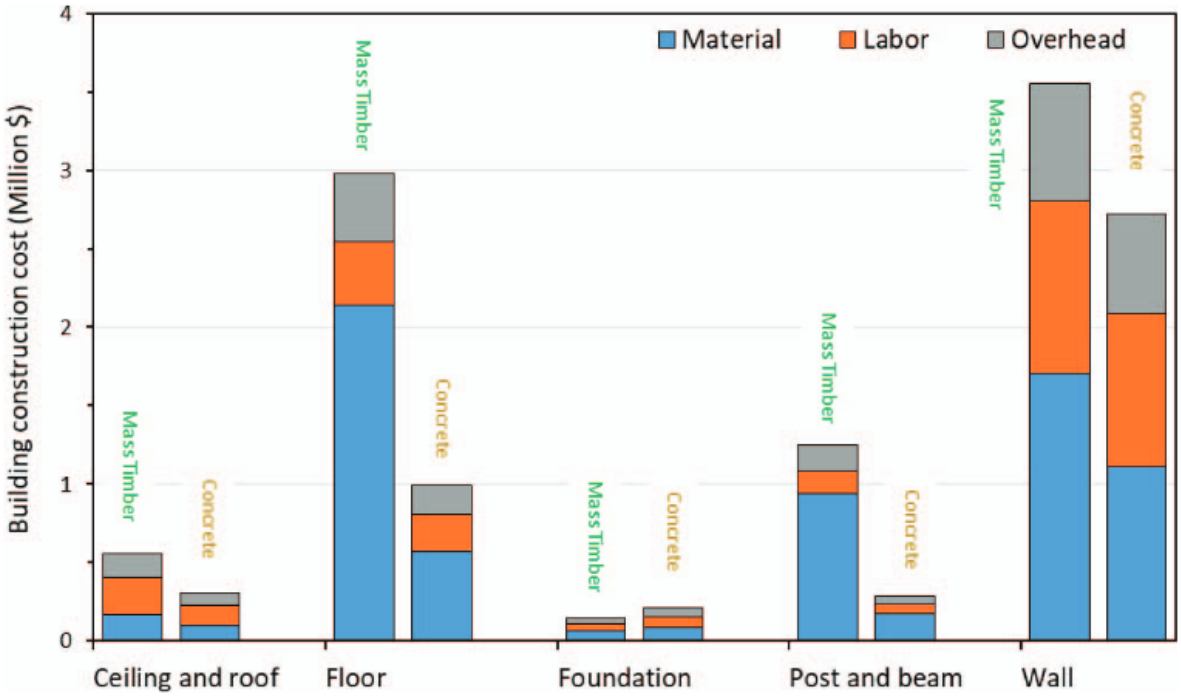

Figure 2-21: Front-end construction costs by assembly type for high-rise mass timber and concrete buildings (Gu, Liang, and Bergman 2020)

It is important to note, the work of Gu et al. (2020) draws from the findings of O'Connor et al. (2004). This study conducted a demolition survey in Minneapolis/St. Paul, MN, the findings of which oppose common assumptions about building service life and the relationship between structural materials and longevity. The study concluded that the majority of steel and concrete buildings were demolished less than 50 years into their service lives. Whereas, the majority of demolished wood buildings were older than 75 years (O'Connor 2004). Drawing from this, Gu et al. (2020) used a longer life span for the mass timber building (100 years) than for the concrete alternative (75 years). Sensitivity analysis revealed that the LCCA was heavily

impacted by study period variation. When mass timber and concrete life spans were equal, mass timber was unable to overcome high front-end costs.

Additionally, O'Connor et al. (2004) reported that majority of buildings in study fell into only three categories for demolition motivation. Those being: area redevelopment (34%), lack of maintenance (24%), and building no longer suitable for intended use (22%). As a result, the authors concluded acknowledgment of short service lives favors structural materials which enable easy building modification for changing needs, as well as materials that are easy to recover at the end of service life.

Another study, conducted by Burback and Pei (2017) recognizes that CLT can be cost competitive against steel and concrete options in certain scenarios. However, their work focused on using CLT as an alternative to light-frame wood construction in a single-family residential home. The study analyzed only initial costs. They compared traditional light-frame, all CLT, optimized CLT + glulam designs. The designs resulted in homes that cost $390,000, $510,000 , and $480,000 , respectively. Meaning the CLT and optimized CLT designs increased the home's construction costs, as compared to the light-frame, by 30.0% and 21.2%, respectively.

2.3.4 International Building Code Allowances

The *2021 International Building Code* (*IBC 2021*) introduced three new building construction classifications: Type IV-A, IV-B, and IV-C. Type IV construction now has four classifications total; the fourth being Type IV-HT—previously known as only "Type IV" in *IBC 2018*. The new classifications are based on IV-HT, but allow taller story heights and require additional fire-resistance as the building height increases (Breneman et al. 2019). A summary of the IBC provisions for each Type IV classification is seen in Figure 2-22.

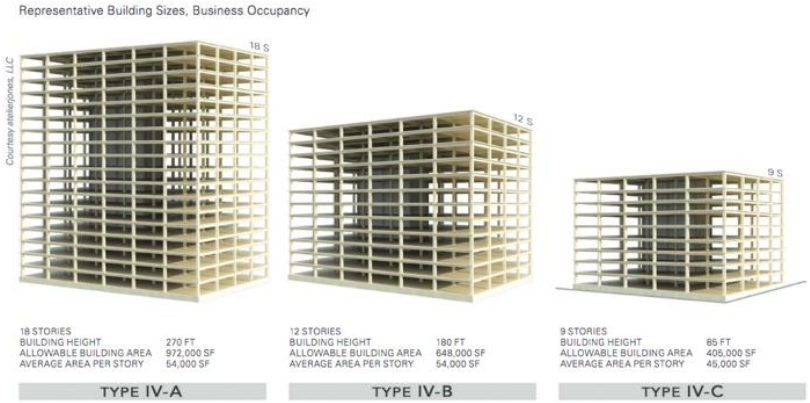

Figure 2-22: IBC 2021 code allowances for business occupancy mass timber structure (Breneman et al. 2019)

2.3.5 Inherent Fire Resistance and Fireproofing Requirements

Mass timber is able to perform architecturally, structurally, and sustainably—while, on top of this, provide passive fire-resistance to a building as well (McLain and Breneman 2019). Passive fire-resistance in mass timber is a consequence of char that forms on the exterior face of a wood element directly exposed to fire. With continued exposure to fire, charring occurs at a very slow, predictable rate on the surface. This char layer creates a protective barrier between the inner portion of the mass timber element and the flame. The resulting reduction is called the *effective char depth* (NDS 2018). The thickening char layer removes oxygen from the inner depths of the member, which extinguishes the burning component—creating an insulative char layer. Figure 2-23 displays the reduction of width and depth that occurs while char forms. Atkins et al. 2022 determined that test results have proven large wooden components can maintain their structural integrity for extended periods of time, even when exposed directly to flames and intense heat—this is largely due to the char layer.

Fire-resistance ratings (FRR) for all structural materials are specified in *IBC 2021 Table 601* (Table 2-5). This is the length of time a given assembly can be exposed to high temperature

conditions before losing critical performance characteristics. *IBC 2021 Section 602.4* states that mass timber elements shall meet the FRR requirements via either the FRR of noncombustible protection, the mass timber itself, or a combination of both. Noncombustible protection requires a material (such as gypsum wall board) be applied to exposed faces of the mass timber. Resulting in a loss of the aesthetic and biophilic benefits of the material.

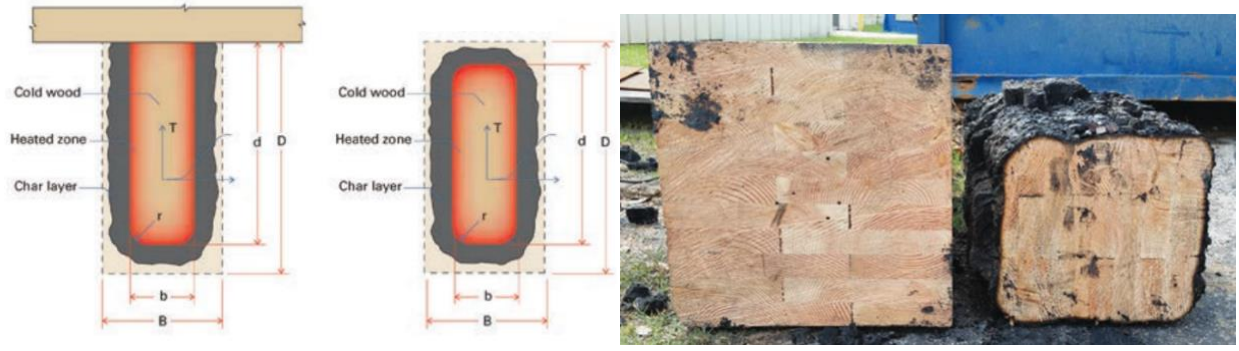

Figure 2-23: Charring in mass timber.The reduction in member width and depth over time (left). Partially charred glulam column pre and post 2-hour fire test (right) (McLain and Breneman 2019).

Table 2-5: Fire resistance ratings for mass timber per IBC 2021 Table 601 (Breneman, Timmers, and Richardson 2019)

Building Element	IV-A	IV-B	IV-C	IV-HT
Primary Structural Frame	3	2	2	HT
Ext. Bearing Walls	3	2	2	2
Int. Bearing Walls	3	2	2	1/HT
Floor Construction	2	2	2	HT
Roof Construction	1½	1	1	HT

Table 2-6: Non-combustible protection requirements for mass timber per IBC 2021 (McLain and Breneman 2019)

Required Noncombustible Protection on Mass Timber Elements by Construction Type

	IV-A	IV-B	IV-C	IV-HT
Interior Surface of Building Elements	Always required. 2/3 of FRR, 80 minutes minimum	Required with exceptions. 2/3 of FRR, 80 minutes minimum	Not required*	Not required*
Exterior Side of Exterior Walls	40 minutes	40 minutes	40 minutes	Not required*
Top of Floor (above Mass Timber)	1" minimum	1" minimum	Not required*	Not required*
Ceiling (below Mass Timber)	Per interior protection	Per interior protection	Not required*	Not required*
Shafts	2/3 of FRR, 80 minutes minimum, inside and outside	2/3 of FRR, 80 minutes minimum, inside and outside	40 minutes minimum, inside and outside	Not required*

**Not required by construction type. Other code requirements may apply. 5/8" Type X gypsum = 40 minutes.*

Some Type IV construction specifies a minimum amount of contribution from noncombustible protection (Table 2-6). In summary, no timber exposure is explicitly allowed per *IBC 2021* in Type IV-A, but exposure increases as construction type progresses toward Type IV-HT, where 100% of mass timber may be exposed.

2.4 Viability and Advantages of Steel-Timber Composite Systems

2.4.1 Growing Implementation of Cross Laminated Timber

The *2019 Canadian Cross Laminated Timber* (CLT) *Handbook* defines CLT as an engineered wood product with orthogonal layers of graded sawn lumber, or structural composite lumber, laminated together with structural adhesives. The product has been developing in the global market during the last two decades, but originated in Europe in the mid-nineties (Ahmed and Arocho 2021; Crespell and Gagnon 2010; Karacabeyli and Gagnon 2019). Initially, CLT panels faced implementation challenges due to lack of experience and acceptance in the AEC community, code limitations for wood construction, and lack of generic or proprietary standards (Crespell and Gagnon 2010). However, CLT has gained momentum in recent years, developing

into a major player in large-scale modern timber construction due to advancements in code allowances and the recognition of advantages by investors and the public (Burback and Pei 2017; Crespell and Gagnon 2010; Ahmed and Arocho 2021). Code allowances in the United States include the recognition of CLT panels as a structural material in the 2015 edition of the NDS and the adoption of the 2021 International Building Code, which includes new mass timber construction types (see *2.2.5 International Building Code Allowances*) (Burback and Pei 2017). Advantages of the panels as a structural material include desirable rigidity, stability, and mechanical properties (Crespell and Gagnon 2010; Ahmed and Arocho 2021).

Data indicates that CLT panels are becoming more common as a building material, not only as a whole in the market, but also relative to other mass timber products. CLT is currently the most common mass timber product being researched in North America (Ahmad et al., in press). Similarly, CLT is the most common mass timber product being constructed. The 2022 International Mass Timber Report, supported by data from WoodWorks, estimated that 71% of the square footage and 65% of mass timber building projects in the United States are accounted for by CLT alone.

2.4.2 Efficiency and Optimization in CLT as a Floor Element

Research by AISC found that steel framing paired with a composite mass timber floor system maximizes the advantages of each material (Skidmore, Owings, and Merrill 2017). Steel frames provide superior spanning capabilities, and composite mass timber floor systems are lightweight, able to span long distances while maintaining a flat soffit. Research indicates these benefits would not be economically feasible in system comprising only mass timber. Equivalent span lengths would require excessively deep beams or a tighter column spacing for a flat soffit

condition. Therefore, a steel-timber composite (STC) harnesses the strengths of each material and applies them to suit (Skidmore, Owings, and Merrill 2017).

Studies show that between one-half to two-thirds of mass in a traditional steel frame structural system is the concrete floor (Allan and Phillips 2021; Chiniforush et al. 2018). Similarly, up to 80% of a structure's weight is accounted for by the floor in buildings over 10 stories tall (Block and Paulson 2019). This suggests that greater efficiency could be achieved by using lighter alternatives to cast-in-place concrete slabs, particularly in tall buildings (D'Amico and Pomponi 2020; Block and Paulson 2019; Allan and Phillips 2021). Tall structures require larger columns at lower levels, to support the self-weight above, therefore, a lighter floor system could result in smaller member sizes and further decrease the weight of the structure.

As a result of the large concentration of mass, as well as the embodied carbon intensive production processes of concrete, studies have shown that up to half of a structure's embodied carbon is in the concrete floor & foundation elements (Allan and Phillips 2021). Therefore, replacing the floor system with a carbon sequestering material, rather than a carbon intensive material has potential to substantially lower the environmental impact of a structure. Mass timber has been recognized as a catalyst for green construction, as its products contribute to the sustainability of cities by turning urban structures into carbon sinks (Scouse et al. 2020). Therefore, replacing concrete and steel floor systems with CLT could have significant benefits and likely be achievable at a global scale (Hart, D'Amico, and Pomponi 2021; Chiniforush et al. 2018).

2.4.3 Impact on Dynamic Response and Lateral Force Resisting Systems

Seismic forces are inertial; resulting from, and are directly correlated with, the mass of a building (Chapra 2007). In the most basic analysis, seismic forces can be simplified as the product of building mass and acceleration, as seen in Figure 2-24. However, more comprehensive analyses should consider the external dynamic force (p) as the sum of inertia ($m\ddot{u}$), damping resistance ($c\dot{u}$), and structural stiffness (ku), as seen in Equation 2.4.1. Where $\ddot{u}$ is the acceleration of the mass, $\dot{u}$ is its velocity, *u* is its displacement, *k* is the lateral stiffness of the system, and *c* is the viscous damping coefficient (Chapra 2007).

$$m\ddot{u} + c\dot{u} + ku = p(t) \qquad \textit{(Equation 2.4.1)}$$

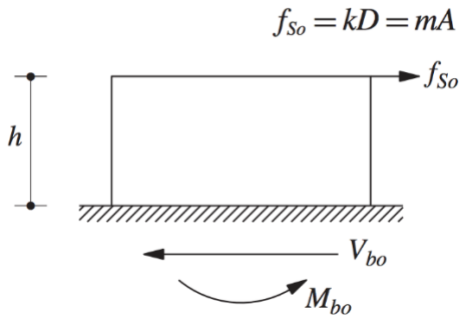

Figure 2-24: Equivalent static (f_{So}) force resulting from dynamic loading of a structure The static force is a product of the structure's mass (m) and pseudo acceleration (A). (Chapra 2007)

As a result of the inertial nature of seismic forces, resulting lateral loads are proportional to the permanent weight, or seismic weight, of the structure (Skidmore, Owings, and Merrill 2017). Therefore, the member sizes in lateral force resisting systems are also directly proportional to the seismic weight. Smaller member sizes will result in less material use and cost savings. In the recognition of CLT as a lightweight replacement to concrete floor systems, research on the topic often includes data on seismic weight or LFRS designs.

For example, a study comparing an all mass timber (MT) structure with an RC alternative, reported a total weight reduction of 33% in the MT structure (Gu, Liang, and Bergman 2020). The influence of replacing concrete floor slabs with CLT has been analyzed. One study in particular, compared a thirty-story all concrete structure and the same structure with a concrete-timber hybrid system. The hybrid structure consisted of concrete slabs at every third floor and CLT floors between. The seismic demand reduction was substantial; so much so, that wind became the governing lateral load case over seismic loads due to the reduction of building mass (Schuirmann et al. 2019). Similarly, steel-timber systems show substantial decreases in seismic weight when compared to traditional steel-concrete systems. One publication reported a 35% reduction in seismic weight (Skidmore, Owings, and Merrill 2017).

2.5 Environmental Research on Steel-Timber Structural Systems

In recognition of the need to replace concrete with a lighter, less energy and carbon intensive material, timber hybrid systems are being recognized as viable alternative. These alternative structural systems are intended to compete financially and functionally with traditional systems (Chiniforush et al. 2018; Skidmore, Owings, and Merrill 2017). Currently, there have been various efforts to quantitatively measure and report the competitiveness of steel-timber systems with conventional systems, some reporting on various criteria. The efforts are expanded upon in the following sections and ultimately summarized in a table at the end of this section.

2.5.1 Energy Implications of Using STC Elements in Buildings

Extensive research on the viability of STC structural systems has been completed in Australia by a team of civil engineers. One associated paper, by Chiniforush et al. (2018), evaluated the life cycle energy implications of adopting mass timber elements as floor and shear wall systems. STC gravity systems utilized CLT panels bearing on hot-rolled WF steel shapes, connected with fasteners to enable composite action (see Figure 2-25). The study quantified the embodied energy as well as operating energy of several structural systems with varying LFRS. Results showed substantially lower cradle-to-gate embodied energy in the STC floor systems when compared to steel-concrete composite (SCC) and RC floor systems; decreasing 59.1% and 20.4%, respectively (see figure 2-27). The authors reported that the life cycle energy saving was found to be mainly associated with a significant drop in the embodied energy of the structure, despite a slight increase in the operating energy demand.

Chiniforush et al. (2018) designed, analyzed, and compared four structural systems, each at three different heights (Figure 2-26). Therefore, results compared various combinations of gravity and lateral systems. The authors reported the steel-timber composite (STC) with CLT shear walls (designated as "STCXXT" in Figure 2-26) had the lowest construction energy use, which contributes to cradle-to-gate energy. The second lowest energy use was the STC with reinforced concrete (RC, designated "STCXXC") shear walls. This was largely due to the energy required to lift CLT panels is substantially lower than the energy required to lift steel or precast concrete panels. Additionally, the authors found that the energy consumption in pumping concrete was 230% higher than those associated with lifting the steel structural elements using a tower crane.

Figure 2-28 displays the total embodied energy of each studied structure. The average total (cradle-to-grave) embodied energy of the RC, steel-concrete composite (SCC), STCC, and STCT structural systems are 1741, 1300, 851, 793 [MJ/m^2], respectively. Therefore, the STC structures have the lowest embodied energy, while the RC structures have the highest. It is important to note, however, when end-of-life recycling is neglected, SCC structures have the highest embodied energy. Ultimately, the STCT structure embodied 58.1% and 111.8% lower energy than the SCC and RC structures (Chiniforush et al. 2018). Additionally, the STCT system was found to be 5 times lighter than the RC system. Because of this substantial weight difference, the authors expect embodied energy saving benefits of STC structures to increase significantly in earthquake prone regions where lateral loads are proportional to the permanent weight of the structures.

The authors go on to state the importance of a CLT provider's location. The influence of a local supplier, versus an overseas supplier, results in up to a 105% decrease in transportation-related consumed energy of the STC structure. However, the effect this decrease in transportation energy has on total embodied energy in STC structures was not specified.

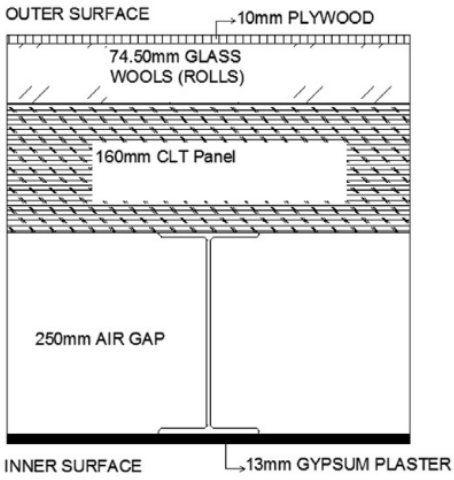

Figure 2-25: STC floor system utilized by Chiniforush et al. (2018)

	Structure	Floor	Shear wall
RCXX	RC	RC slab	RC
SCCXX	Steel	SCC	RC
STCXXC	Steel	STC	RC
STCXXT	Steel	STC	CLT

*XX indicates number of stories (05, 10, and 15)

Figure 2-26: Structural systems investigated by Chiniforush et al. (2018)

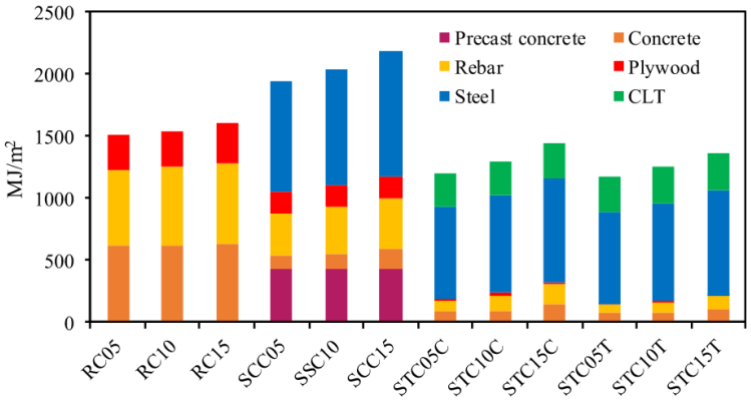

Figure 2-27: Cradle-to-Gate embodied energy per unit floor area (Chiniforush et al. 2018)

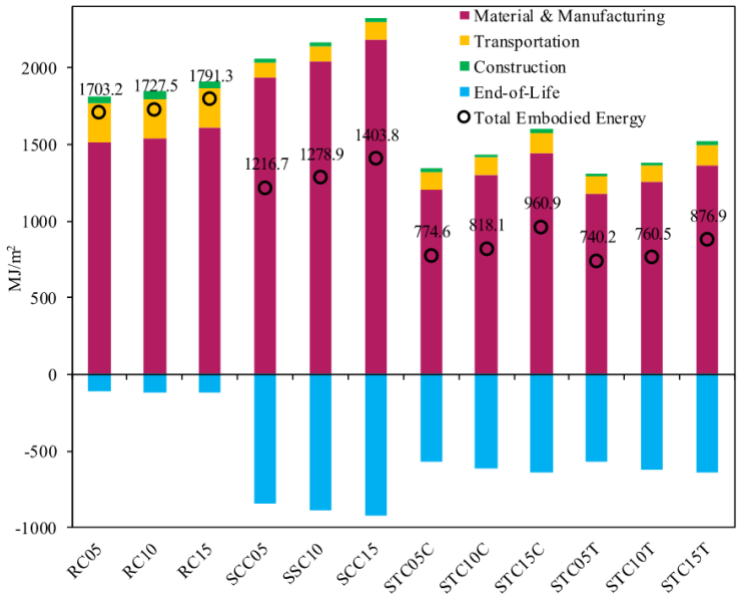

Figure 2-28: Total embodied energy of the studied structures per unit area (Chiniforush et al. 2018)

2.5.2 AISC Steel and Timber Research for High-Rise Residential Buildings

Steel and Timber Research for High-Rise Residential Buildings by the American Institute of Steel Construction (AISC) focused on marketability, serviceability, constructability, and cost of a steel-timber composite system. However, gravity beams were hot-rolled WT steel shapes, relying on cast-in-place concrete to enable composite action. CLT floor panels and concrete topping were connected with angled screws, achieving composite action to increase stiffness of the floor panel and mitigate CLT span deflections. The system utilizes CLT bearing on WT flanges without fasteners, or composite action between the steel and timber (Figure 2-29). The benefits of the light-weight structural system were clear, as the steel-timber system resulted in a seismic mass 35% lower than an equivalent RC structure. The publication results claimed marketable bay sizes and floor-to-floor heights by utilizing flat soffits and thin ceiling sandwiches. Furthermore, the study reports clear advantages due to the lightweight and prefabricated system, as well as viability in the high-rise residential market due to reasonable material quantities, fabrication techniques, erection sequences, and indications of financial competitiveness.

The 6-ply CLT decks in the AISC study were 8” thick with 2.5” of concrete topping, governed by pre and post-composite deflections (Skidmore, Owings, and Merrill 2017). The CLT-concrete composite system allowed a level soffit, with no interior support beams, and column bay sizes consistent with concrete flat plate construction. AISC considered the flat soffit an achievement in marketability, as this attribute is consistent with concrete flat plate construction. This benefit, would not be economically feasible with an all mass-timber system, as it would require deep beams for the bay sizes or a tighter column spacing for a flat soffit

condition (Skidmore, Owings, and Merrill 2017). Additionally, the concrete topping depth allowed it to be utilized as a diaphragm for lateral design.

While proposed STC system utilized two separate composite elements, neither utilized steel and timber connected to create composite action. As seen in Figure 2-29, the CLT and concrete are connected with screws to create composite action; while the concrete is cast-in-place around the steel to create composite action. Resulting in a "steel-timber composite system" without steel-timber composite action.

2.5.3 MCDA of Steel and Mass Timber Prototype Buildings in the PNW

A study by Ahmad et al. (in press) utilized multiple-criteria decision analysis (MCDA) to quantitatively compare steel-concrete and mass timber (MT) structures. The criteria under analysis were global warming potential (GWP), seismic resiliency, superstructure cost, and durability. In effort to harness GWP reductions from the MT structures, as well as seismic resiliency and cost performance from steel framing and LFRS, Ahmad et al. (in press) combined the two systems into a steel-timber hybrid (STH) system. The STH was a simplified structural design which merged the CLT floors of the MT structure with the gravity and lateral framing of the steel structures. Results indicated that the STH system was most preferred when GWP is moderately prioritized in decision making and comparable to the conventional STC and MT buildings in the four other cases (see Figures 2-30 and 2-31). Ultimately, the study demonstrated that a steel-timber structure combines the seismic and low-cost benefits of steel construction with the low embodied carbon benefits of mass timber construction. Demonstrating that the STH case may represent the broadest appeal across decision makers (Ahmad et al., in press).

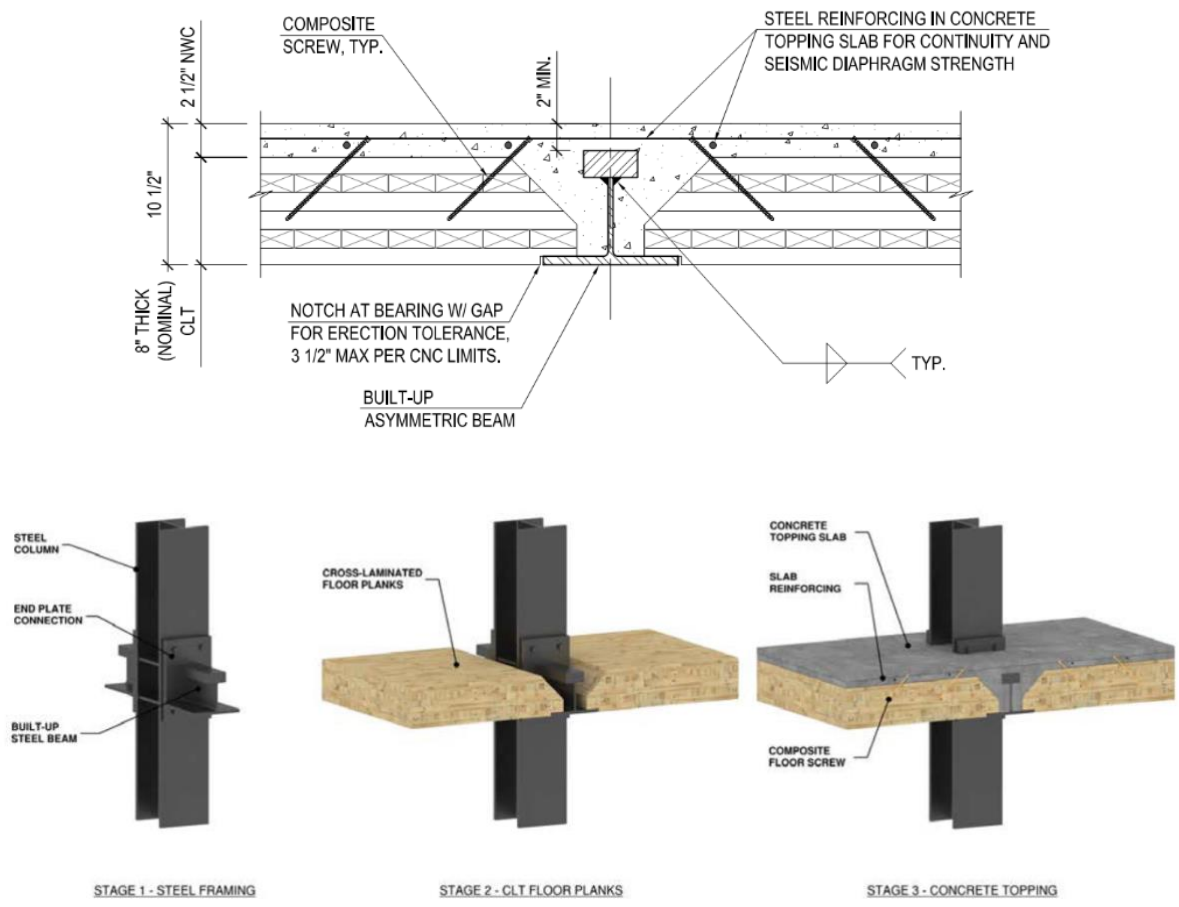

Figure 2-29: STC floor system utilized by AISC

Interestingly, this study concluded that a full MT structure is only the most optimal system when GWP is weighted very heavily in decision making. Whereas, when preference is placed on cost, durability, or seismic resiliency the SCC structure was preferable. However, because the STH system was a small portion of the study, the design was not optimized fully. The steel framing and lateral system were designed for the gravity and lateral loads of concrete floor slabs, neglecting the lightweight benefits of a CLT floor system as well as added stiffness from steel framing in vibration considerations. However, the comparability of the decision analyses suggest if the steel-timber system should be researched further, it may be the most preferable option (Ahmad et al., in press).

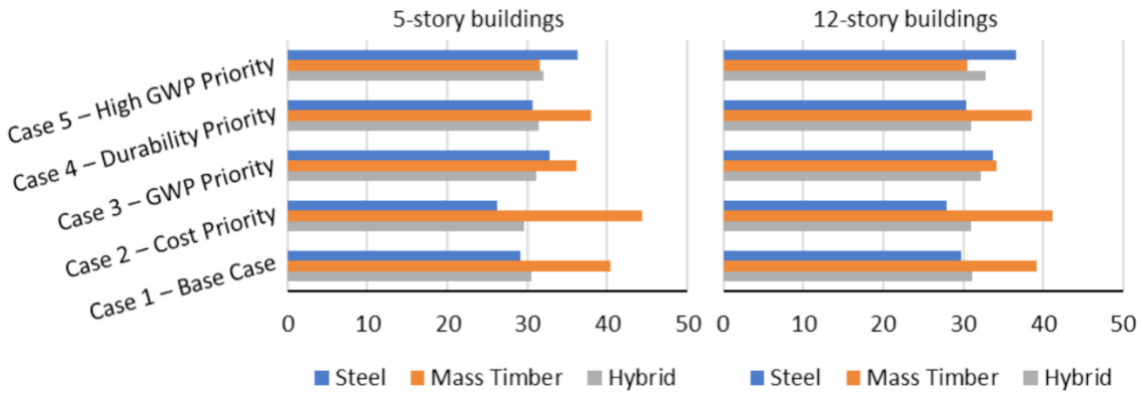

Figure 2-30: Decision analysis results of the structures compared by Ahmad et al. (in press) Low score is preferred.

Decision Maker (DM) Case	GWP Emissions	Seismic Resiliency	Durability/ Maintenance	Construction Cost
1: Base Case	20%	20%	20%	40%
2: Cost/Durability priority	10%	10%	20%	60%
3: Sustainability priority	50%	5%	20%	25%
4: Resiliency/Durability priority	15%	30%	30%	25%
5: High Sustainability priority	70%	5%	20%	5%

Figure 2-31: Decision maker scenarios and weights utilized by Ahmad et al. (in press)

Table 2-7: Summary of included literature on steel-timber structural systems

Authors	***Chiniforush et al. (2018)***	***Barber et al. (2022)***	***AISC Steel-Timber Research (2017)***	***Ahmad, Allan, and Phillips (in press)***
Composite or Hybrid	Composite	Hybrid	Composite	Hybrid
Steel-Timber Floor System	250 mm Deep WF + 160 mm (6-ply) CLT	W27x84 + 5 ply CLT	Built Up WT5 or WT6 + 6-ply CLT + 2.5" Concrete	W16x36 or W18x46 + 5-ply CLT
Composite Components	WF + CLT	N/A	WT + Concrete CLT + Concrete	N/A
Composite Connection	Unspecified	N/A	Steel and Concrete: Cast in Place Timber and Concrete: Screw	N/A
Non-Structural Floor Topping	74.5 mm Glass Wools + 10 mm Plywood	1" acoustic mat + 2" Normal Weight Concrete	None	50 mm Light Weight Concrete
Reported Vibration Analysis	Met General Serviceability Criteria	Unspecified	Determined Acceptable	Unspecified
STC Lateral System	Steel Moment Frame + CLT or RC Shear Walls	Not Considered	Steel Eccentrically Braced Frame	Steel Buckling Restrained Braced Frames
Building Specs	5, 10, and 15 Stories Office Use	Horizontal Structure of a Typical Interior Bay	8 Story Residential	5 Story Office 12 Story Residential
LCA Boundary	Cradle to Grave	Cradle to Grave	No LCA Conducted	Cradle to Gate + End of Life
Biogenic Carbon Sequestration	Not Considered	Both Included and Exlcuded	N/A	Not Considered
LCI Database	Inventory of Carbon and Energy (ICE)	EPDs, Athena, and GaBi; via Athena and Tally	N/A	EPDs and Athena; via Athena
End of Life Assumptions	Steel: 100% Recycled Concrete: 77 - 80% Recycled; 20- 23% landfilled CLT: 80% recycled 20% landfilled	Unspecified, likely Athena and Tally generic assumptions	N/A	Steel: 98% Recycling 2% Not Specified Concrete: Not Specified CLT: Not Specified
Compared Systems	RC, SCC, and STC	PT Slab, SCC, and STC	RC and STC	SCC, MT, and STH
Notes	Valipour et al. published accompanying papers on this STC system	--	Atypical composite floor system, utilizing WTs	Merely an approximation for STC design; Ref. Allan and Phillips (2021)

2.6 Vibration Analysis of Steel-Timber Floor Systems

2.6.1 Current Knowledge of Steel-Timber Vibration

STC floor systems are lightweight and relatively stiff, creating a susceptibility to undesirable vibration under service load conditions. Lightweight and long-span systems (such as steel-concrete, steel-timber, and full mass timber systems) in general, are susceptible to vibrations within ranges of human sensitivity, which require vibration analyses. Performance in vibration serviceability often controls member sizing and material selection (Breneman and Zimmerman 2021). Consequently, the low mass and damping ratio in timber slabs necessitate careful assessment for serviceability vibrations in preliminary design stages of STC floor systems (Chiniforush et al. 2017; Hassanieh et al. 2019).

Investigations of STC vibration behavior have been carried out by a team of researchers in Australia. Vibration performance was assessed with respect to available guidelines and provisions, as well as in physical experiments. Physical tests were conducted at typical spans for residential buildings (5.8 m clear span), in which deliberate variations of shear connector type, shear connector spacing, and orientation of CLT panels were studied. Results indicated natural frequencies near 24 Hz for beams of residential span length; significantly higher than limits (8-9 Hz) recommended by *Euro Code 5*, as well as U.S. recommendations in *AISC Design Guide 11*, and ISO 2631-2 (A. Chiniforush et al. 2019; Chiniforush et al. 2017). Additionally, STC beams with differing shear connectors showed similar vibration frequencies throughout various flexural modes. Leading to the conclusions that connector type was not a determining factor in dynamic response. Conversely, the spline connecting CLT panels was found to significantly affect the vibration response. This conclusion was drawn in recognition that analytical models

overestimated the fundamental frequencies, as they did not account for multiple panels, but a unit slab (Chiniforush et al. 2017).

2.6.2 Vibration Analysis Methods

The methodology and approach presented in *AISC Design Guide 11*, is typically referenced and followed in Steel-Timber and full mass timber floor system vibration evaluation and design (A. Chiniforush et al. 2019; Breneman and Zimmerman 2021; Hassanieh et al. 2019). Other analysis methods, utilized in academia and recommended in the U.S. Mass Timber Vibration Design Guide, include those methods detailed in the *Canadian CLT Handbook*, *AISC Design Guide 11*, the *ECCS Guideline*, *BS EN 1995-1-1*, *SCI P354*, and C*CIP-016* (Hassanieh et al. 2019; Breneman and Zimmerman 2021). Figure 2-31 details some of these methods as well as respective limitations.

Analysis Method	Design Guide	Attributes	Limitations
Empirical formula	CLT Handbook	Relationship from tested simply-supported, single-span bare CLT	Limited applicability due to extent of tested systems; no consideration of support flexibility; no consideration of different target performance levels
Simplified modal formulas	AISC Design Guide 11, SCI P354, CCIP-016	For wall- or beam-supported systems	Existing methods calibrated to steel or concrete systems and not necessarily appropriate for mass timber floors
Modal response analysis	AISC Design Guide 11, SCI P354, CCIP-016	Accommodates different damping ratios, floor mass, span or fixity conditions, and excitation/response locations	Sensitive to excitation and modeling assumptions
Time history analysis	AISC Design Guide 11, SCI P354, CCIP-016	Directly accounts for time effects (number of strides taken, etc.) and spatial effects (walking path, etc.)	Difficult to implement; high sensitivity to excitation and modeling assumptions; user judgement required to properly select walking paths and other inputs

Figure 2-32: Vibration analysis methods applicable to mass timber. As detailed in the U.S. Mass Timber Vibration Design Guide (Breneman and Zimmerman 2021)

2.6.3 AISC Design Guide 11 Approach

The crucial parameter, used to evaluate floor vibration serviceability, in *AISC Design Guide 11* is natural frequency. In general, humans are most sensitive to accelerations in structures with natural frequencies within the range of their own internal organs' natural frequencies. At these frequencies, resonance, or the build-up of the motion tends to occur, making the accelerations more bothersome or uncomfortable than those at higher or lower frequencies. Most often resonance occurs at frequencies between 4 and 8 Hz. However, acceptance of vibration by humans varies depending on what they are doing. For example, humans in an office or residence will most likely be bothered by accelerations as they approach 0.005g (0.5% gravity). However, humans in motion or amidst activity often tolerate accelerations 10-30 times greater, 0.05g - 0.15g (Murray et al. 2016).

The AISC approach does not condemn floor systems with natural frequencies between 4 and 8 Hz. Instead, the approach evaluates peak accelerations of the low-frequency floor systems as fractions of gravity and suggests limits relative to building occupancy. Table 2-8 summarizes the recommended limits.

Table 2-8: Recommended upper bounds for floor acceleration
Adapted from *AISC Design Guide 11* (Murray et al. 2016)

Occupancy	Acceleration Limit
Office, Residences, Churches, Schools, and Quiet Areas	0.05% gravity
Shopping Malls	1.5% gravity

Chapter 3: Methodology

3.1 Parameters and Materials

3.1.1 Schematic Design

In this thesis, the following two structural systems were compared in the life cycle analyses: steel-timber composite (STC) and steel-concrete composite (SCC). The SCC system was chosen as a benchmark structure—those to which the STC structure would be compared—because of its established structural codes and common use. Both of the structural systems were designed at two heights. Dimensional constraints of the buildings comply with the upper and lower bounds of the recently introduced Type IV height and area constraints in IBC 2021: Type IV-A being the upper bound, and IV-C being the lower bound.

As the majority of mass timber construction projects are multi-family use (Leafblad, Peters, and Cullen 2021), STC systems have potential to expand the mass timber market into commercial and business use projects. Thus, all buildings were designed for business use. All geometric constraints for the design of the structures (regardless of structural system) were in accordance with IBC 2021, and met requirements for Occupancy B, Type IV. This ensured designs of each structural system, and corresponding life cycle analyses, were comparable. Table 3-1 summarizes IBC 2021 provisions for Class B Type IV construction. Allowable area per floor was calculated in accordance with IBC 2021 section 506.2.

Type IV-A and IV-C were boundaries, functioning as constraints for the buildings' dimensions. A 12' – 0" story height was suggested by a panel of industry professionals and utilized in all structures. As a result, total building heights were 84 ft and 216 ft in the 7-story and 18-story structures, shown in Figure 3-1. Similarly, 30 ft by 30 ft bay sizes were chosen to maintain dimensional consistency in framing plans. Each structure has (7) – 30 ft bays in the

north and south directions. Table 3-2 and Figure 3-1 present typical layout and framing plans of the buildings.

Table 3-1: IBC 2021 limits, for class B occupancy, mass timber construction

Construction Type	**IV-A**	**IV-B**	**IV-C**	**IV-HT**
Allowable Height [ft.]	270	180	85	85
Allowable Stories	18	12	9	6
Allowable Area per Floor [ft.^{2}]	54,000	54,000	45,000	54,000

Internal optimization analyses, in conjuncture with advice from a panel of industry professionals, determined practically efficient spans of concrete and timber floor slabs of 10 ft and 15 ft, respectively, as seen in Figure 3-1. 10 ft spans resulted in optimally thick concrete slabs with 5” concrete on 2” deep metal decks that was sufficient for unshored construction, adequate vibration mitigation, and avoidance of excessive concrete material use. Furthermore, industry professionals (architect and engineer) suggested 10 ft is industry standard for beam spacing in steel-concrete floor systems. In STC floor assemblages, 5-ply CLT (6-7/8” panel thickness) provided efficient fire-resistance and behavior in service level vibrations, resulting in a floor slab with sufficient bending and shear capacity, capable of long spans between beams. Therefore, 15’–0” CLT spans resulted in optimal utilization of capacity of the materials.

Structural analysis and design of all columns and SCC floor framing was completed in ETABS. Whereas, analysis and design of the STC floor and roof systems resulted from internally developed calculations (see *3.3.1 Steel-Timber Composite Analysis and Design*). All buildings

Table 3-2: Design constraints for the two buildings in each of the three structural systems

Limiting Construction Type	IV-A	IV-C
Design Height [ft.]	216	84
Design Stories	18	7
Design Story Height	12’-0”	12’-0”
Design Area per Floor [ft.^{2}]	44,100	44,100

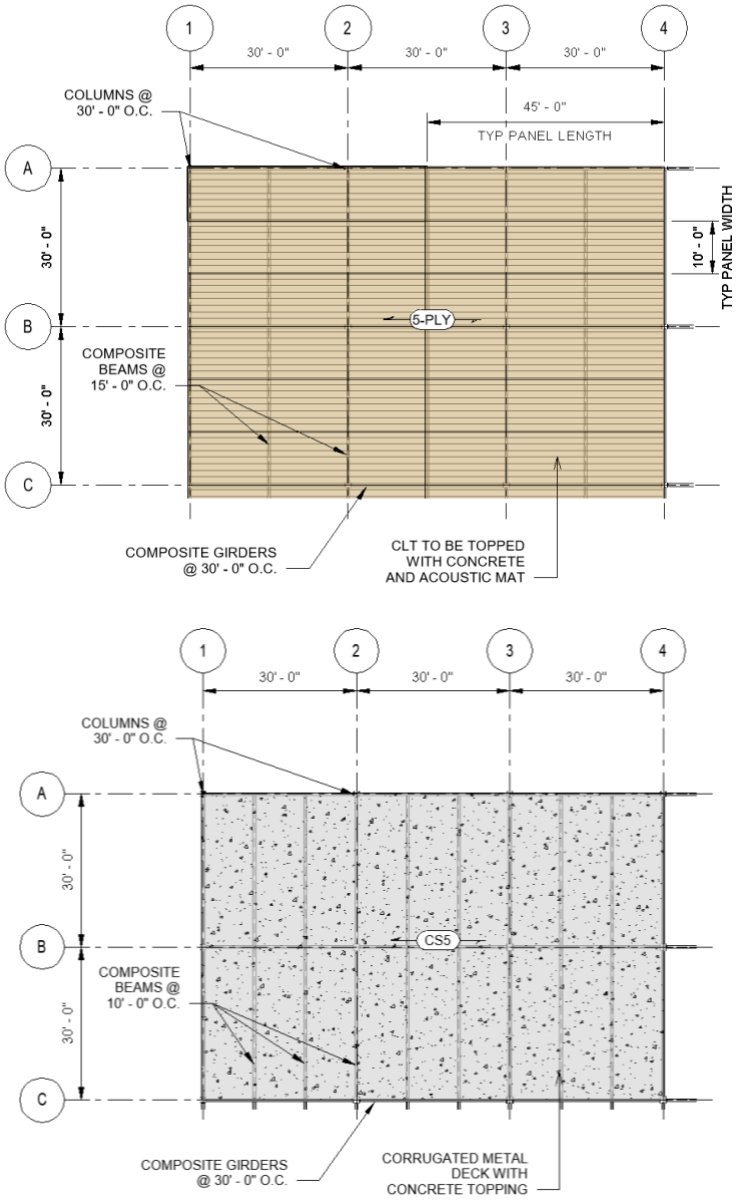

Figure 3-1: Typical SCC framing plan

were all designed in accordance with IBC 2021 and ASCE 7-16. The modeling and design processes for the structural systems are discussed, in detail, in the following sections.

3.1.2 Material Properties

The following tables (Table 3-3 and Table 3-4) display the structural materials and corresponding properties within each system. In addition to the materials reported in Table 3-3, the STC floor assemblages included rubber matting and concrete topping for acoustic transmission and vibration mitigation (Figure 3-2). These materials are not reported in Table 3-3 as they were non-structural. The unit weight of the concrete topping was taken as 145 pcf and the compressive strength as 2500 psi. Whereas, the unit weight of structural reinforced concrete was taken as 150 pcf and the compressive strength as 4000 psi.

STC is heavily impacted by the orientation of the CLT panel's major axis. Analytical models that include each individual lam's material properties are necessary for accuracy. Studies (Hassanieh et al. 2016; 2017) indicate the effective modulus of elasticity of perpendicular lams are 3-4% the modulus of elasticity of the parallel lams. As a result, the modulus of elasticity

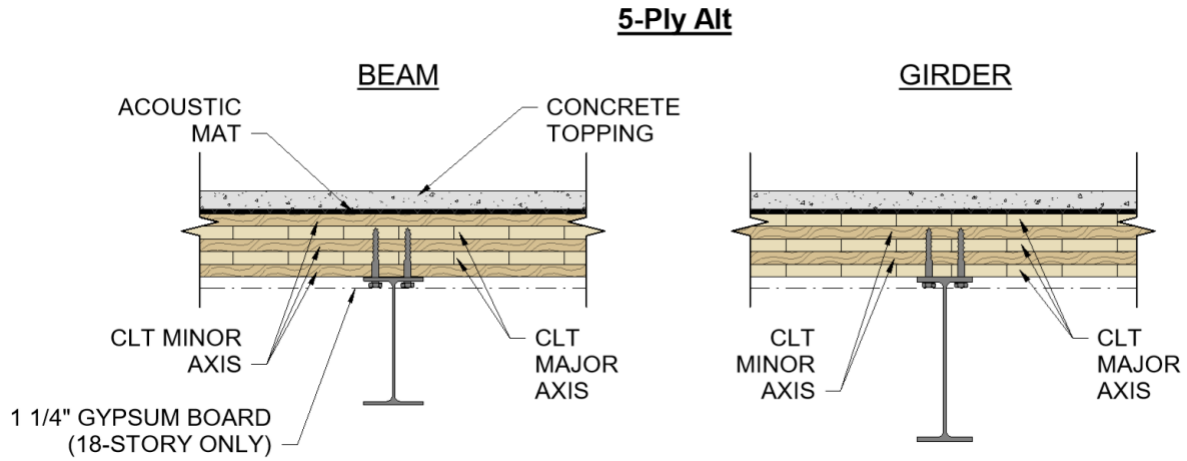

Figure 3-2: STC floor system cross sections

Table 3-3: Materials utilized in the steel-timber composite structures

Steel-Timber Composite Structures: Material Properties		
Material	**Cross Laminated Timber**	**Structural Steel**
Specifications	Southern Pine No. 2	ASTM A992 Gr. 50
$\mathbf{E_{parallel}}$	1400 ksi	29000 ksi
$\mathbf{E_{perpindicular}}$	42 ksi	--
$\mathbf{f_{c,parallel}}$	2.51 ksi	--
$\mathbf{f_{c,perpindicular}}$	0.85 ksi	--
$\mathbf{f_y}$	--	50 ksi
$\mathbf{f_u}$	--	65 ksi

Table 3-4: Materials utilized in the steel-concrete composite structures

Steel-Concrete Composite Structures: Material Properties				
Material	**Concrete**	**Reinforcement**	**Steel Deck**	**Structural Steel**
Specifications	Normal Weight Concrete	Welded Wire Reinforcement	ASTM A653 Gr. 50	ASTM A992 Gr. 50
$\mathbf{f'_c}$	4000 psi	--	--	--
$\mathbf{f_y}$	--	70 ksi	50 ksi	50 ksi
$\mathbf{f_u}$	--	--	65 ksi	65 ksi

design values for perpendicular lams in this study, are 3% of the modulus of elasticity of the parallel lams. Similarly, *NDS 2018* recommends compressive strength design values that are relative to grain orientation. Those values, adjusted in accordance with *NDS 2018 Chapter 4* are utilized in this thesis and are reported in Table 3-3 (American Wood Council 2018).

3.1.3 Fire Requirements of Structural Elements

Fire requirements for structures in the U.S. are governed by the International Building Code. Fire-resistance rating (FRR) of various elements within a structure are dependent on the occupancy, size, and presence or absence of automated sprinkler systems. For the sake of this study, all structures have the occupancy classification of Business Group B; and all are assumed to have automated sprinkler systems present.

Table 3-5 summarizes fire-resistance ratings of building elements, as defined in *IBC 2021 Table 601*. Table 3-6 summarizes dimensional constraints of various elements resulting from the respective required FRR. To maintain consistency and comparability between structures, Primary Structural Frames and various structural elements were designed for the same FRRs (in hours). Note, however, that the RC and SCC structures would not be Type IV construction, and may have potential to be designed for lower FRRs. The variance in FRR between construction types is due to the material properties corresponding to each type. Concrete is Type I construction, which has lower FRRs because the material is non-combustible. Mass Timber is Type IV construction, which has higher FRRs because the material is combustible. In practice, these structures would not require the same FRRs or corresponding constraints.

Table 3-5: Fire-resistance rating for various structural elements as required by IBC 2021 Table 601.

Limiting Construction Type	***IV-A***	***IV-C***
Structural Element	**Fire-Resistance Rating [hrs.]**	
Primary Structural Frame	3	2
Bearing Walls	3	2
Floor	2	2
Roof	1 ½	1

Table 3-6: Constraints applicable to Type IV construction

Limiting Construction Type	***IV-A***	***IV-C***	**IBC 2021 Reference**
Constraint	**Minimum**		
CLT Panel Floor Thickness	4”	4”	2304.11.3.1
Floor Noncombustible Protection	1”	--	602.4.1.3
Floor Noncombustible FR Contribution	80 min	0 min	602.4.1.2.1

3.2 Design Loads

Design loads, applicable to office occupancy, were determined by ASCE 7-16 Sections 3, 4, and C3. Floor live loads were taken as 50 psf with an additional 15 psf partition weight. Superimposed dead load represents floor finish. Roof dead and live loads are typical (*ASCE/SEI 7-16*, 2017), see Table 3-7. Self-weight of structural elements was accounted for in gravity analyses and contributed to total dead load and all live loads were reducible.

Table 3-7: Superimposed loads applied to all structures in analysis and design

Superimposed Load	**Floor**	**Roof**
Dead Load [psf]	10	20
Live Load [psf]	65	20

3.3 Structural Analysis and Design

All structural frames were composed entirely of wide-flange steel while floor systems varied between structural systems. The structures were each independently designed at two heights. The floor assemblages were designed in consideration of strength demands, deflections under service loads, airborne and impact sound transmission, vibration, and fire-resistance. All

horizontal framing members were designed under the assumption of 25% composite action as research has shown this level results in roughly 50% increases of strength and stiffness relative to ignoring composite action, and that returns diminish at higher levels of composite action (Potuzak 2023). Structural analysis and design was completed for the superstructure as a gravity frame and ignored lateral load design considerations.

Member sizing was completed via either design calculations, based on AISC/ACI/etc, or using design features of ETABS (CSi 2022). Vertical framing members in the STC and SCC systems and horizontal framing members within the SCC system were designed within ETABS. Conversely, horizontal framing members within the STC system were sized using manual design calculations because proprietary design software does not have established methods to account for the composite design of steel members with timber slabs. Established composite design modules within software, such as ETABS, currently is best suited for steel-concrete composite design. Therefore, internally developed steel-timber composite strength calculations were utilized. Example calculations for steel-timber composite member design can be found in the appendix of this document.

Floor and roof decks were included in models and calculations to supply self-weight, capture accurate floor deck geometry, and to capture composite action in horizontal members. Decking was assumed to supply continuous bracing to the top flanges of horizontal members, while bottom flanges were assumed braced at quarter points. This ensured lateral-torsional buckling would not control design of the beams and girders. All member connections were considered pinned. As moment transfer was not considered in any members, gravity design alone is reported in this document.

3.3.1 Steel-Timber Composite: Analysis and Design

Two steel-timber composite (STC) structures were analyzed and designed via manual calculations and ETABS version 20.0.1. The design parameters for the structures are detailed in *3.1.1 Schematic Design*. As previously stated, the structures were dimensionally consistent in all ways except total height. One structure had seven stories, while one had eighteen stories. Likewise, gravity loads were consistent between all structures.

STC framing was composed of 5-Ply Southern Pine CLT and steel wide flanges spaced at 15 ft. on-center. Composite action was enabled by assuming that self-tapping screws connecting steel floor beams/girders and CLT panels transferred interfacial shear. The floor beams framed into composite wide-flange girders on the column lines. In addition to CLT, concrete topping contributed to acoustic transmission mitigation and vibration damping. The concrete topping was considered as part of the dead load in the analyses but did not contribute strength or stiffness to the system.

One unique aspect of CLT panels, in comparison to concrete decks, is dependency on outer ply orientation. This is due to the orthotropic nature of timber as a structural material. CLT panels possess more desirable structural properties (flexural strength, stiffness) when outer plies are oriented with wood fibers parallel to the span direction (strong axis). The strong axis for the CLT panels were oriented perpendicular to the steel beam, resulting strong axis spanning between these elements. Therefore, this orientation resulted in the CLT panel strong axis to be perpendicular to floor beams, and parallel to girders.

This is consequential because laboratory testing of timber products has indicated a significantly lower structural material properties in perpendicular oriented laminations, relative to parallel laminations (see *3.1.2 Material Properties*). As a result, steel-timber composite

members generally have improved performance when the majority of CLT laminations are oriented parallel with the beam span (Figure 3-3). In this study, it was necessary to orient the strong axis of the CLT floor panel perpendicular to the beam to efficiently span between supports. As a result, the CLT strong axis was parallel with girders which generally resulted in greater improvements of stiffness and strength relative to non-composite sections.

For instance, laboratory testing has shown lower modulus of elasticity in perpendicular oriented laminations (E_{perp}). These laminations have a modulus of elasticity as low as 3-4% that of the parallel laminations (E_{para}), (Bodig and Jayne, 1982; Christovasilis et al., 2016; Hassanieh et al., 2016, 2017). As a result, modular ratios, n, of CLT laminations vary respective to orientation and influence composite section parameters such as transformed section properties and stiffness (Figure 3-4). Similar to modulus of elasticity, compressive strength, f_c, varies between perpendicular and parallel laminations which influences flange compressive force capacity. Therefore, CLT panel orientation influences both strength and serviceability calculations in STC design. Equations 3.3.1—3.3.4 are exemplary of transformed flange width calculations relative to beams in this study.

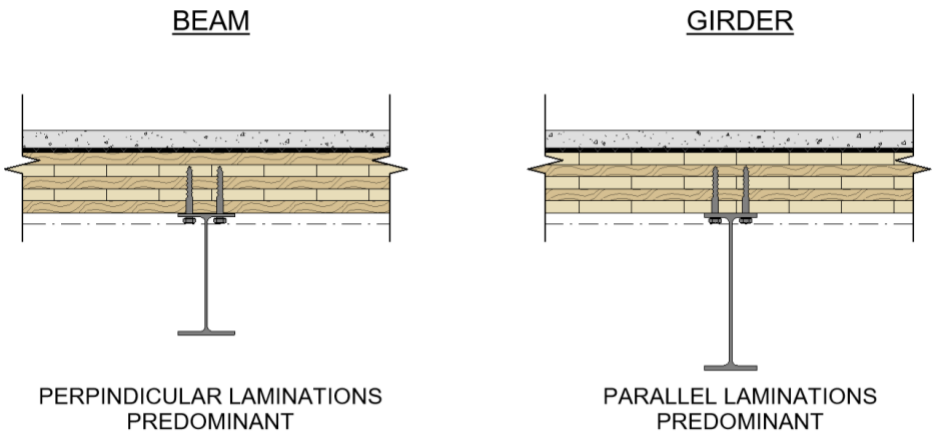

Figure 3-3: CLT panel orientation

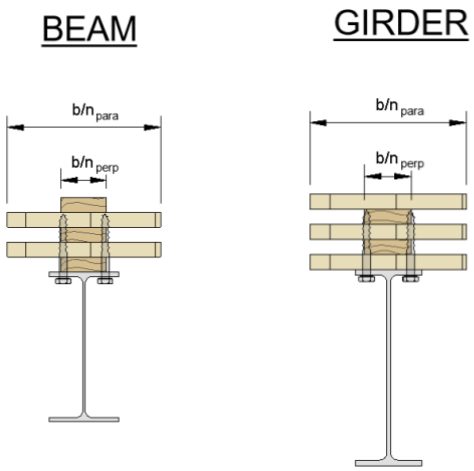

Figure 3-4: Flange widths of clt laminations relative to transformed section analysis (not to scale)

Parallel Lamination Transformed Properties

$$n_{para} = \frac{E_{steel}}{E_{para}} = \frac{29000\ ksi}{1400\ ksi} = 20.7 \qquad \textit{(Equation 3.3.1)}$$

$$b_{transf,para} = \frac{b_{eff}}{n_{para}} = \frac{144\ in}{20.7} = 6.95\ in \qquad \textit{(Equation 3.3.2)}$$

Perpendicular Lamination Transformed Properties

$$n_{perp} = \frac{E_{steel}}{E_{perp}} = \frac{29000\ ksi}{42\ ksi} = 390 \qquad \textit{(Equation 3.3.3)}$$

$$b_{transf,perp} = \frac{b_{eff}}{n_{perp}} = \frac{144\ in}{390} = 0.21\ in \qquad \textit{(Equation 3.3.4)}$$

Design calculations of steel-timber composite members were internally developed due to lack of guidance design procedure for the system. A method consistent with steel-concrete composite design was utilized (Segui 2018). Therefore, the flexural capacity of a STC member was resultant of the internal resisting force couple and the force couple moment arm. The compressive capacity of the CLT was a summation of the compressive strength of each

lamination. As previously stated, lamination compressive strength is dependent on orientation to the beam span and varied with panel orientation. Because the STC members were designed to 25% composite action the depth of the compression block corresponded to 0.25 the compressive force. Tension in the CLT was ignored in this thesis; therefore, tension capacity was resultant of the tensile capacity of the steel WF alone.

Equations 3.3.5—3.3.8 reflect the method utilized to determine the nominal capacity of a STC member. A comprehensive design example can be found in the appendix of this thesis. In summary, steel-timber composite section capacity is a function of steel yield strength, steel area, steel depth, the area of steel in compression, the depth of the compression block, and the geometry of the CLT in the compression block. An effort to understand screw shear capacity and behavior in full-scale flexural members is being conducted in parallel with this research (Merryday et al. 2023); because it is still undergoing experimental and numerical study, design specifications of shear connections were largely ignored in this thesis.

$$C = T = min\begin{cases} A_s F_y \\ \sum f_{c,lam} A_{lam} \end{cases} \quad \textit{(Equation 3.3.5)}$$

$$\Sigma Q_n = 0.25C \quad \textit{(Equation 3.3.6)}$$

$$A_{sc} = \frac{F_y A_s - \Sigma Q_n}{2F_y} \quad \textit{(Equation 3.3.7)}$$

$$M_n = \left(F_y A_s \frac{d_s}{2}\right) - \left(2A_{sc} F_y \overline{y}\right) + \sum_{i=0}^{n} a_i b_{eff,i} f_{c,i} (d_{CLT} - y_i) \quad \textit{(Equation 3.3.8)}$$

C = compressive capacity of flange (kips)

T = tensile capacity of the steel section (kips)

A_s = area of steel (in^2)

F_y = yield strength of steel (ksi)

$F_{c,lam}$ = compressive strength of the CLT lamination, relative to orientation (ksi)

A_{lam} = area of wood in lamination (in^2)

ΣQ_n = partial composite compressive force (25%) (kips)

A_{sc} = area of steel required to balance partial composite compression block (in^2)

d_s = depth of steel cross section (in)

y = neutral axis of the partial composite section (in)

a_i = depth of lamination *i* (in)

$b_{eff,i}$ = effective flange width of lamination *i* (in)

$f_{c,i}$ = compressive strength of lamination *i* (ksi)

d_{CLT} = total depth of the CLT panel (in)

y_i = neutral axis of lamination *i* (in)

3.3.2 Steel-Concrete Composite: Analysis and Design

Two steel-concrete composite (SCC) structures were analyzed and designed in ETABS version 20.0.1. The design parameters for the structures are detailed in *3.1.1 Schematic Design*.

All SCC structures were designed with composite floor systems. The floor assemblage consisted of a metal deck with concrete topping. Steel wide-flanges spaced at 10 ft on-center supported the floor deck. The floor beams framed into composite wide-flange girders on the column lines.

The web-based *Vulcraft Composite Deck Slab Strength* design tool (Vulcraft 2022) was utilized to select deck depth, gauge, and concrete thickness. Shoring was not considered in design; thus, unshored span length controlled steel deck thickness. Concrete slabs were assumed to have 6x6 – W1.4xW1.4 welded wire reinforcement as it was sufficient for minimum

reinforcement temperature and shrinkage steel (*ACI 318-19*, 2020; *SDI-C 2017*, 2017). Concrete topping thickness was optimized to mitigate excessive material use, while ensuring unshored construction and adequate vibration performance in the floor assembly. Independent designs were completed for the floor decks and the roof deck.

3.3.3 Deflection and Vibration Considerations

Structural member design may be controlled by deflection or vibration limits rather than strength capacities. As a result, *ASCE 7-16* provides guidance to structural engineers on appropriate limitations of structures in these categories. All STC and SCC structures were designed in accordance with these guidelines. Table 3-8 summarizes the deflection and vibrations limitations imposed on all structures in this study.

Table 3-8: Deflection and vibration limits

Reference Document	**Consideration**	**ASCE 7 Load Combination**	**Element in Consideration**	**Limit**
ASCE 7-16	Superimposed Load Deflection	$D_{super} + L$	Horizontal Members	L/240
ASCE 7-16	Live Load Deflection	1.0L	Horizontal Members	L/360
ASCE 7-16	Superimposed Load Deflection	$D_{super} + L$	Floor Slabs	L/360
SDI-CD/NC	Unshored Deflection	$D_{self} + C$	Metal Floor Decking	L/90
AISC DG 11	Vibration due to Walking Excitation	N/A	Steel-Concrete Floor Systems	$a_p/g \leq 0.005$
U.S. Mass Timber Floor Vibration Design Guide	Vibration due to Walking Excitation	N/A	Steel-Timber Floor Systems	$a_p/g \leq 0.005$

Vibration was considered in both structural systems and was assumed to be due to human walking excitation in an office outfitted with electronic systems. Floor system vibration limits, demands, and capacity were guided by *AISC Design Guide 11*, for SCC, and the *U.S. Mass Timber Floor Vibration Design Guide* (Murray et al. 2016; Breneman and Zimmerman 2021).

3.4 Vibrations of Steel-Timber Structural Systems

3.4.1 Vibration Evaluation of Steel-Timber Floor Systems

Vibrations due to walking excitation were evaluated by the guidelines published in *AISC Design Guide 11: Vibrations of Steel-Framed Structural Systems (DG11)* as recommended by the *U.S. Mass Timber Floor Vibration Design Guide* (Murray et al. 2016; Breneman and Zimmerman 2021). *DG11* recommends floor systems with natural frequencies less than 9 Hz (low-frequency floors) be evaluated for human comfort as resonance in the human's core is likely to occur between 3 and 8 Hz. As a result, acceleration limits of low-frequency floors in an office building are to be 0.005g to avoid resonance and discomfort to building occupants.

Unlike strength or deflection analysis, vibration analysis is a holistic assessment of the floor assembly. It takes into account expected superimposed loads as well as all structural elements including the slab, beam, and girder. Separate analysis of beam and girder properties are required prior to combined properties. The combined analysis then provides evaluation of all floor elements as one system. Particulars of floor geometry must be precise in preliminary deck geometry calculations, transformed section properties, and effective floor panel weight calculations. As a result, manual vibration assessments are detail intensive and the majority of calculations are not provided in the main body of this thesis, but rather in an example in the appendix.

Also unlike strength or deflection analysis, the steel-timber composite section was assumed 100% composite in vibration assessment. This is used based on AISC DG11, which recommends 6-8 psf service level live loads (for electronic outfit offices) and 4 psf dead load (Murray et al. 2016). At this levels of loading, minimal slip will occur between the steel member and floor deck, allowing the member to behave as a full composite member may, regardless of shear transfer capacity of the connections (Murray et al. 2016).

Peak floor acceleration was evaluated by Equation 3.4.1. Floor system acceleration is related to natural frequency, damping, and the floor system weight. The natural frequency of the system is a function of both the beam and girder deflection (Δ_b, Δ'_g) as shown in Equation 3.4.2. The vibration performance of a floor system can generally be improved by increasing the system's stiffness, mass, or damping ratio. Stiffness and mass may be enlarged by deepening steel framing sections, deepening the CLT, or applying weight with topping. The damping ratio is the sum of component damping values recommended in *AISC DG11*. This study assumed a damping coefficient (β) of 0.03, assuming contribution from the structural system, ductwork, electronic office fit-out, and minor partitions in bay.

$$\frac{a_p}{g} = \frac{P_0 e^{-0.35 f_n}}{\beta W} \leq 0.005 \qquad \textit{(Equation 3.4.1)}$$

$$f_n = 0.18 \sqrt{\frac{g}{\Delta_b + \Delta'_g}} \qquad \textit{(Equation 3.4.2)}$$

a_p/g= peak floor acceleration ratio

g = gravity (in/s^2)

P_0 = amplitude of the driving force, 65 lb

f_n = fundamental natural frequency of the floor assemblage (Hz)

β = damping ratio

W = effective effective panel weight (lbs)

Δ_b = beam deflection under vibration service loads (in)

Δ'_g = reduced girder deflection under vibration service loads (in)

Table 3-9: Total floor system loads in vibration studies. Adapted from *AISC DG11 (Murray et al. 2016)*

Component	Damping Ratio, β_i
Structural System	0.01
Ceiling and Ductwork	0.01
Electronic Office Fit-Out	0.005
Paper Office Fit-Out	0.01
Churches, Schools, and Malls	0.0
Full-Height Dry Wall Partitions in Bay	0.02-0.05

3.4.2 Considerations for Timber Panel Floor Slabs in Vibration Assessment

The *AISC DG11* approach was developed for steel-concrete floor systems. When utilizing this method for timber, the approach is similar to the original, however additional refinement for composite beam properties necessary for accuracy. Specifically, accounting for the transformed area, respective to the modulus of elasticity of the parallel and perpendicular lams is crucial (see *3.3.1 Steel-Timber Composite: Analysis and Design*). Therefore, in addition to steel-timber beam transformed moment of inertia and girder transformed moment of inertia, calculations of the deck's effective moment of inertia were resultant of the timber transformed section (Figure 3-4).

3.4.3 Steel-Timber Vibration Studies

In effort to understand the performance of steel-timber composite floor systems in vibration serviceability a vibration study was performed. Beyond increasing awareness of STC vibration behaviors it aided the author in determining efficient concrete topping thickness, and ultimately the floor system assembly utilized in the LCA study of this thesis. The study focused on steel-timber beams, analyzing them at various span lengths with varying depths of concrete topping and utilized the analytical approach outlined in *Section 3.4.1*. Each instance was designed to meet vibration, strength, and deflection limits for office occupancy. Superimposed dead loads were the same as utilized in this paper, and are reported in section *3.2.1 Gravity Loads*. Vibration and strength limits are reported in Table 3-8.

The floor system was comprised of 5-Ply CLT panels (6-7/8" deep) spanning between support beams. The CLT density was assumed to be 39 pcf, simulating Southern Pine. CLT material properties were the same as utilized in this paper, and are reported in section *3.1.2 Material Properties*. The concrete topping was assumed to be unreinforced normal weight concrete, with a density of 145 pcf.

The support beams, spaced 15 ft. O.C., varied in length, and spanned to girders. The girders' span lengths were kept constant, at 30 ft. Each floor system was designed to account for the mass of the variable normal weight concrete topping depth; resulting in total dead load variances between each floor system, live load remained constant throughout the study. STC beams and girders were designed to supply the minimum required strength, stiffness (deflection adequacy), and provide floor system accelerations below 0.005g. Resulting design sections and loads of each system are reported in Table 3-10.

Figure 3-5 displays resulting natural frequencies corresponding to the topping depth and beam span length of interest. All configurations resulted in low-frequency floor systems, indicating that an acceleration limit of 0.005g was appropriate. Note that the natural frequencies decreased as concrete thickness increased however, all floor systems were still within the range of human discomfort (3-8 Hz).

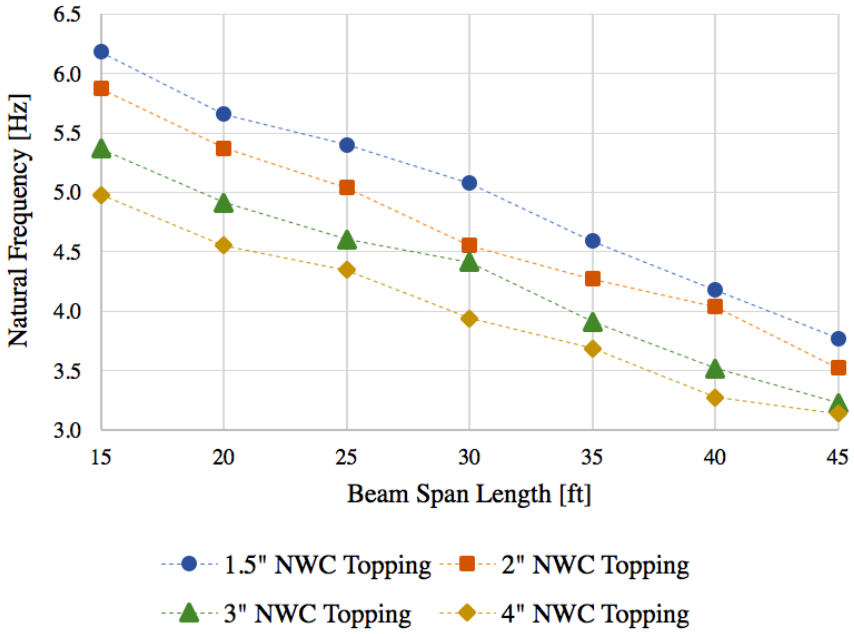

Figure 3-5: Natural frequency of 5-ply CLT floor panels with various topping depths

Table 3-10: Vibration study design sections and loads

System	STC + 1.5" NWC		STC + 2" NWC		STC + 3" NWC		STC + 4" NWC	
L_{beam} [ft]	Beam	Girder	Beam	Girder	Beam	Girder	Beam	Girder
15	W10x17	W16x36	W10x17	W16x36	W10x17	W16x36	W10x17	W16x36
20	W14x22	W18x40	W14x22	W18x40	W14x22	W18x40	W14x22	W18x40
25	W16x31	W21x48	W16x31	W21x44	W16x31	W21x44	W16x31	W21x48
30	W18x40	W24x55	W18x40	W21x50	W18x40	W24x55	W18X35	W24X55
35	W21x48	W24x55	W21X44	W24x55	W21X44	W24x55	W21X44	W24X62
40	W24x55	W24x55	W24X55	W24x62	W21x57	W24x62	W21x55	W24x68
45	W24X68	W24x62	W24X62	W24x68	W24x62	W24x68	W24x68	W24X76
DL [psf]	50		57		69		81	
LL [psf]	65		65		65		65	

Table 3-11: Vibration utilization of stc floor assemblages with varying topping depths

L_{beam} [ft]	1.5" NWC	2" NWC	3" NWC	4" NWC
15	0.95	0.96	0.96	0.95
20	0.98	0.98	0.97	0.95
25	0.98	0.99	0.96	0.93
30	0.98	1.00	0.94	0.97
35	0.98	1.00	0.95	0.90
40	0.97	0.93	0.94	0.89
45	0.97	0.97	0.90	0.81

When studying Table 3-10, one may observe that despite varying concrete depths, the adequate steel section designs of the same span length decreased in cross sectional size only mildly (0 to 14 lbs/ft) as concrete topping thickness increased. Furthermore, through observation of controlling utilization factors (demand divided by capacity for strength and deflection, observed acceleration divided by allowable acceleration for vibration) at various span lengths (Figure 3-6), it becomes clear that vibration is the controlling parameter in design of all floor beams until reaching spans above 35 ft. with 3-4" of concrete topping. Conversely, girders

overcome vibration control regardless of topping depth as the bearing beam length increases beyond 35-40 ft.

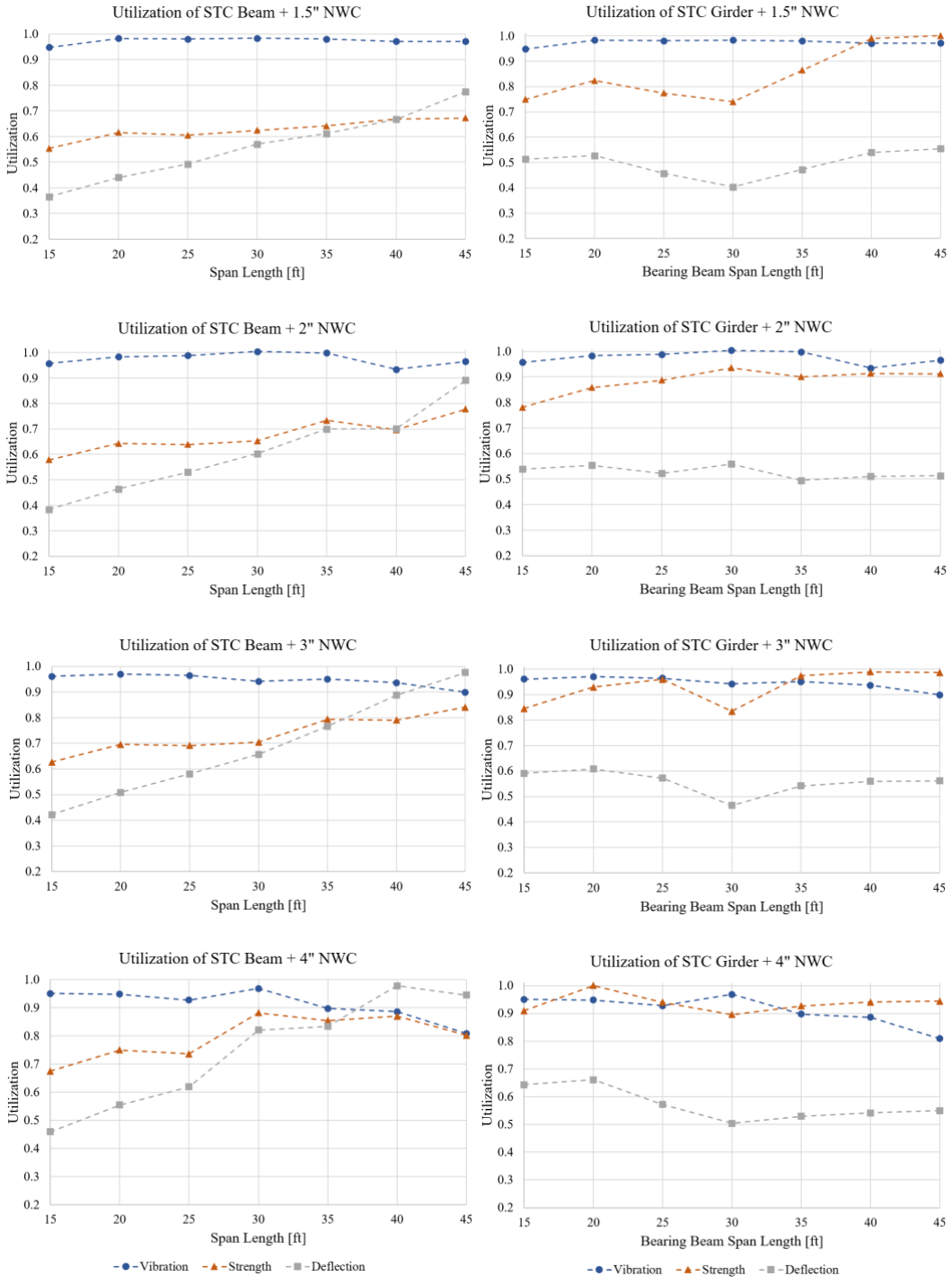

Figure 3-6: Utilization of STC design parameters in systems with varying topping depths

Results indicated the steel framing contributed more substantially to stiffness and vibration mitigation than the additional concrete topping. This was apparent as systems were not often able to decrease cross-sectional steel sizes even as concrete depth increased and additionally, vibration utilizations only slightly decreased in designs that were vibration controlled. To further understand the impact of framing, the system with 1.5" NWC topping was assessed with various beam design sections (Table 3-12). Design 1 was taken to be the minimum required beam section reported in table 3-10. Design 2 increased the beam cross-section by one member size, generally leading to a member of the same depth with a larger cross-sectional area. As a result, Design 2 cross sections are 2-8 plf heavier and decreased in vibration utilization by 2-9% relative to Design 1. Design 3 increased the beam by one more member size, generally resulting in an increase of both depth and cross-sectional area. As a result, Design 3 cross sections are 0-3 in. deeper, 2-16 plf heavier, and decreased vibration utilization by 9-19% relative to Design 1. In light of the recognition that steel framing contributes more substantially than concrete topping to vibration mitigation, STC with 1.5" of normal weight concrete topping was utilized in the study described in this thesis to mitigate inefficient concrete material use.

Table 3-12: Vibration utilization of various STC beam sections with 1.5” NWC topping

L_{beam} [ft]	Design 1	Design 2	Design 3
15	0.95	0.89	0.77
	W10x17	W10x19	W12x19
20	0.98	0.89	0.79
	W14x22	W14x26	W16x26
25	0.98	0.90	0.83
	W16x31	W16x36	W18x35
30	0.98	0.91	0.81
	W18x40	W18x46	W21x44
35	0.98	0.96	0.82
	W21x48	W21x50	W24x55
40	0.97	0.92	0.88
	W24x55	W24x62	W24x68
45	0.97	0.93	0.82
	W24x68	W24x76	W27x84

3.4.4 Steel-Timber Utilization Studies

In recognition of relatively low strength and deflection utilization ratios of STC members due to vibration controlled design, the need to justify composite action was identified. In effort to understand the benefits of a STC system, composite members were juxtaposed with the same steel cross section in a non-composite design scenario (steel-timber hybrid). The purpose was to compare the strength and deflection utilization ratios of underutilized composite members with the utilization ratios of non-composite members.

The study utilized the WF design sections of the vibration study as they were adequate in composite strength, composite deflection, and vibration. Identical to the vibration studies, beam span lengths varied from 15-45 ft. while girder span lengths remained constant at 30 ft. Applied loads and concrete topping depths were consistent with vibration studies as well. Steel design sections, topping depths, and floor system loads are reported in Table 3-10.

The steel cross sections were checked in an identical design scenario (loads, span length, topping depth etc.) for non-composite strength and deflection adequacy. Vibration utilization of non-composite members was not a concern as *AISC DG11* recommends utilizing transformed moment of inertia (as if 100% composite) in vibration assessments if a floor deck is attached to a framing member regardless of the presence of shear connectors *(Murray et al. 2016)*. Therefore, as member sizes were originally designed to provide peak floor accelerations within recommended limits, the vibration utilizations remained constant between composite and non-composite design scenarios.

Results of the study showed non-composite girders at all span lengths and applied loads were inadequate (Figure 3-7). Non-composite beams were generally inadequate, with the exception of spans shorter than 25-30 ft. in systems with loads of lesser magnitudes. As such, composite design was shown to have substantial benefits as the design sections would have majorly been impossible in a non-composite design scenario. Therefore, steel-timber composite design was shown to reduce steel material usage despite vibration controlled design.

Detailed results of composite and non-composite utilization ratios pertaining to the buildings of the LCA in this thesis are reported in Chapter 4. This study lead to the conclusion that STC is efficient and advantageous to steel-timber hybrid design in the design scenario of this study. Furthermore, the results of this study indicate STC systems are particularly efficient for long span members, heavy load scenarios, or the combination of the two.

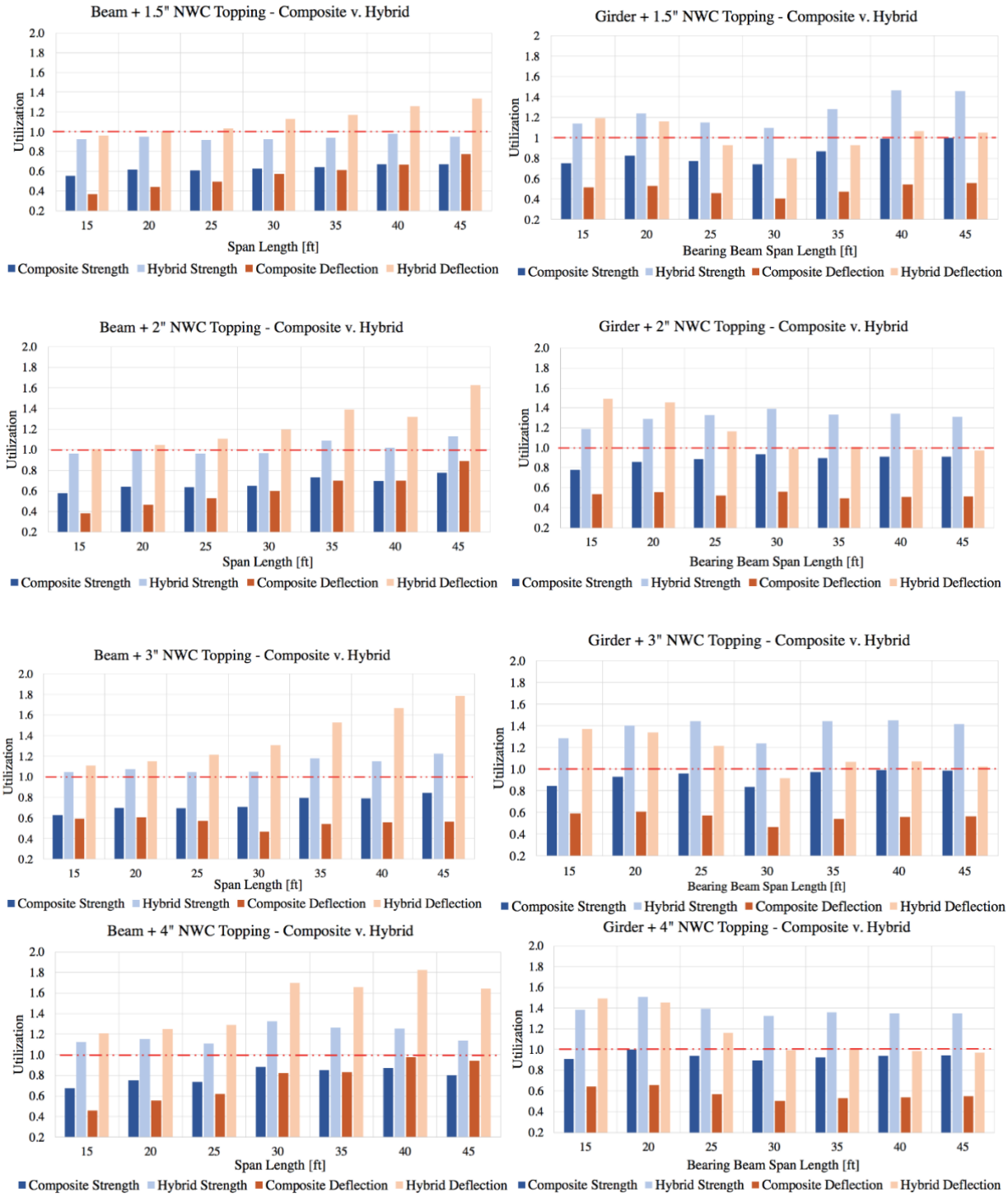

Figure 3-7: Steel-timber composite and non-composite utilization ratios
Note that a member is insufficient if either strength or deflection is above 1.0 utilization.

3.5 Life Cycle Assessment

The comparative WBLCA was performed for the portfolio of buildings using the commercial software Tally (KT Innovations 2022). There are many different available software for performing WBLCA, but Tally was chosen because (1) it is integrated within Revit, which in turn is able to import ETABS structural models to automatically perform material volume calculations; and (2) it is has experienced widespread use in the academic literature on WBLCA (refs). The following sections describe the specifics of the WBLCA, including the system boundaries, choice of functional units, selection of life cycle inventory, and major assumptions.

3.5.2 System Boundary

The comparative analysis was constrained by the boundary displayed in Figure 3-8. Embodied energy and carbon were the focus. The boundary was cradle-to-gate (A1-A3), including construction transportation (A4), end-of-life impacts (C2-C4, D). All structural elements were subjected to analyses across these stages. The building life expectancy was 60 years for all structures. Biogenic carbon, in CLT, was accounted for in modules A1-A3.

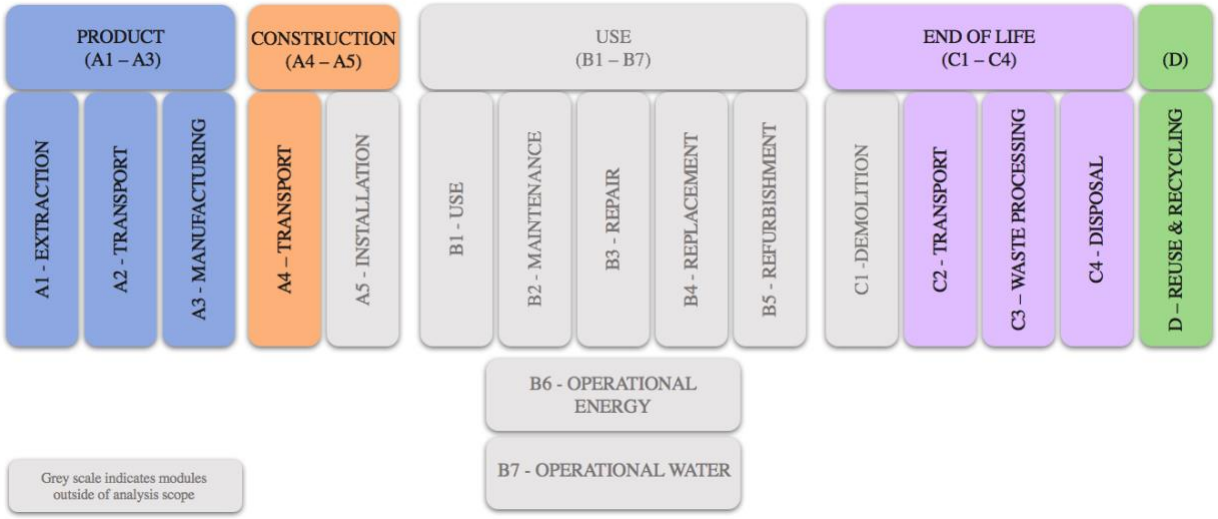

Figure 3-8: System boundary of life cycle analysis

Modules B1-B7 account for operational energy and emissions, which fall outside of the scope of embodied environmental impacts. Therefore, all the energy required to use the building and associated emissions were not accounted for in the assessment. Similarly, on-site construction environmental impacts were not considered (A5 and C1) due to the complexities of estimating the environmental impacts associated with construction equipment and processes.

3.5.3 Outputs and Functional Units

Mass, embodied carbon, and embodied energy are reported in the units of Table 3-13. Total values are reported, as well as normalized values, to aid in quantitative comparison between structures of varying scopes. All normalized values are divided by net floor area or respective material mass; the 7 and 18 story structures were 28,679 m^2 (308,700 ft^2) and 73,746 m^2 (793,800 ft^2), respectively.

Table 3-13: Functional units of the life cycle analysis

Parameter	**Raw Unit**	**Normalized Unit**	
Mass	kg	kg / m^2	--
Embodied Carbon	kg CO^2-eq	kg CO^2-eq / m^2	kg CO^2-eq / kg
Primary Energy Demand	MJ	MJ / m^2	MJ / kg

3.5.4 Life Cycle Inventory

Life Cycle Inventory (LCI) is the compilation of inputs and outputs for the buildings in analysis. This study utilized Revit's innate features to determine total material quantities, or quantity take off. This required a detailed Building Information Model, with all elements accurately represented in size, location, and material properties. Once modeled, elements were

paired with LCI materials defined within the Revit add-in *Tally*. Table 3-14 details environmental data sources, assumptions, and life cycle scenarios of the analyses. The software draws from the commercial LCI database GaBi 8.5 (2018) and EPDs for LCI. Despite a robust internal database of Tally, preliminary analyses determined generic CLT environmental impacts to be unrepresentative of current CLT manufacturing practices in the United States. Similarly, the database lacked a rubber material analogous to an acoustic mat.

In certain instances, Tally may allow the user to add product specific environmental data (EPDs) via technical support from the developer. However, the current version does not support manual database additions. As a result, further refinement of the models was required to obtain outputs reflective of appropriate EPDs. This was achieved by applying adjustment factors to material volumes during LCI to result in appropriate unit production environmental impacts. In effect, the generic CLT and acoustic mat material environmental impacts were scaled to match the appropriate data published in EPDs, creating a pseudo material in the model. Examples of the adjustment process for the CLT and acoustic mat materials are reported in the appendix of this thesis. The utilized EPDs reflected in the production stage data only (stages A1-A3). Accordingly, environmental impacts of the remaining life stages were products of the assumptions made for transportation, end-of-life processing, and post-life re-use or recycling. Therefore, end-of-life (Module C) and Module D environmental data was not modified and includes the original database life stage scenarios.

3.5.5 Assumptions in Analysis

Assumptions are necessary in LCA. However, analysis tools, such as *Tally*, enable the user to avoid inputting most assumptions. Instead, the software is framed with data from national

or global averages. Assumptions are influential in LCI; utilizing a software provides assumptions that are consistent, where applicable, throughout various LCA models.

Assumptions in this study, applied by Tally, encompassed transportation distances, end-of-life scope, and module D scope. Table 3-14 reports all assumptions. The author assumed all individual elements to have life spans greater than, or equal to, the building service life. This applied the assumption of no component maintenance, repair, or replacement in the LCA. Beyond these assumptions, Tally assumes hot-rolled steel and steel decks are fabricated with 100% and 28% scrap material, respectively. This is accounted for by applying a "credit" in module D, as opposed to the product stage.

Results of this study present environmental impacts and mass of structural assemblages as a one unit. As a result, the LCA outputs of hot-rolled steel framing and its associated cementitious fireproofing are presented under one label: *Framing*. Similarly, the concrete associated with SCC structures is an assemblage of 4000 psi concrete and minimum steel reinforcing.

Table 3-14: Life cycle inventory of the analyses

Element	LCI Materials	LCI Source	Trucking Distance	End-of-Life Scope	Module D Scope
Cross-Laminated Timber	Proxied by Glulam	- Glulam CORRIM (2011) - *SmartLam, Dothan: Cross Laminated Timber (2021)*	332 km	- 14.5% Recovered - 22% Incinerated with Energy Recovery - 63.5% Landfilled	Avoided burden for recovered wood products
Acoustic Mat	SBS Rubber Tile	- EU-28: Rubber Flooring Profiled (2017) - *U.S. Rubber: QuietSound Acoustical Underlayment (2019)*	805 km	- 17.5% Recovered - 82.5% Landfilled	Avoided burden for recovered material, includes grinding energy
Type X Gypsum Wall Board	- Gypsum - Boric Acid - Cement - Sodium Lignin Sulfonate - Glass Fiber - Silane - Polyglucose - Perlite - Paper - Casein Glue	Gypsum Plaster Board (Fire Protection) (2017)	172 km	100 % Landfilled	None
W-Shape Steel	Hot Rolled Structural Steel	American Institute of Steel Construction: Hot Rolled Steel (2010)*	431 km	- 98% Recovered - 2% Landfilled	Burden reflects landfilled material only
Steel Deck	Coated Steel Panels, 1 ½ - 3" Deep, 22 - 16 Ga.	Steel Deck Institute: Steel Deck**	431 km	- 98% Recovered - 2% Landfilled	Avoided burden for 72% of material
Steel Reinforcing	Steel Reinforcing; cut, bent, or modified by the design professional	Concrete Reinforcing Steel Institute: Fabricated Steel Reinforcement (2017)	431 km	- 70% Recovered - 30% Landfill	Burden reflects landfilled material only
Concrete Topping	- 43% Coarse Aggregate - 37% Sand - 9% Portland Cement - 8% Water - 2% Fly Ash - <1% Slag - <1% Admix.	- PCA (2014) - Pumice Gravel (2017) - Gravel (2017) - Fly Ash (2017) - Slag-tap granulate (2017) - Expanded Clay (2017) - Calcium Nitrate (2017) -Sodium Ligninsulfonate (2017) …	24 km	- 55% Recycled into Coarse Aggregate - 45% Landfilled	Avoided burden for coarse aggregate; includes grinding energy
Reinforced Concrete	- 41% Coarse Aggregate - 36% Sand - 12% Portland Cement - 8% Water - 2% Fly Ash - 1% Slag - <1% Admix.	- PCA (2014) - Pumice Gravel (2017) - Gravel (2017) - Fly Ash (2017) - Slag-tap granulate (2017) - Expanded Clay (2017) - Calcium Nitrate (2017) -Sodium Ligninsulfonate (2017) …	24 km	- 55% Recycled into Coarse Aggregate - 45% Landfilled	Avoided burden for coarse aggregate; includes grinding energy
Cementitious Fireproofing	- 65% Cement - 15% Vermiculite - 10% MICA - 10% Calcium Carbonate	- PCA (2014) - Vermiculite (2017) - Silica Sand (2017) - Limestone Flour (2017) -Electricity Grid Mix (2014)	172 km	100% Landfilled	None

*EPD Expired 3/31/2021
**EPD Expired 12/15/2020
Notes:
1. Environmental data reports component impacts. The framing component accountings for hot-rolled steel and associated cementitious fireproofing. Similarly, the reinforced concrete component accounts for plain concrete and associated steel reinforcing.
2. Italicized *LCI Source* bullets are the EPDs utilized to verify and adjust database environmental impacts.

3.6 Life Cycle Inventory Data

3.6.1 Material Environmental Impacts

The environmental impacts associated with structural components are reported in Figure 3-9 and Table 3-15. These values are reflective of the LCAs reported in Chapter 4 of this paper and were largely resultant of *Tally* database specifics. However, as discussed in section *3.5.4 Life Cycle Inventory* adjustments were applied to generic CLT and rubber mat materials within Tally to more accurately reflect current environmental impacts of U.S. produced materials.

Concrete data varies slightly between structural systems as the concrete topping in STC floor assemblages was assumed to be plain 2500 psi concrete. Whereas the structural concrete in SCC floor assemblages was assumed to be reinforced 4000 psi concrete. Therefore, reinforced concrete data accounts for associated steel reinforcing as well. Similarly, hot rolled steel data and associated cementitious fireproofing are reported as one component: fireproofed steel.

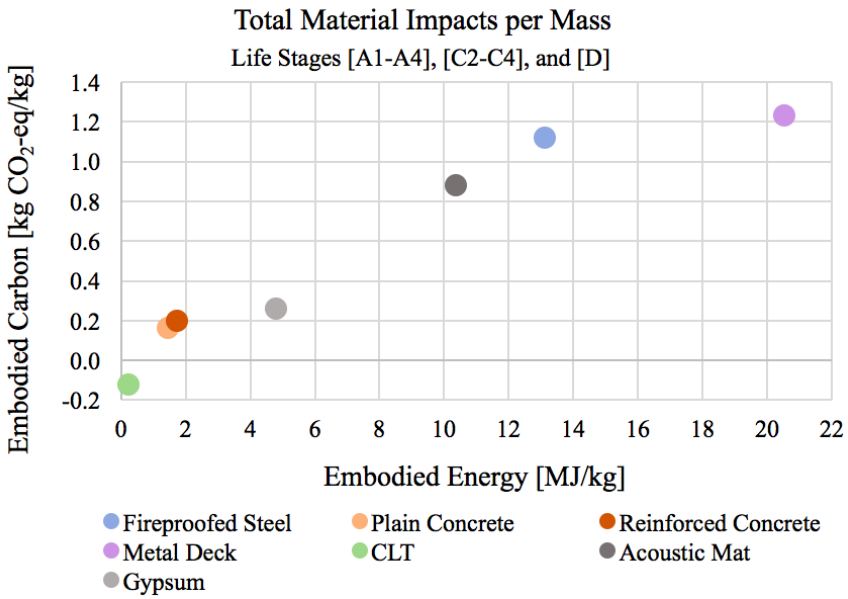

Figure 3-9: Embodied emissions and energy of materials by mass

Table 3-15: Embodied emissions and energy of materials by mass. Life Stages [A1-A4], [C2-C4], and [D]

Material	Embodied Carbon [kg CO_2-eq/kg]	Embodied Energy [MJ/kg]
CLT	-0.12	0.24
Acoustic Mat	0.88	10.4
Hot Rolled Steel and Fireproofing	1.12	13.1
Metal Deck	1.23	20.5
2500 psi Plain Concrete	0.16	1.44
4000 psi Reinforced Concrete	0.20	1.72

3.6.2 Data Validation

In effort to validate EPD and *Tally* database environmental figures with external data, material impacts utilized in this study were compared with a literature review which encompassed more than 70 relevant studies (Cabeza et al. 2021). A more detailed synopsis of the document is presented in section *2.1.4 Embodied Energy and Embodied Carbon in Structural Materials*. Plotting the environmental data utilized in this study on the tables presented by Cabeza et al. (2021) indicates the environmental data in this study was reasonable. Data comparisons are reported in Figure 3-10 and Table 3-16.

Comparable materials between studies were CLT, concrete, and steel. The materials were compared for environmental impacts resulting from material production only. The cradle to gate boundary aided in validating comparisons obtained from a broad range of studies which have potential for vast differences in building use, end of life, and post life scenarios. Potential inequalities may result from regional influence on environmental impacts as the study by Cabeza

et al. encompassed world-wide data although most predominately, the majority of reported data was resultant of project locations outside of the United States.

The embodied energy of CLT and concrete were slightly smaller than the lower bound of the literature review data. However, the variation of this study's data point is relatively low: only 0.25 MJ/kg below the lower bound of literature data. As the range of the reported data points is 6.56, it is reasonable to assume this study's data point are reasonable and not outliers. Additionally, by studying the deeper hues of the data bars, one may conclude that CLT is more likely to have data point concentrations at the lower end of the spectrum than concrete. As a result, the utilized environmental data may err in the favor of concrete, as opposed to skewing the data toward larger concrete embodied energies which is more representative of the coefficients commonly used in the literature.

The literature review source lacked CLT embodied carbon data. However, the data utilized in this study was sourced from an EPD. As EPDs are known within the industry to provide reliable and accurate environmental data (Gu, Liang, and Bergman 2020; Feng, Sadiq, and Hewage 2022), the lack of validation is not a concern. Note however, that the CLT data point plotted in Figure 3-10 is within the range of glulam data and comparable to other timber products.

Furthermore, both steel data points in this study are assumed 98% recovered for recycling of material. However, *recycled steel* as reported in the literature review appears to be tied to few sources. Whereas *general steel* appears to be associated with a larger number of sources which encompass varying proportions of recycled content, unspecified recycled content, or no recycled content. The accepted value in this study laid between the recycled steel concentration and the lower bound of general steel. As a result, the embodied impacts of fireproofed steel appear

reasonable, as it would be expected to have greater impacts than plain recycled steel. Furthermore, the same data is utilized in both the STC and SCC assessments. As a result, any error is equal between the two studies which nullifies potential inequalities in comparison.

Table 3-16: Cradle to gate embodied emissions and energy of materials by mass

Material	**Embodied Carbon [kg CO_2-eq/kg]**	**Embodied Energy [MJ/kg]**
CLT	-1.01	0.30
Acoustic Mat	0.86	10.2
Hot Rolled Steel and Fireproofing	1.01	12.0
Metal Deck	2.34	30.0
2500 psi Plain Concrete	0.12	1.07
4000 psi Reinforced Concrete	0.15	1.33

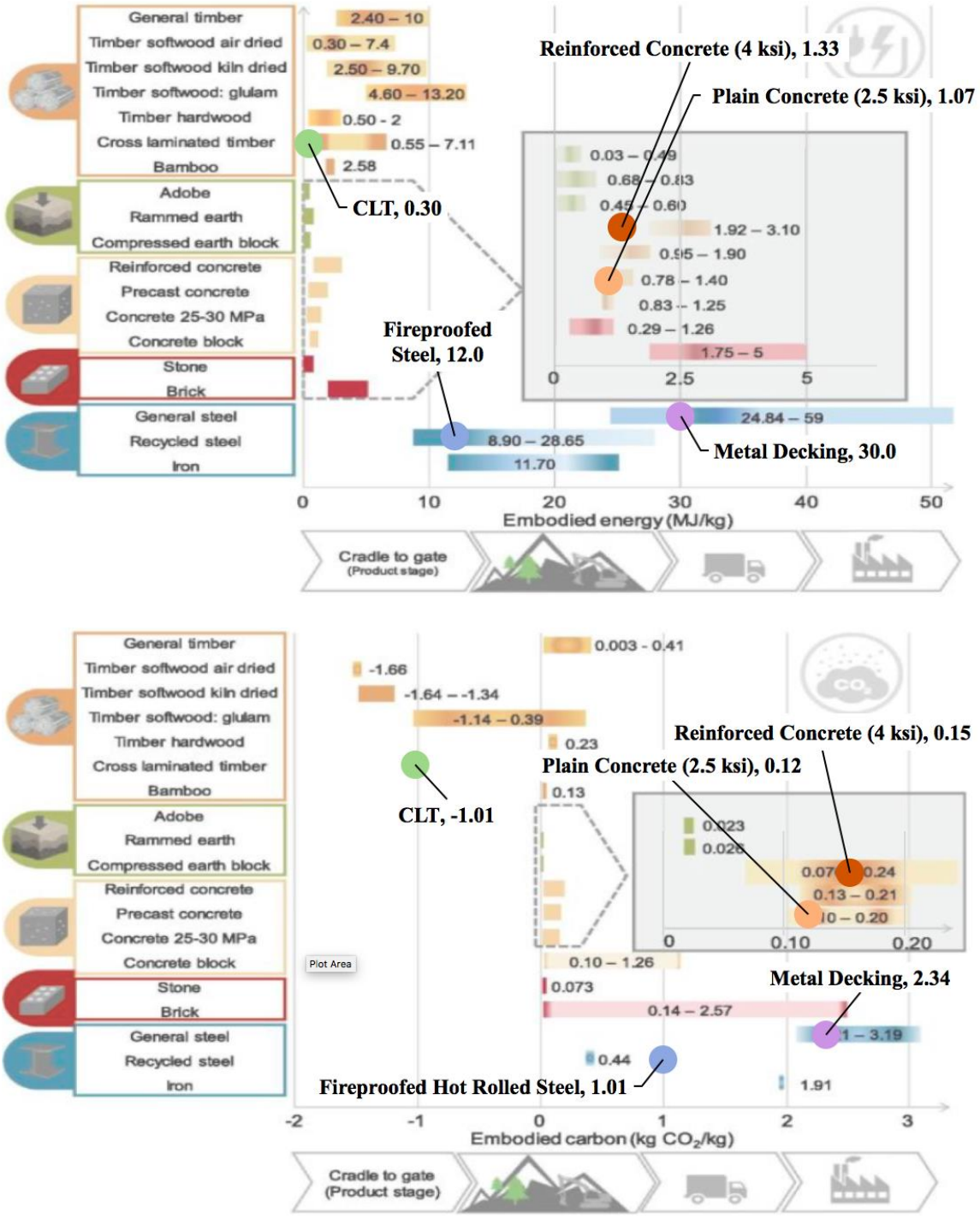

Figure 3-10: Comparison of environmental data with literature review data.Data Encompasses Production, or Life Stages [A1-A3]; Figure adapted from Cabeza et al. (2021)

Chapter 4: Results and Discussion

4.1 Structural Design Summaries

Lightweight STC floor systems are advantageous for gravitational force and deflection demands in composite systems. Floor systems were evaluated for vibration due to walking excitations per *AISC Design Guide 11 (Murray et al. 2016)* that indicated STC and SCC floor systems were both low-frequency (f_n < 9 Hz), requiring the office use acceleration limit of 0.005g to avoid resonance and discomfort to occupants. The low mass timber floor system requires additional stiffness contribution from steel framing or mass contribution from concrete topping in vibration design. As a result, STC floor member sizes were generally controlled by vibration requirements, leaving strength and deflection utilizations in the range of 0.40-0.80. Similarly, the relatively low acceleration limit for office use structures generally resulted in vibration controlled member sizing for SCC members as well. However, strength and deflection utilizations were not generally lower than 0.85.

Final member sizes for each structural system are summarized in Tables 4-1 and 4-2. STC floor beam and girder cross sections were generally larger than those of the SCC system due to the vibration-controlled design. However, roof members were subjected to less stringent vibration requirements, resulting in the strength-controlled design of the composite sections. Consequently, roof members are generally lighter than the SCC alternative despite larger tributary areas of the floor beams. In summary, member sizing of the STC system was controlled primarily by vibration limits, which resulted in relatively low demand/capacity (utilization) ratios for flexural strength and deflection.

4.1.1 Steel-Timber Composite: Design Summary

All STC floor systems were composed of 5-ply Southern Pine CLT with 1.5” normal weight concrete topping. 5-ply panels were necessary to provide fire-resistance and behavior for service level vibrations and deflections. Typical floor framing consisted of W18x40 beams, framing into W24x55 girders. Typical roof framing consisted of W14x22 beams, framing into W18x35 girders. Floor beams and girders were designed to approximately 25% composite action. Figure 3-2 shows a typical floor section. Girders are framed into steel WF columns, together acting as the gravity framing system. Member sizes for STC structures are summarized in Tables 4-1 and 4-2.

4.1.2 Steel-Concrete Composite: Design Summary

All SCC floor systems were composed of a 5” slab on a 2” deep 20-gauge deck. Typical floor framing consisted of W12x26 beams, framing into W21x50 girders. The roof decking systems were 3.5” slabs on a 1.5” deep 20-gauge deck. Typical roof framing consisted of W12x19 beams, framing into W18x40 girders. Floor beams and girders were designed to approximately 25% composite action. Figure 4-1 shows a typical floor section. Girders are framed into steel WF

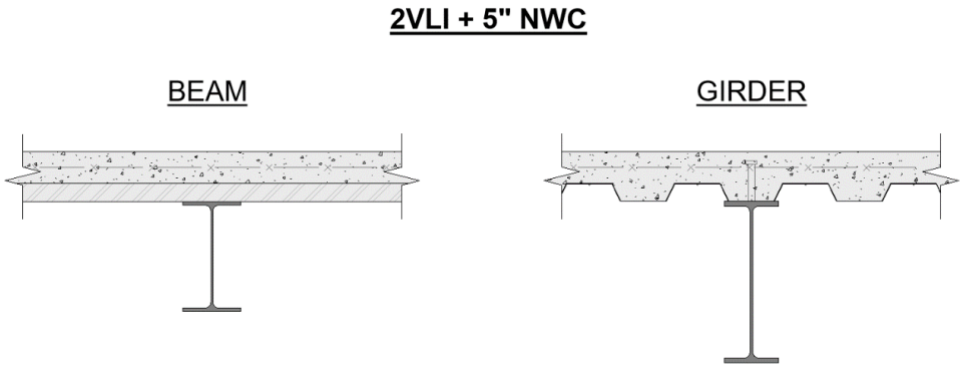

Figure 4-1: SCC floor system sections

columns, together acting as the gravity framing system. Member sizes for SCC structures are summarized in Tables 4-1 and 4-2.

Table 4-1: 7-Story member summaries

7-Story Member Sizes		
Description	**Steel-Timber**	**Steel-Concrete**
Roof Beam	W14x22	W12x19
Roof Girder	W18x35	W18x40
Roof N-S Spandrel	W10x15	W10x17
Roof E-W Spandrel	W14x22	W12x26
Floor Beam	W18x40	W12x26
Floor Girder	W24x55	W21x50
Floor N-S Spandrel	W16x26	W12x26
Floor E-W Spandrel	W16x31	W14x30
Interior Column Levels 1-4	W14x61	W12x65
Interior Column Levels 5-7	W12x30	W10x33
Exterior Column Levels 1-4	W14x38	W12x40
Exterior Column Levels 5-7	W12x26	W12x26

Table 4-2: 18-Story member summaries

18-Story Member Sizes		
Description	**Steel-Timber**	**Steel-Concrete**
Roof Beam	W14x22	W12x19
Roof Girder	W18x35	W18x40
Roof N-S Spandrel	W10x15	W10x17
Roof E-W Spandrel	W14x22	W12x26
Floor Beam	W18x40	W12x26
Floor Girder	W24x55	W21x50
Floor N-S Spandrel	W16x26	W12x26
Floor E-W Spandrel	W16x31	W14x30
Interior Column Levels 1-6	W14x145	W14x159
Interior Column Levels 7-10	W14x99	W12x106
Interior Column Levels 11-14	W10x68	W12x72
Interior Column Levels 15-18	W10x39	W10x39
Exterior Column Levels 1-6	W12x87	W12x87
Exterior Column Levels 7-10	W12x65	W12x65
Exterior Column Levels 11-14	W12x45	W12x45
Exterior Column Levels 15-18	W12x30	W12x30

4.1.3 Juxtaposition of Steel-Timber Composite and Non-Composite Systems

Lightweight STC floor systems were advantageous for flexural demands and deflection of composite members. However, the low-mass floor system required additional stiffness contribution from steel framing in vibration design. As a result, STC floor member sizes

were generally controlled by vibration demands. Sizing controlled by vibration resulted in relatively low demand/capacity ratios for composite flexural strength and composite deflection. Despite this, the composite design proved auspicious.

Preliminary analyses (reported in *3.4.4 Steel-Timber Utilization Studies*) indicate the non-composite design of the members would result in larger cross sections throughout, see Table 4-3. Note that STC floor members were controlled by vibration design. However, roof members were subjected to less stringent acceleration limits, allowing full strength development of the composite sections. Harnessing the full composite strength of the roof members, resulted in non-composite utilizations significantly above the capacity of the steel section alone.

Table 4-3: Comparison of composite and non-composite steel-timber sections in identical design scenarios at 30 ft. span length

		Composite Design		**Non-Composite Design**	
Description	**Member**	**Controlling Parameter**	**Utilization Ratio**	**Controlling Parameter**	**Utilization Ratio**
Floor Beam	W18x40	Vibration	0.98	Deflection	1.12
Floor Girder	W24x55	Vibration	0.98	Strength	1.10
Floor Spandrel	W16x26	Vibration	0.90	Deflection	1.22
Floor Spandrel	W16x31	Vibration	0.90	Deflection	1.49
Roof Beam	W14x22	Strength	0.90	Deflection	2.02
Roof Girder	W18x35	Strength	0.93	Strength	1.40
Roof Spandrel	W10x15	Strength	0.89	Deflection	3.08
Roof Spandrel	W14x22	Strength	0.93	Deflection	1.61

4.1.4 Secondary Design Considerations

Secondary design considerations were non-structural design items that ensured equivalent performance between the systems in non-structural capabilities; namely, acoustics and fire-resistance. This was achieved by having the systems comply with the *2021 International Building Code* (International Code Council 2020) requirements for sound transmission and fire-resistance rating. As STC systems are less established, only the methods and components utilized to meet standards are reported below.

To provide satisfactory acoustic performance, a combination of acoustic mat and concrete topping was provided for the STC system. Rubber membrane was 0.5” thick and paired with 1.5” concrete topping which has been experimentally shown to provide Sound Transmission Class and Impact Insulation Class ratings sufficient for office buildings, as required in IBC 2021 (Barber et al. 2022).

According to IBC 2021, a 2-hour fire rating is required for floor systems of Type IV-C construction. While 5-ply CLT provides adequate fire-resistance for Type IV-C construction, Type IV-A construction requires 80 minutes of non-combustible material contribution to fire resistance. To comply with this requirement, 1-1/4” of Type X gypsum board was included in the 18-story floor assembly.

4.2 Life Cycle Assessment and Comparison

4.2.1 Superstructure Mass

7-story and 18-story STC systems had 9.7% and 4.0% less superstructure mass than the SCC alternatives. Note that the presence of gypsum had a significant impact on the 18-story STC total mass, as the element comprised 8.0% of the total mass. When disregarding gypsum, the 18-

story STC structure had 12% lower mass than the SCC alternative. Figure 4-2, Table 4-4, and Table 4-5 display total values as well as material contributions to the total mass.

STC steel framing and associated cementitious fireproofing are presented in this paper's figures as "framing." Framing mass had only negligible variances between STC and SCC, differing by -1.8% and +1.8% in the 7-story and 18-story structures respectively. Despite fewer framing members, vibration demands increased STC purlin member sizes, resulting in comparable steel mass per bay. Therefore, all significant variances in mass were attributed to the floor systems, which averaged 86% of superstructure mass in all structures.

When studying floor systems alone, timber assemblages reduced floor system mass by 11% and 5% in 7-story in 18-story structures, respectively. Despite this, the presence of concrete topping in the STC floor assemblage had a significant presence. The 1.5" normal weight concrete comprised an average of 16% of depth STC floor assembly depth, but an average of 41% of the mass.

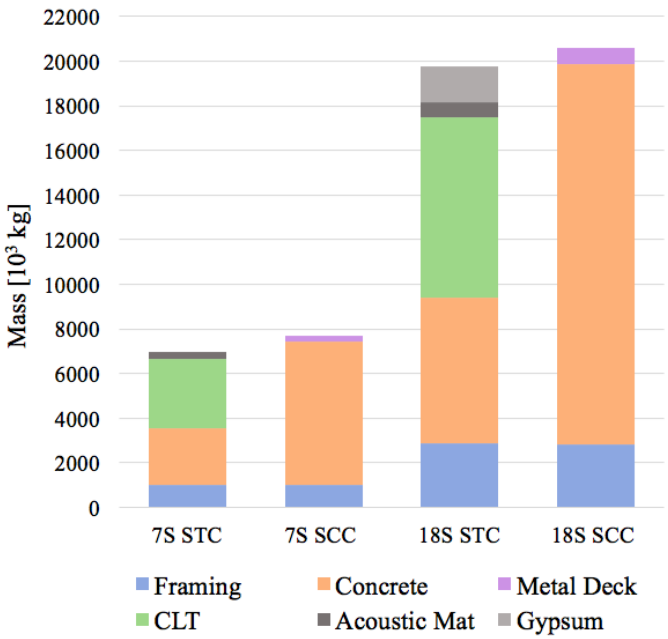

Figure 4-2: Superstructure mass

Table 4-4: 7-Story material quantities

	7S STC		7S SCC	
Material	**Mass [kg]**	**% Total Mass**	**Mass [kg]**	**% Total Mass**
CLT	3,141,482	45.2	--	--
Acoustic Mat	269,713	3.88	--	--
Steel Framing and Fireproofing	984,400	14.2	1,001,859	13.0
Metal Deck	--	--	269,063	3.50
2500 psi Plain Concrete	2,549,167	36.7	--	--
4000 psi Reinforced Concrete	--	--	6,418,060	83.5
Floor Assemblage	5,960,362	85.8	6,687,123	87.0
Total	6,944,763	100	7,688,982	100

Table 4-5: 18-Story material quantities

	18S STC		18S SCC	
Material	**Mass [kg]**	**% Total Mass**	**Mass [kg]**	**% Total Mass**
CLT	8,071,555	40.8	--	--
Acoustic Mat	692,812	3.51	--	--
Steel Framing and Fireproofing	2,864,601	14.5	2,813,673	13.7
Metal Deck	--	--	688,284	3.35
2500 psi Plain Concrete	6,549,564	33.1	--	--
4000 psi Reinforced Concrete	--	--	17,073,677	83.0
Type X Gypsum	1,583,754	8.01	--	--
Floor Assemblage	16,897,685	85.5	17,761,961	86.3
Total	19,762,286	100	20,575,634	100

Note: Instances in which the above percentages do not sum to precisely 100 are due to rounding.

4.2.2 Total Life Environmental Impacts

Total LCA outputs account for all life stages within the boundary. Final values are net, accounting for biogenic carbon, as well as avoided burdens (otherwise referred to as credits), due to recovery and reuse. Tables 4-6 and 4-7 detail all total values obtained in the study. Both STC systems had lower embodied carbon than the SCC alternatives. STC systems prompted 50% and 42% reductions in total embodied carbon. Similarly, both STC systems had lower embodied energy than the SCC alternatives. STC systems led to 32% and 21% reductions in total embodied energy.

The most significant contributor to both embodied carbon and embodied energy in STC systems was framing. However, the most significant contributor in SCC systems varied, with concrete being the largest contributor to embodied carbon and framing being the largest contributor to embodied energy. Furthermore, the impacts of STC floor assemblages were less significant than the impacts of framing alone. The opposite of which was found in SCC systems—floor system impacts were greater than those of framing. Figure 4-3 displays component contributions to total environmental impacts.

As previously discussed, steel framing mass varied less than 2% between structural types. Likewise, the portion of both total embodied carbon and embodied energy associated with steel framing varied by roughly 2% between structural types. Therefore, environmental benefits due to fewer framing members in the STC system were found to be negligible. Consequently, the environmental benefits of the steel-timber system stemmed primarily from CLT floors.

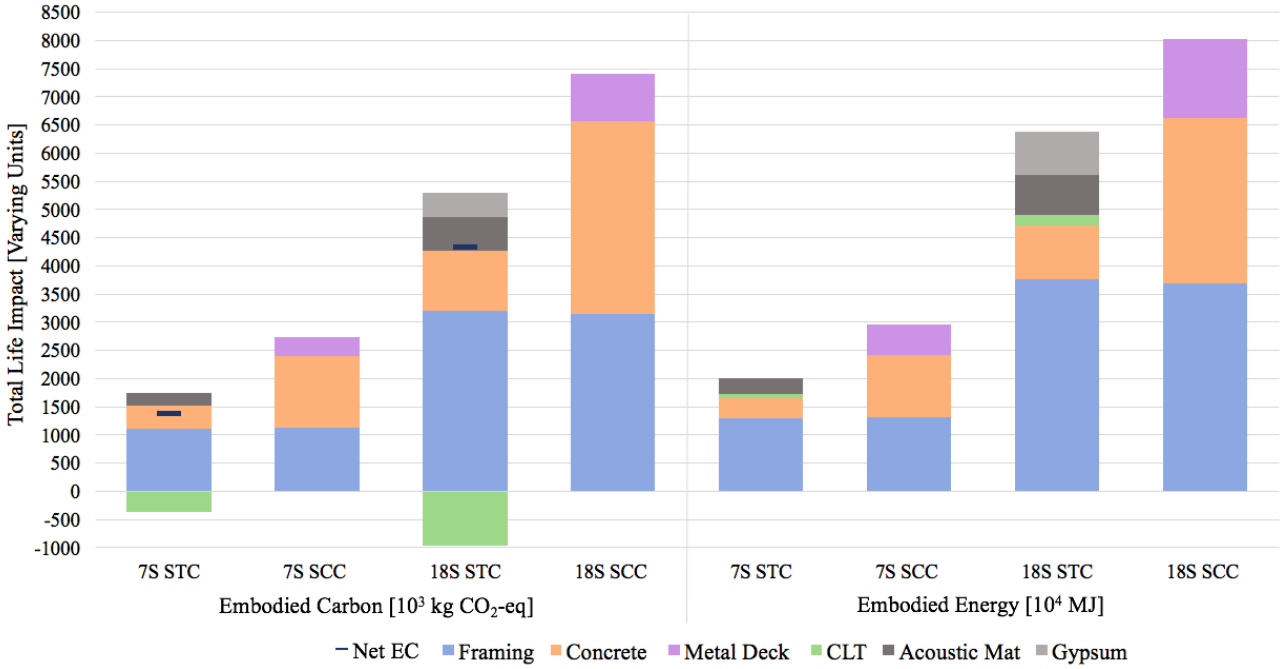

Figure 4-3: Total embodied carbon and embodied energy of structures. Life stages [A1-A3], [C2-C4], and [D]

Table 4-6: 7-Story total environmental impacts. Life stages [A1-A3], [C2-C4], and [D]

	7S STC				7S SCC			
Material	**EC [kg CO_2-eq]**	**% Total EC**	**EE [MJ]**	**% Total EE**	**EC [kg CO2-eq]**	**% Total EC**	**EE [MJ]**	**% Total EE**
CLT	-374,607	-27.2	758,668	3.77	--	--	--	--
Acoustic Mat	237,934	17.2	2,800,391	13.9	--	--	--	--
Steel Framing and Fireproofing	1,101,957	79.9	12,899,810	64.1	1,122,671	41.0	13,093,578	44.2
Metal Deck	--	--	--	--	332,134	12.1	5,520,449	18.6
2500 psi Plain Concrete	414,324	30.0	3,662,010	18.2	--	--	--	--
4000 psi Reinforced Concrete	--	--	--	--	1,283,842	46.9	11,034,420	37.2
Floor Assemblage	277,651	20.1	7,221,068	35.9	1,615,976	59.0	16,554,869	55.8
Total	1,379,608	100	29,120,878	100	2,738,647	100	29,648,447	100

Table 4-7: 18-Story total environmental impacts. Life stages [A1-A3], [C2-C4], and [D]

	18S STC				18S SCC			
Material	**EC [kg CO_2-eq]**	**% Total EC**	**EE [MJ]**	**% Total EE**	**EC [kg CO2-eq]**	**% Total EC**	**EE [MJ]**	**% Total EE**
CLT	-962,478	-22.2	1,949,518	3.06	--	--	--	--
Acoustic Mat	606,683	14.0	7,163,625	11.2	--	--	--	--
Steel Framing and Fireproofing	3,201,512	74.0	37,693,268	59.1	3,148,329	42.5	36,911,416	45.9
Metal Deck	--	--	--	--	849,626	11.5	14,121,735	17.6
2500 psi Plain Concrete	1,064,521	24.6	9,408,787	14.8	--	--	--	--
4000 psi Reinforced Concrete	--	--	--	--	3,411,613	46.0	29,308,365	36.5
Type X Gypsum	415,563	9.61	7,571,243	11.9	--	--	--	--
Floor Assemblage	1,124,289	26.0	26,093,173	40.9	4,261,239	57.5	43,430,100	54.1
Total	4,325,802	100	63,786,441	100	7,409,568	100	80,341,516	100

4.2.3 Cradle to Gate Environmental Impacts

Cradle-to-gate boundaries encompass product stages only (A1-A3). Environmental impacts associated with material production have the potential to account for a significant portion of overall environmental impact. Additionally, these values may provide a comparable output in studies of varying system boundaries. Varying techniques and methodologies of LCI may account for biogenic carbon in different life stages, or neglect it altogether. As previously stated, this study accounts for biogenic carbon in stage A1—resulting in negative values for net cradle-to-gate embodied carbon in the STC structures.

Table 4-8 displays cradle-to-gate environmental impacts, normalized by floor area, and Figure 4-4 displays material contributions. Note that variances between the STC proportions are

due to the presence of gypsum in the 18-story structure. The results indicate that carbon sequestered by the lumber in CLT is significant enough to offset all emissions associated with

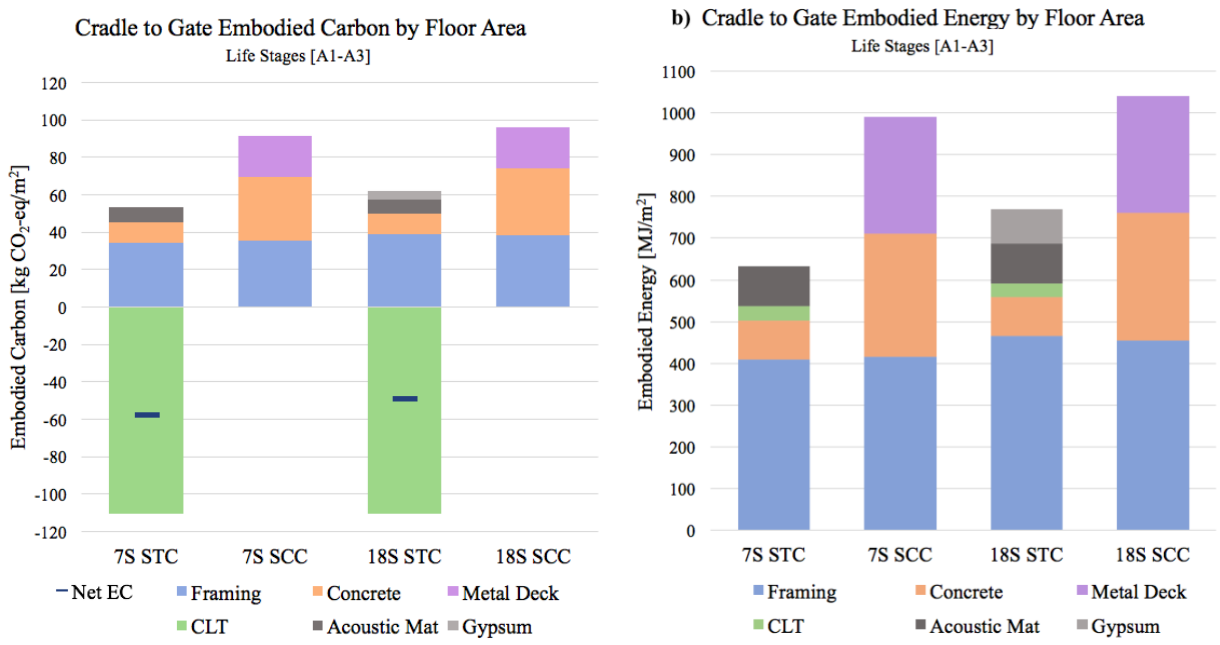

Figure 4-4: Cradle to gate embodied environmental impacts

Table 4-8: Cradle to gate embodied environmental impacts by floor area

Structure	Net Embodied Carbon [kg CO_2-eq/m^2]	Portion of Total Embodied Carbon	Embodied Energy [MJ/m^2]	Portion of Total Embodied Energy
7S STC	-57	-120%	630	90%
7S SCC	92	96%	990	96%
18S STC	-49	-83%	770	90%
18S SCC	96	96%	1040	96%

the product life stages. However, despite significant sequestration, nearly 1.5 times the amount of sequestered carbon is emitted throughout the structure's total life cycle—causing the largest portions of the STC structures' carbon footprints to appear in the post-life stage (see section

4.2.4 Environmental Impacts per Life Stage). Conversely, the SCC structures' carbon footprints are heavily front-loaded, as the production stages account for the bulk of the structures' embodied carbon. This is due to concrete's carbon offsets, associated with recycling and re-use, occurring during end-of-life.

In all structures, the largest contributor to cradle-to-gate embodied energy was the framing component. In the STC structures, the energy associated with the production of framing accounted for an average of 63% of cradle to gate embodied energy and 56% of total embodied energy. In the SCC structures, the energy associated with the production of framing accounted for an average of 43% of cradle to gate embodied energy and 41% of total embodied energy.

4.2.4 Environmental Impacts per Life Stage

A deeper examination of LCA outputs attributed to life stages allows one to understand the variances between structural material environmental impacts and their associated causes. The impacts associated with stages A1-A3, known as cradle to gate impacts, account for significant portions of total impacts. Additionally, cradle to gate values are commonly presented as LCA outcomes, as they are valuable for comparison between assessments of varying scopes. As a result, cradle to gate outcomes are reported and discussed independently (section *4.2.3 Cradle to Gate Environmental Impacts*). As previously discussed, carbon sequestration of lumber products causes the largest portions of the STC structures' carbon footprints to appear at the end-of-life stages. This is because Module A avoids net carbon emissions due to the large amount of carbon sequestered in lumber. Conversely, the SCC structures' carbon footprints are heavily front-loaded. This is due to the production stages accounting for the bulk of SCC structures' embodied carbon. Conversely, the end-of-life and post-life stages of concrete are associated with

the material's environmental credits, due to recycling and re-use. Similarly, the energy required to produce CLT is relatively low compared to the energy required to produce concrete and metal decking. However, the STC structures have no avoided energy burdens throughout their life cycles; whereas, the SCC structures net a negative embodied energy value in Module D. The embodied carbon and embodied energy of the structures are presented by the life cycle stage in Figures 4-5 and 4-6. Tables 4-9 and 4-10 go on to report the life stage values of each structure and their relative percentage of the total impact.

Note that avoided embodied carbon and embodied energy burdens associated with SCC structures in Module D are only a fraction of the avoided burdens associated with STC structures in Module A. In the case of embodied carbon, the avoided burdens attributed to 7-story and 18-story SCC structures (Module D) are 12% and 14% of the avoided carbon burdens attributed to the STC structures (Module A). A similar comparison between net embodied energy in the structural types is not valid. CLT was assumed to be incinerated for energy recovery in the post-life stage. However, the energy produced by incineration was not significant enough to overcome the remaining STC materials' energy demands in Module D. As a result, the net embodied energy associated with Module D of STC structures is positive and contributes to overall energy demand. Therefore, avoided energy burdens are unique to the SCC structure.

More points of interest in the life stage breakdowns are the large embodied carbon values associated with CLT in the product (Module A) and end-of-life stages (Module C). As discussed, lumber products sequester relatively large amounts of carbon before production. As such, the sequestered carbon is accounted for in Module A. This created a very large negative embodied carbon attributed to the production of CLT. However, later in the structure's life, much of the

carbon sequestered within CLT was re-released into the atmosphere. This is due to the assumptions specified for the material end-of-life scenarios; the CLT was assumed 14.5% recovered for reuse, 22% incinerated for energy production, and 63.5% landfilled (Table 3-11). As a result of these assumptions, 81% of the carbon sequestered by CLT was released due to material breakdown in a landfill or emitted due to material recovery and energy production. This resulted in relatively high embodied carbon impacts during end-of-life stages for the STC structures. Note the comparability of the embodied carbon of STC in Module C and SCC in Module A (Table 4-9).

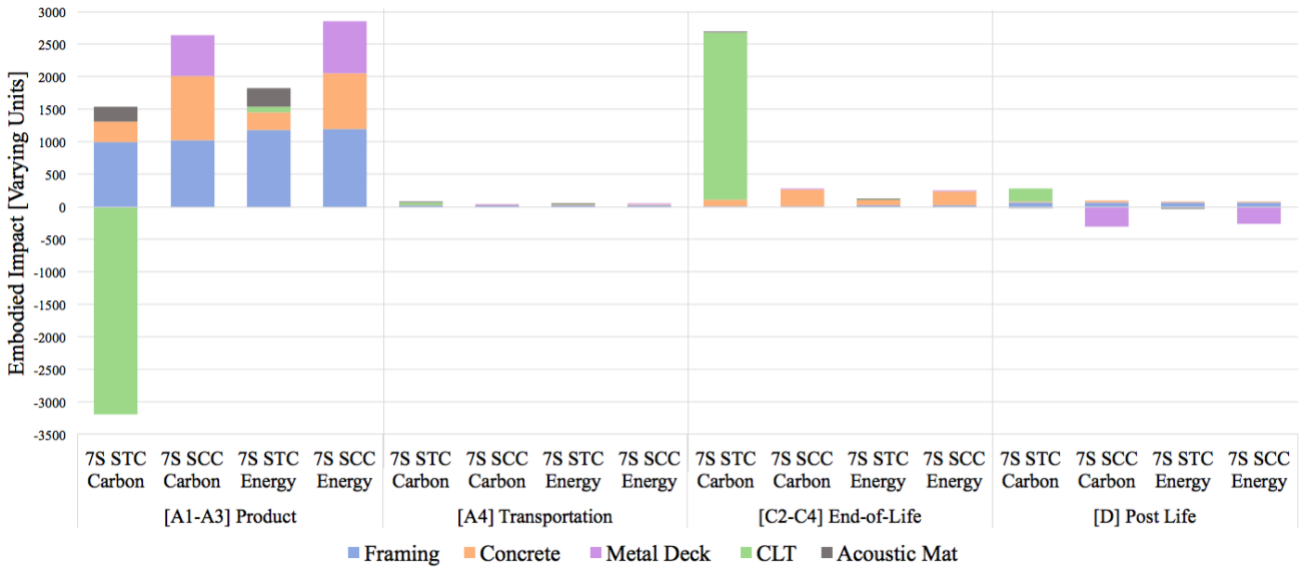

Figure 4-5: 7-Story embodied environmental impacts per life stage

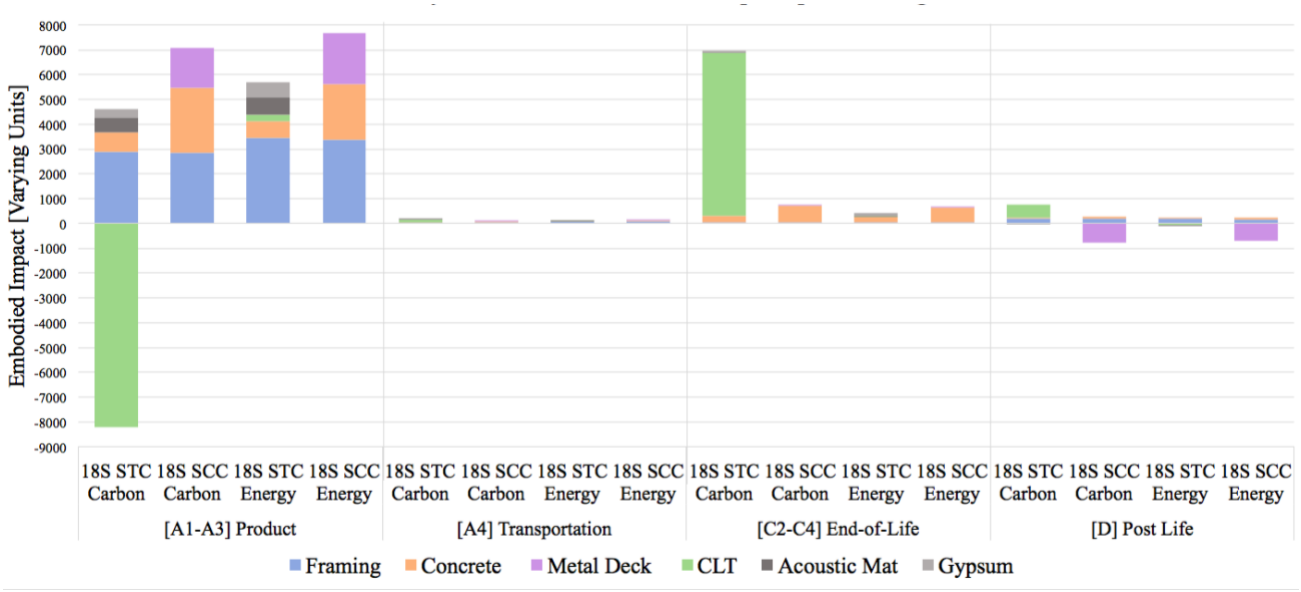

Figure 4-6: 18-story embodied environmental impacts per life stage

Table 4-9: Net embodied carbon per life stage

Net Embodied Carbon [kg CO_2-eq]									
Structure	[A1 – A3] Product		[A4] Transportation		[C2 – C4] End-of-Life		[D] Post Life		Total
7S STC	-1,653	-120%	66.70	5%	2,686	195%	280.0	20%	1,380
7S SCC	2,639	96%	34.75	1%	271.8	10%	-206.6	-8%	2,739
18S STC	-3,590	-83%	193.6	4%	6,972	161%	750.3	17%	4,326
18S SCC	7,095	96%	95.35	1%	722.7	10%	-504.0	-7%	7,410

Table 4-10: Net embodied energy per life stage

Net Embodied Energy [MJ]									
Structure	[A1 – A3] Product		[A4] Transportation		[C2 – C4] End-of-Life		[D] Post Life		Total
7S STC	1,819	90%	37.11	2%	114.5	6%	41.38	2%	2,012
7S SCC	2,853	96%	50.53	2%	241.0	8%	-180.0	-6%	2,965
18S STC	5,701	89%	127.7	2%	416.6	7%	133.1	2%	6,379
18S SCC	7,694	96%	138.7	2%	640.6	8%	-439.3	-5%	8,034

4.2.5 Floor System Environmental Impacts

Isolating floor systems provides insightful data by displaying disproportionality of environmental impacts and component depth. Despite composing only 17% and 15% of STC floor system depths, concrete accounted for 150% and 95% of floor system embodied carbon as well as 51% and 36% of embodied energy. Conversely, CLT composed 77% and 68% of STC floor system depths but accounted for -135% and -86% of embodied carbon as well as 11% and 7.5% of embodied energy.

7-Story and 18-Story STC floor assemblies resulted in $1/6^{th}$ and $1/4^{th}$ of the embodied carbon of SCC floor assemblies (Figure 4-7). Similarly, substantial decreases in embodied energy resulted from the timber floor alternatives, with the systems demanding 57% and 40% less energy. Despite substantial benefits to the alternative, the presence of gypsum in STC floors had a significant impact—increasing timber floor assembly mass, embodied carbon, and embodied energy by 10%, 59%, and 41%, respectively. Tables 4-11 and 4-12 detail the total outputs obtained from floor system analyses and the relative percentage of total floor impacts. Table 4-13 summarizes the results normalized by floor area.

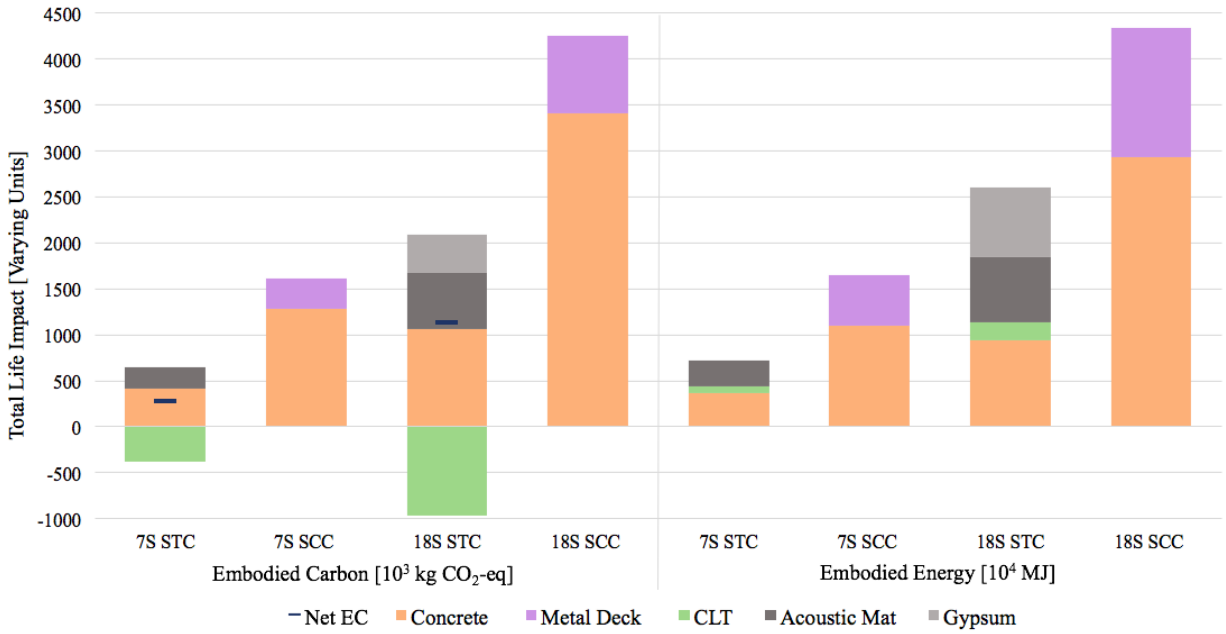

Figure 4-7: Total embodied carbon and embodied energy of floor assemblages. Life stages [A1-A3], [C2-C4], and [D]

Table 4-11: Floor assemblages - 7-story total life environmental impacts. Life stages [A1-A3], [C2-C4], and [D]

	7S STC				7S SCC			
Material	**EC [10^3 kg CO_2-eq]**	**% Floor EC**	**EE [10^4 MJ]**	**% Floor EE**	**EC [10^3 kg CO_2-eq]**	**% Floor EC**	**EE [10^4 MJ]**	**% Floor EE**
CLT	-374.6	-135	75.87	10.5	--	--	--	--
Acoustic Mat	237.9	85.7	280.0	38.8	--	--	--	--
Metal Deck	--	--	--	--	332.1	20.6	552.0	33.3
2500 psi Plain Concrete	414.3	149	366.2	50.7	--	--	--	--
4000 psi Reinforced Concrete	--	--	--	--	1,284	79.4	1,103	66.7
Total Floor Assemblage	277.7	100	722.1	100	1,616	100	1,655	100

Table 4-12: Floor assemblages - 18-story total life environmental impacts. Life stages [A1-A3], [C2-C4], and [D]

	18S STC				18S SCC			
Material	**EC [10^3 kg CO_2-eq]**	**% Floor EC**	**EE [10^4 MJ]**	**% Floor EE**	**EC [10^3 kg CO_2-eq]**	**% Floor EC**	**EE [10^4 MJ]**	**% Floor EE**
CLT	-962	-85.6	195	7.47	--	--	--	--
Acoustic Mat	607	54.0	716	27.5	--	--	--	--
Metal Deck	--	--	--	--	850	0.93	1,412	32.5
2500 psi Plain Concrete	1,065	94.7	941	36.1	--	--	--	--
4000 psi Reinforced Concrete	--	--	--	--	3,412	99.1	2,931	67.5
Type X Gypsum	416	37.0	757	29.0	--	--	--	--
Total Floor Assemblage	1,124	100	2,609	100	4,261	100	4,343	100

Table 4-13: Summary of mass and environmental impacts of floor assemblages. Life stages [A1-A3]

Floor Assembly	Embodied Carbon [kg CO^2-eq/m^2]	Embodied Energy [MJ/m^2]	Mass [kg/m^2]
CLT + Acoustic Mat + Concrete (7-Story STC)	9.64	251	207
CLT + Gypsum + Acoustic Mat + Concrete (18-Story STC)	15.2	353	228
Concrete + Metal Deck + Steel Reinforcing (SCC)	56.8	581	236

4.3 Sensitivity Analysis

4.3.1 Influence CLT Sourcing

The need to understand how product-specific environmental data impacts life cycle assessment was identified during this study. To close the knowledge gap, a sensitivity analysis

was conducted utilizing five North American CLT EPDs. Various mass timber producers in North America publish EPDs for specific manufacturing centers. To better understand how regional data may affect environmental impacts, the sensitivity analysis included manufacturing centers from various regions of North America. The data obtained from EPDs was global warming potential, fossil fuel depletion, and sequestered carbon associated with CLT at produced the relative manufacturing centers. Figure 4-8 and Table 3-14 report CLT environmental data and the associated regions.

It is important to note that embodied energy had one outlier data point. The reported cradle to gate energy of the CLT produced in Eastern Canada was roughly 10 times higher than the remainder of the data set. Further review of the published data reveals citations of proper development standards and techniques. However, the EPD reports no third-party LCA review, as is commonly declared within these documents. As a result, this paper reports the data obtained from CLT produced in Eastern Canada but does not include it in statistical analysis.

The dispersion of CLT production data in this paper is relatively low. Net embodied carbon had a coefficient of variance of -17%. Similarly, embodied energy had a coefficient of variance of 18%. The negative coefficient of variance in embodied carbon is due to a negative mean value. This is a valid metric of analysis as all net embodied carbon data points are negative.

Despite a limited set, data indicated the lowest embodied carbon occurs in CLT manufactured in the PNW. Embodied carbon associated with the two CLT products of this region averaged 19% lower than the data set mean value. On the contrary, the highest cradle to gate embodied carbon resulted from CLT produced in the Northern U.S. Rockies. Embodied

carbon produced in this region was 17% higher than the data set mean value. It is interesting to note that the PNW and Northern Rockies regions of the U.S. are adjoining.

A comparative WBLCA was conducted in an effort to determine the impact of CLT sourcing. The only variances in LCI data were the cradle to gate impact data of CLT. Wood density, CLT transportation distances, CLT end-of-life scenarios, as well as all other structural material inputs remained constant. Despite the divergent embodied energy data point in the Eastern Canadian-produced CLT, the WBLCA utilized the producer-reported cradle to gate values (Table 4-14). Consequently, the WBLCA embodied energy output related to Eastern CAN is likely an anomaly. Therefore, impacts of varying CLT densities such as structural framing design due to self-weight variance were not considered. The sensitivity analysis considered 7-story building heights only. Total LCA outputs are reported in Figure 4-9 and Table 4-15, reported embodied carbon values account for biogenic carbon. The impact of CLT data variations on WBLCA resulted in coefficients of variation of 5% and 1% for embodied carbon and embodied energy respectively.

The conclusions drawn from the sensitivity analysis were twofold. Firstly, cradle to gate embodied carbon and embodied energy may vary up to 20% between North American produced CLT products. Secondly, the impact of CLT sourcing does not greatly influence WBLCAs' environmental impacts. This is due to the remaining structural materials accounting for a significantly larger portion of emissions and energy use.

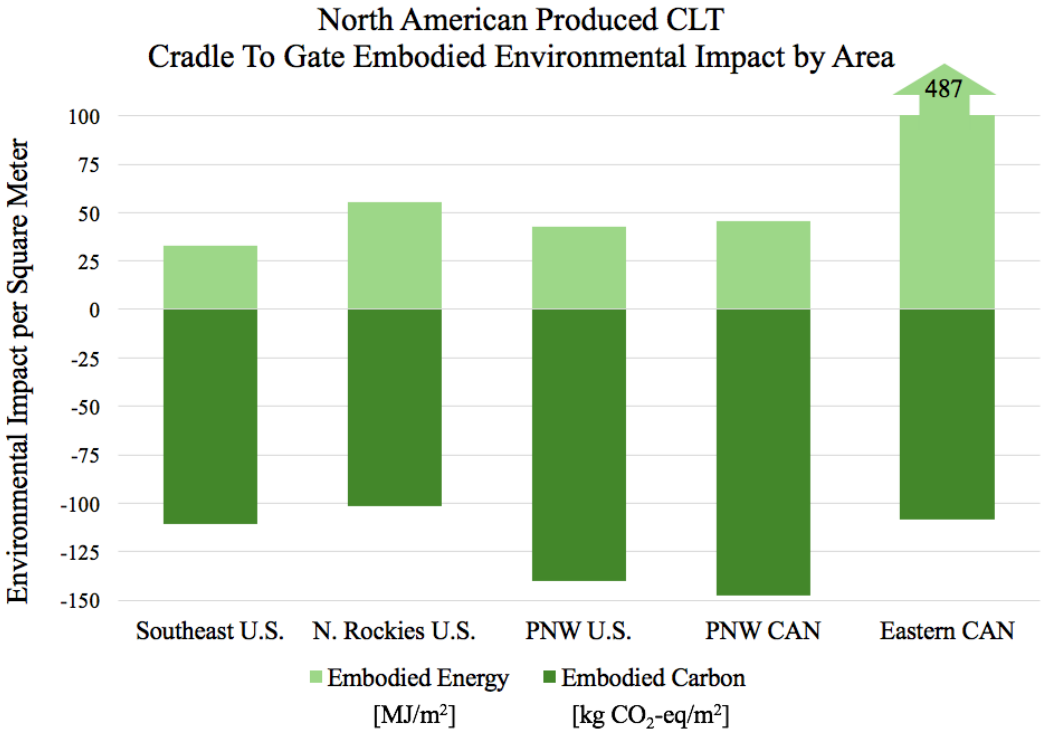

Figure 4-8: Reported production environmental impacts of North American produced CLT

Table 4-14: Cradle to gate environmental impacts of North American produced CLT Life Stages [A1-A3]

Identifier/ Region	**Source**	**Embodied Carbon [kg CO_2-eq/m^2]**	**Embodied Energy [MJ/m^2]**
Southeastern U.S.	SmartLam Alabama	-110.6	33.00
Northern U.S. Rockies	SmartLam Montana	-101.6	55.36
Pacific North-West (U.S.)	Vaagen Washington	-140.2	42.76
Pacific North-West (Canada)	StructureLam British Columbia	-147.7	45.82
Eastern Canada	Nordic Quebec	-108.2	486.6
	Mean, μ =	-121.7	44.23*
	Standard Deviation, σ =	20.78	9.212*
	Coefficient of Variation, CV =	-0.17	0.18*

*Embodied energy statistics exclude outlier data point

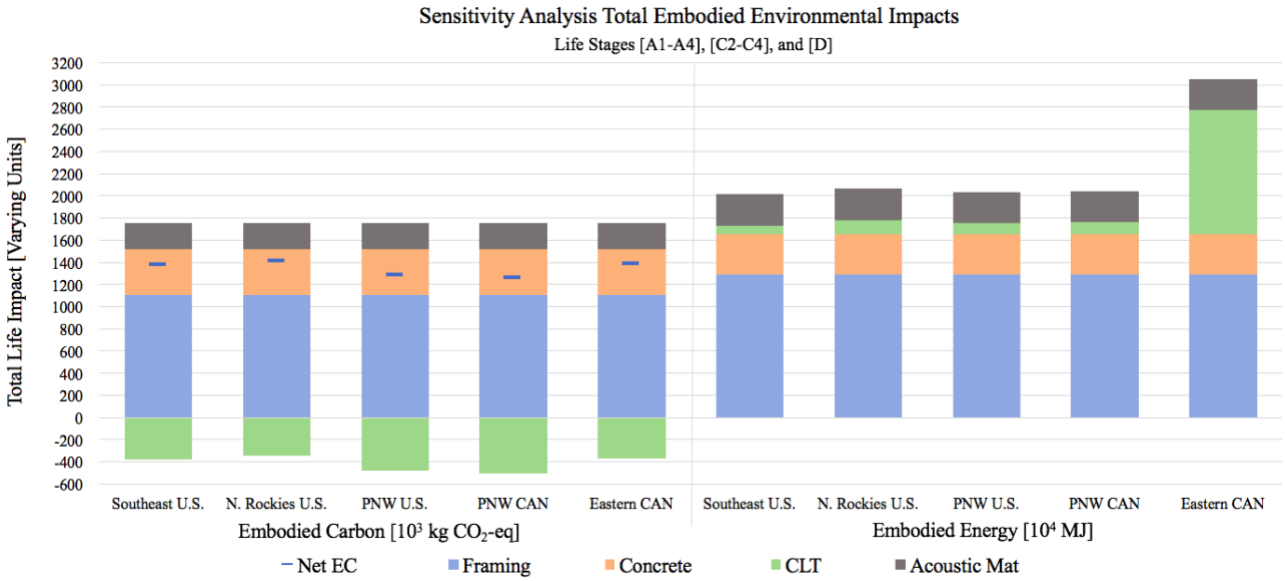

Figure 4-9: Total LCA outputs associated with North American produced CLT

Table 4-15: Net environmental impacts associated with North American produced CLT.Life Stages [A1-A4], [C2-C4], [D]

Source	Region	Embodied Carbon [10^3 kg CO_2-eq]	Embodied Energy [10^4 MJ]
SmartLam Alabama	Southeastern U.S.	1,380	2,012
SmartLam Montana	Northern U.S. Rockies	1,410	2,063
Vaagen Washington	Pacific North-West (U.S.)	1,280	2,035
StructureLam British Columbia	Pacific North-West (Canada)	1,254	2,042
Nordic Quebec	Eastern Canada	1,388	3,055
	Mean, μ =	1,342	2,038*
	Standard Deviation, σ =	70.37	21.18*
	Coefficient of Variation, CV =	0.05	0.01

**Mean embodied energy excludes outlier data point*

The results of the main body of work in this thesis are focused on CLT manufactured in the Southeastern United States. This data was chosen in part because of its relevance to the experimental and numerical study being conducted at Auburn University in a parallel effort to this paper to develop design guidelines and calculation methodologies. Additionally, Southeastern embodied carbon and energy demand are close to the mean values for all regions and are thus representative of broader studies.

4.3.2 Sensitivity Analysis: Biogenic Carbon

The need to understand how biogenic carbon impacts LCA results was identified during this study as the outcome is influenced by its inclusion and is often disregarded or the inclusions are unspecified within LCAs (Andersen et al. 2021). In an effort to close the knowledge gap, a sensitivity analysis was conducted which contrasted the inclusion or exclusion of biogenic carbon in both STC and SCC life cycle assessments. Results indicate the consideration of biogenic carbon is paramount to the environmental performance of the STC system. Whereas the consideration of biogenic carbon only negligibly impacts the environmental performance of the SCC system. Figure 4-10 and Table 4-16 report the total life assessment outputs of STC and SCC systems, both excluding and including biogenic carbon.

This paper reports total life sensitivity analyses. The only variances were the inclusion or exclusion of biogenic carbon. The exclusion of biogenic carbon was carried out by turning off the consideration within the analysis software as well as modifying input data that was extracted from EPDs to exclude carbon sequestration. All material quantities, wood density, transportation distances, end of life scenarios, as well as all other structural material inputs remained constant.

Biogenic carbon data for all products besides CLT was reflective of *Tally* database specifics and not user inputs. The sensitivity analysis considered 7-story building heights only.

Resulting variances of total life embodied carbon due to biogenic carbon consideration were less typically than 2% except in CLT which decreased total life embodied carbon by 130%. This was expected due to the carbon sequestered within lumber which causes lumber products to act as carbon sinks. As a result, lumber products often have net negative embodied carbon.

One may note that biogenic carbon decreased embodied carbon values in all products except the acoustic mat. This product was manually adjusted to reflect appropriate EPD data (see section *3.2.4 Life Cycle Inventory*. However, the product had no reported biogenic carbon and was not inputted to account for such. Therefore, the nearly negligible increase in total embodied carbon is likely a result of the generic rubber material's life-cycle scenario assumptions within *Tally*.

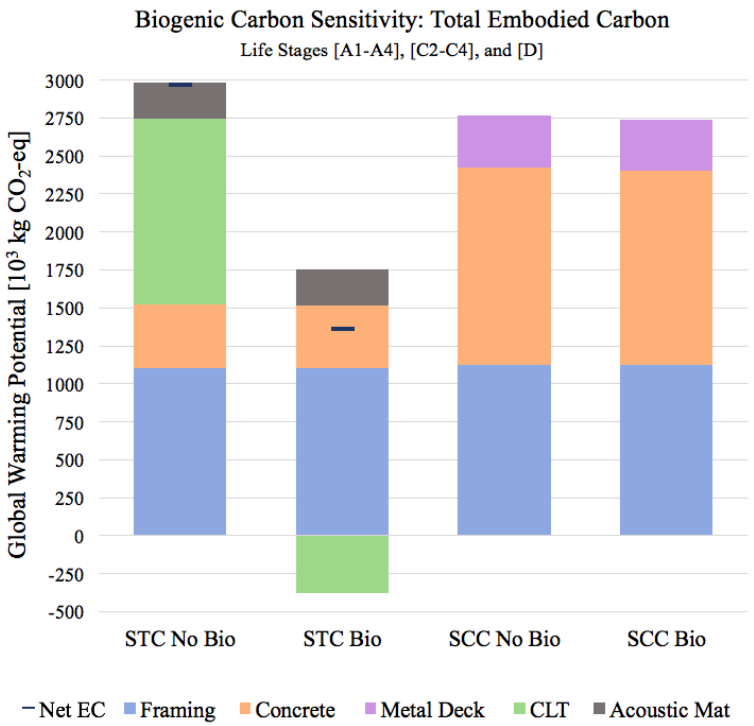

Figure 4-10: Juxtaposition of total LCA outputs: excluding or including biogenic carbon

Table 4-16: Total life embodied carbon when excluding or including biogenic. Life stages [A1-A4], [C2-C4], [D]

Embodied Carbon [10^3 kg CO_2-eq]						
	Steel-Timber Composite			**Steel-Concrete Composite**		
Element	No Biogenic Carbon	Biogenic Carbon Included	Difference	No Biogenic Carbon	Biogenic Carbon Included	Difference
CLT	1,221	-374.6	130%	--	--	--
Acoustic Mat	236.2	237.9	0.76%	--	--	--
Steel Framing and Fireproofing	1,105	1,102	0.26%	1,126	1,123	0.27%
Metal Deck	--	--	--	340.2	332.1	2.4%
2500 psi Plain Concrete	418.7	414.3	1.0%	--	--	--
4000 psi Reinforced Concrete	--	--	--	1,299	1,284	1.1%
Total	2,981	1,380	54%	2,765	2,739	0.94%
Floor Assemblage	1,876	277.7	85%	1,639	1,616	1.4%

Chapter 5: Summary, Conclusions, and Recommendations

5.1 Summary

The primary objective of this study was to comparatively investigate the environmental impacts of the novel steel-timber composite structural system with an established structural system counterpart, in this case a steel-concrete composite system. To explore the sustainable merits associated with STC and SCC systems, the superstructures of functionally equivalent office buildings at 7- and 18-story heights were designed and the components of each were analyzed in rigorous life cycle assessment.

Both structural systems were designed to comply with industry standards and recommendations for serviceability in office buildings. The design of the STC structures provided insight into the structural performance and nuances introduced when CLT panels are employed as a composite floor slab. Additionally, the steel-timber composite design was contrasted with non-composite design, shedding light on the advantages in stiffness and strength when harnessing composite action in steel-timber systems.

The environmentally focused module of this thesis revealed the material usage (mass), embodied carbon, and embodied energy associated with the final STC and SCC designs. Reports of environmental impacts within the boundaries of cradle to gate, constituent life stages, and total life were reported. Additionally, the weighty influence of the floor systems on the whole building environmental impacts were highlighted.

5.2 Conclusions

5.2.1 Steel-Timber Composite Design

The structural designs provided insight into nuances associated with the steel-timber composite system. The following results are notable, particularly in guidance to designers that may be unfamiliar with steel-timber composite design.

1. Vibration was a significant factor in the design of steel-timber composite members. Studies focused on floor system vibration in this thesis indicated the stiffness contributed by steel framing more significantly mitigated peak accelerations than additional concrete topping.
2. The orthotropic nature of CLT panels result in varying material properties (modulus of elasticity, compressive strength, etc.) in individual laminations that are relative to steel-to-panel orientation. As a result, transformed section properties varied between composite beams and girders.
3. CLT panel depth was controlled by fire-resistance requirements. As so, efficient floor panel span lengths for the steel-timber composite system were 15 ft, which exceed typical floor spans of concrete composite floor decks (10 ft).
4. Significant advantages were found to be associated with STC design relative to non-composite design. The design sections utilized in the structures of this thesis would have failed in non-composite design scenarios.

5.2.1 Life Cycle Assessment

Environmental advantages were found to be associated with the STC structures, relative to the SCC structures. The analyses provided valid whole building comparisons and the following results were achieved.

1. Embodied carbon, or global warming potential, was lower in the STC systems than the SCC systems. Total embodied carbon was reduced by 50% and 42% in the 7-story and 18-story structures, respectively.
2. Embodied energy, or primary energy demand, was lower in the STC systems than the SCC. Total embodied energy was reduced by 32% and 21%.
3. Steel framing mass and its associated environmental impacts were comparable between systems of the same height. As a result, environmental benefits attributed to STC structures stem predominately from floor assemblages, which compose an average of 86% of total superstructure mass.
4. STC systems had lower embodied carbon, embodied energy, and mass associated with floor assemblages by an average of 380%, 98%, and 10%, respectively.
5. In whole building comparisons, cross laminated timber floor panels averaged 130% lower embodied carbon, 93% lower embodied energy, and 52% lower mass than concrete on metal deck slabs.
6. Although the volumes of steel frame were nearly equivalent between structural types, the environmental impacts of the material far exceed its proportion to structural mass. In STC structures, hot-rolled steel averaged 14% of total mass, 77% of total embodied carbon, and 62% of total embodied energy. In SCC structures, hot-rolled steel averaged 13% of total mass, 42% of total embodied carbon, and 45% of total embodied energy.

5.3 Study Assumptions and Limitations

Assumptions surrounding product involvement and variances in LCI methodology have the potential to create discrepancies in environmental impact calculations. The LCI data of this study is representative of the *Tally 2023* internal database (Version 2022.04.08.01; Building Transparency 2022), as well as the environmental product declarations and life stage scenarios detailed in Chapter 3. Data beyond this study may only be comparably valid if building components, material proportions, upstream production processes, production regions, system boundaries, biogenic carbon considerations, environmental data collection, and life stage scenarios used in the study are transparent and functionally equivalent.

Steel-timber composite design calculations were developed internally due to a lack of design guidance on the novel system. Steel-timber composite beam nominal capacity and screw shear capacity assumptions were gathered from an experimental and numerical study conducted at Auburn University in a parallel effort to develop design guidelines and calculation methodologies. Vibration design methodology for the STC system was established by modifying the calculation procedure provided in *AISC Design Guide 11*, a design document intended for steel-concrete systems. The STC design was primarily controlled by vibration requirements, which designers commonly disregard as a design consideration. Design scenarios in which vibration is not a factor in design are expected further improve the environmental impact benefits of STC system. Further studies on the vibration characteristics and applicability of *AISC DG11* on STC systems are recommended.

5.1 Recommendation #1: Vibration of Long Span Steel-Timber Composite Floor Systems

5.1.1 Need for Laboratory Testing

Exploration of vibration of STC floor systems has been carried out by research teams in Australia (A. Chiniforush et al. 2019; Hassanieh et al. 2019; Chiniforush et al. 2017). However, physical tests were limited to relatively short span lengths (20 ft clear span), more typical of residential use buildings. As a result, there is a need for vibration studies in long-span (30 ft or greater) steel-timber composite systems with loads representative of various occupancy types.

Preliminary analyses indicate that expected superimposed loads of greater magnitudes may dampen vibration and lead to decreased reliance on steel member stiffness in vibration mitigation. Furthermore, variations of parameters that influence floor system vibration and acceleration would be beneficial. This would supply further knowledge as to efficient span lengths, occupancy types, and load intensities. Physical experiments which vary span lengths may encompass a broader range of occupancy types and the corresponding efficient bay sizes. Physical experiments which vary load intensities may encompass a variety of occupancy types and appropriate loadings of such.

5.1.2 Uncertainty in Empirical Vibration Evaluation

In parallel with vibration studies, there is a need for current timber floor analysis methods to be verified or developed further for steel-timber systems as new knowledge is developed. *AISC Design Guide 11* methods are popular for vibration analysis of steel-framed and timber structures (Breneman and Zimmerman 2021; Murray et al. 2016). However, the empirical formulas were designed for steel-concrete floor systems and may not be entirely accurate for the lighter-weight, greater depth, concrete topping, or composite action of steel-timber composite floor systems. As

a result, laboratory testing and methodology adaptations may be most beneficial to the structural engineering industry when completed in tandem.

5.2 Recommendation #2: Impact on Foundation and Lateral Force Resisting Systems

Steel-timber composite systems have shown the potential to decrease superstructure mass by up to 35% when compared to steel-concrete and 500% when compared to reinforced concrete systems (Chiniforush et al., 2018; SOM, 2017). As a result, the adoption of STC structures in earthquake-prone regions has the potential to supply further design benefits when compared to more established systems. As earthquake loads are inertial, structural design is dependent on superstructure mass and the lightweight STC floor system has the potential to result in smaller cross-sectional framing. Similarly, the decreased superstructure mass has the potential to decrease concrete foundation sizes which may significantly vary concrete material use and alleviate associated environmental impacts.

5.3 Recommendation #3: Constructability and Cost Studies

Beyond biophilic aesthetics and a decreased environmental impact, the use of mass timber panels in composite timber-steel floor systems has become increasingly attractive to owners, installers, and designers because of its benefits for on-site safety and scheduling efficiencies (Zuo et al. 2017). These benefits are largely attributed to the modular installation process, which decreases the number of required employees and can reduce construction schedules by 30 to 50 percent (Atkins et al. 2022). Given the potential constructability benefits, there is a need to quantify the potential labor hours and schedule duration of composite steel-mass timber structural systems relative to other common structural systems. To do so, cost estimates and schedule durations for each of the benchmark structures in the current study were

compiled. This included the exact size of members and material quantities of the structures. The results will be the total project cost, estimated required employees on site, and schedule duration.

While a body of research exists into the comparison of steel, concrete, and mass timber, the financial implications of structures comprising only mass timber make them economically incomparable. Steel-timber composite alternatives create an efficient and affordable innovation in the mass timber market.

5.4 Recommendation #4: Steel-Timber and Concrete-Timber Comparative WBLCA

Literature review and the results of this thesis indicate steel structural systems and framing have embodied carbon and energy coefficients higher than other structural materials (Hart, D'Amico, and Pomponi 2021; De Wolf et al. 2016). In light of the extreme environmental impacts associated with steel, concrete-timber hybrid systems may provide a structural system environmentally competitive with steel-timber. Therefore, a whole building life cycle assessment that compares functionally equivalent steel-timber and steel-concrete structures would clarify the environmental efficiency of concrete framing, as well as juxtapose the environmental impacts of concrete and steel framing.

References

A. Chiniforush, A., M. Makki Alamdari, U. Dackermann, H.R. Valipour, and A. Akbarnezhad. 2019. “Vibration Behaviour of Steel-Timber Composite Floors, Part (1): Experimental & Numerical Investigation.” *Journal of Constructional Steel Research* 161 (October): 244–57. https://doi.org/10.1016/j.jcsr.2019.07.007.

Ahmad, Fokruddin, Kevin Allan, and Adam Phillips. In Press. “Multiple-Criteria Decision Analysis of Steel and Mass Timber Prototype Buildings in the Pacific Northwest.”

Ahmed, Shafayet, and Ingrid Arocho. 2021. “Analysis of Cost Comparison and Effects of Change Orders during Construction: Study of a Mass Timber and a Concrete Building Project.” *Journal of Building Engineering* 33 (January): 101856. https://doi.org/10.1016/j.jobe.2020.101856.

———. 2022. “Cost Analysis of a Mass Timber Building Project: Comparison of Budgeted and Actual Construction Cost.” In *Construction Research Congress 2022*, 493–501. Arlington, Virginia: American Society of Civil Engineers. https://doi.org/10.1061/9780784483978.051.

Allan, Kevin, and Adam R. Phillips. 2021. “Comparative Cradle-to-Grave Life Cycle Assessment of Low and Mid-Rise Mass Timber Buildings with Equivalent Structural Steel Alternatives.” *Sustainability* 13 (6): 3401. https://doi.org/10.3390/su13063401.

American Concrete Institute. 2020. *ACI 318-19: Building Code Requirements for Structural Concrete*. American Concrete Institute.

Andersen, C. E., F. N. Rasmussen, G. Habert, and H. Birgisdóttir. 2021. “Embodied GHG Emissions of Wooden Buildings—Challenges of Biogenic Carbon Accounting in Current

LCA Methods." *Frontiers in Built Environment* 7 (August): 729096. https://doi.org/10.3389/fbuil.2021.729096.

Arowoshegbe, AMOS O, and UNIAMIKOGBO Emmanuel. 2016. "SUSTAINABILITY AND TRIPLE BOTTOM LINE: AN OVERVIEW OF TWO INTERRELATED CONCEPTS," 39.

ASCE. 2017. *ASCE/SEI 7-16: Minimum Design Loads and Associated Criteria for Buildings and Other Structures*. Reston,VA: American Society of Civil Engineers.

Aspila, Aku, Markku Heinisuo, Kristo Mela, Mikko Malaska, and Sami Pajunen. 2022. "Elastic Design of Steel-Timber Composite Beams." *Wood Material Science & Engineering* 0 (0): 1–10. https://doi.org/10.1080/17480272.2022.2093128.

Atkins, Dave, Roy Anderson, Emily Dawson, and Lech Muszynski. 2022. *2022 International Mass Timber Report*. Forest Business Network.

American Wood Council. 2018. *National Design Specification for Wood Construction with Commentary*. 2018 Edition. VA, U.S.A.

Block, Philippe, and Noelle Paulson. 2019. "E4: Efficiency, Economy, Elegance, and Ecology," 4.

Breneman, Scott, Matt Timmers, and Dennis Richardson. 2019. "Tall Wood Buildings in the 2021 IBC." WoodWorks.

Breneman, Scott, and Reid Zimmerman. 2021. "U.S. Mass Timber Floor Vibration Design Guide." WoodWorks.

Budig, Michael, Oliver Heckmann, Amanda Ng Qi Boon, Markus Hudert, Clement Lork, and Lynette Cheah. 2020. "Data-Driven Embodied Carbon Evaluation of Early Building Design Iterations," 10.

Burback, Brad, and Shiling Pei. 2017. “Cross-Laminated Timber for Single-Family Residential Construction: Comparative Cost Study.” *Journal of Architectural Engineering* 23 (3): 06017002. https://doi.org/10.1061/(ASCE)AE.1943-5568.0000267.

Cabeza, Luisa F., Laura Boquera, Marta Chàfer, and David Vérez. 2021. “Embodied Energy and Embodied Carbon of Structural Building Materials: Worldwide Progress and Barriers through Literature Map Analysis.” *Energy and Buildings* 231 (January): 110612. https://doi.org/10.1016/j.enbuild.2020.110612.

Chapra, Anil K. 2007. *Dynamics of Structures: Theory and Applications to Earthquake Engineering*. 3rd ed. Upper Saddle River, NJ: Pearson Education, Inc.

Chau, C.K., T.M. Leung, and W.Y. Ng. 2015. “A Review on Life Cycle Assessment, Life Cycle Energy Assessment and Life Cycle Carbon Emissions Assessment on Buildings.” *Applied Energy* 143 (April): 395–413. https://doi.org/10.1016/j.apenergy.2015.01.023.

Chiniforush, Alireza A, Ali Akbarnezhad, Hamid Valipour, and Ulrike Dackermann. 2017. “DYNAMIC RESPONSE OF STEEL-TIMBER COMPOSITE (STC) BEAMS,” 8.

Chiniforush, Alireza A., Ali Akbarnezhad, Hamid Valipour, and Jianzhuang Xiao. 2018. “Energy Implications of Using Steel-Timber Composite (STC) Elements in Buildings.” *Energy and Buildings* 176 (October): 203–15. https://doi.org/10.1016/j.enbuild.2018.07.038.

Christovasilis, I.P., M. Brunetti, M. Follesa, M. Nocetti, and D. Vassallo. 2016. “Evaluation of the Mechanical Properties of Cross Laminated Timber with Elementary Beam Theories.” *Construction and Building Materials* 122 (September): 202–13. https://doi.org/10.1016/j.conbuildmat.2016.06.082.

Crespell, Pablo, and Sylvain Gagnon. 2010. “Cross Laminated Timber: A Primer.” FP Innovations.

Crowther, Philip. 1999. “Design for Disassembly to Recover Embodied Energy.” *Sustaining the Future: Ecology Architecture PLEA’99*, 95–100.

CSi. 2022. “ETABs.” Computers and Structures inc.

D’Amico, Bernardino, and Francesco Pomponi. 2020. “On Mass Quantities of Gravity Frames in Building Structures.” *Journal of Building Engineering* 31 (September): 101426. https://doi.org/10.1016/j.jobe.2020.101426.

De Wolf, Catherine, Frances Yang, Duncan Cox, Andrea Charlson, Amy Seif Hattan, and John Ochsendorf. 2016. “Material Quantities and Embodied Carbon Dioxide in Structures.” *Proceedings of the Institution of Civil Engineers - Engineering Sustainability* 169 (4): 150–61. https://doi.org/10.1680/ensu.15.00033.

Dean, Brian, John Dulac, Trevor Morgan, and Uwe Remme. 2018. “The Future of Cooling.” *International Energy Agency/OECD*, 92.

Dixit, Manish K., Charles H. Culp, and Jose L. Fernández-Solís. 2013. “System Boundary for Embodied Energy in Buildings: A Conceptual Model for Definition.” *Renewable and Sustainable Energy Reviews* 21 (May): 153–64. https://doi.org/10.1016/j.rser.2012.12.037.

Dodge Data & Analytics, ed. 2018. *Market Share by Construction Material*. Bedford, MA, U.S.A.: Dodge Data and Analytics.

Elkington, John. 2018. “25 Years Ago I Coined the Phrase ‘Triple Bottom Line.’ Here’s Why It’s Time to Rethink It.” *Harvard Business Review*, June 25, 2018.

https://hbr.org/2018/06/25-years-ago-i-coined-the-phrase-triple-bottom-line-heres-why-im-giving-up-on-it.

Feng, H., R. Sadiq, and K. Hewage. 2022. “Exploring the Current Challenges and Emerging Approaches in Whole Building Life Cycle Assessment.” *Canadian Journal of Civil Engineering* 49 (2): 149–58. https://doi.org/10.1139/cjce-2020-0284.

GABC, and UN Environment. 2016. *Global Roadmap for Transition Towards Low-GHG and Resilient Buildings*. Global Alliance for Buildings and Construction.

Gu, Hongmei, Shaobo Liang, and Richard Bergman. 2020. “Comparison of Building Construction and Life-Cycle Cost for a High-Rise Mass Timber Building with Its Concrete Alternative.” *Forest Products Journal* 70 (4): 482–92. https://doi.org/10.13073/FPJ-D-20-00052.

Gu, Hongmei, Shaobo Liang, Francesca Pierobon, Maureen Puettmann, Indroneil Ganguly, Cindy Chen, Rachel Pasternack, Mark Wishnie, Susan Jones, and Ian Maples. 2021. “Mass Timber Building Life Cycle Assessment Methodology for the U.S. Regional Case Studies.” *Sustainability* 13 (24): 14034. https://doi.org/10.3390/su132414034.

Hart, Jim, Bernardino D’Amico, and Francesco Pomponi. 2021. “Whole-life Embodied Carbon in Multistory Buildings: Steel, Concrete and Timber Structures.” *Journal of Industrial Ecology* 25 (2): 403–18. https://doi.org/10.1111/jiec.13139.

Hassanieh, A., A.A. Chiniforush, H.R. Valipour, and M.A. Bradford. 2019. “Vibration Behaviour of Steel-Timber Composite Floors, Part (2): Evaluation of Human-Induced Vibrations.” *Journal of Constructional Steel Research* 158 (July): 156–70. https://doi.org/10.1016/j.jcsr.2019.03.026.

Hassanieh, A., H.R. Valipour, and M.A. Bradford. 2016. “Experimental and Numerical Study of Steel-Timber Composite (STC) Beams.” *Journal of Constructional Steel Research* 122 (July): 367–78. https://doi.org/10.1016/j.jcsr.2016.04.005.

———. 2017. “Experimental and Numerical Investigation of Short-Term Behaviour of CLT-Steel Composite Beams.” *Engineering Structures* 144 (August): 43–57. https://doi.org/10.1016/j.engstruct.2017.04.052.

International Code Council. 2020. *2021 International Building Code*. Country Club Hills, IL: International Code Council, INC.

Karacabeyli, Erol, and Sylvain Gagnon, eds. 2019. *Canadian CLT Handbook*. 2019th ed. Vol. 1. FP Innovations.

Kensler, Mike. 2014. “Director’s Corner: Interconnectedness and the Compass of Sustainability.” Auburn Univeristy, Office of Sustainability. January 20, 2014.

KT Innovations. 2022. “Tally.” Building Transparency, KT Innovations, Autodesk. https://choosetally.com/.

Kuzman, Manja K., and Dick Sandberg. 2017. “Comparison of Timber-House Technologies and Initiatives Supporting Use of Timber in Slovenia and Sweden-the State of the Art.” *IForest - Biogeosciences and Forestry* 10 (6): 930–38.

Leafblad, Janelle, Jeff Peters, and Laura Cullen. 2021. “2021 Year in Review: Trends in Light-Frame and Mass Timber Construction.” Presented at the A 2021 Snapshot: Challenges, Trends and Advancements in Wood Design and Construction, November 4.

Lewis, Meghan, Monica Huang, Stephanie Carlisle, and Kate Simonen. 2021. “Measuring Embodied Carbon.” *AIA - CLF Embodied Carbon Toolkit for Architects*, October, 11.

Lewis, Simon L., and Mark A. Maslin. 2015. “Defining the Anthropocene.” *Nature* 519 (7542): 171–80. https://doi.org/10.1038/nature14258.

Lindsey, Rebecca. 2022. “Climate Change: Atmospheric Carbon Dioxide.” NOAA. June 23, 2022. https://www.climate.gov/news-features/understanding-climate/climate-change-atmospheric-carbon-dioxide.

LWA. 2022. “John W. Olver Design Building.” Leers Weinzapfel Associates. 2022.

Malmqvist, Tove, Mauritz Glaumann, Sabina Scarpellini, Ignacio Zabalza, Alfonso Aranda, Eva Llera, and Sergio Díaz. 2011. “Life Cycle Assessment in Buildings: The ENSLIC Simplified Method and Guidelines.” *Energy* 36 (4): 1900–1907. https://doi.org/10.1016/j.energy.2010.03.026.

Marhani, Mohd Arif, Aini Jaapar, Nor Azmi Ahmad Bari, and Mardhiah Zawawi. 2013. “Sustainability Through Lean Construction Approach: A Literature Review.” *AMER International Conference on Quality of Life* 101 (November): 90–99.

McLain, Richard, and Scott Breneman. 2019. “Fire Design of Mass Timber Members.” WoodWorks.

Merryday, Hugh, Kadir Sener, and David Roueche. 2023. “Pushout Tests on Steel-Timber Connections Using Self-Tapping Screws.” In .

Murray, Thomas M., David E. Allen, Eric E. Ungar, and D. Brad Davis. 2016. *AISC Design Guide 11: Vibrations of Steel -Framed Structural Systems Due to Human Activity*. 2nd ed. American Institute of Steel Construction.

Nguyen, Phuong, Brian Lines, Dan Tran, and Ph D Student. 2018. “Best-Value Procurement in Design-Bid-Build Construction Projects: Empirical Analysis of Selection Outcomes.” *Construction Research Congress*, 11.

NOAA “Trends in Atmospheric Carbon Dioxide.” n.d. NOAA Global Monitoring Laboratory. https://gml.noaa.gov/ccgg/trends/.

Nwodo, Martin N., and Chimay J. Anumba. 2019. “A Review of Life Cycle Assessment of Buildings Using a Systematic Approach.” *Building and Environment* 162 (September): 106290. https://doi.org/10.1016/j.buildenv.2019.106290.

Obafemi, A.P. Olukoya. 2017. “Built Heritage as Catalysts of Environmental Sustainability: A Pragmatic Paradigm for Anthropocene.” In *Vernacular and Earthen Architecture: Conservation and Sustainability*, edited by C. Mileto, F. Vegas López-Manzanares, L. García-Soriano, and V. Cristini, 1st ed., 657–62. CRC Press. https://doi.org/10.1201/9781315267739.

O’Connor, Jennifer. 2004. “Survey on Actual Service Lives for North American Buildings,” 9.

Pacheco-Torgal, Fernando, Luisa F. Cabeza, João Labrincha, and Aldo Giuntini de Magalhaes. 2014. *Eco-Efficient Construction and Building Materials*. Woodhead Publishing.

Petersen, Ann Kristin, and Birger Solberg. 2002. “Greenhouse Gas Emissions, Life-Cycle Inventory and Cost-Efficiency of Using Laminated Wood Instead of Steel Construction. Case: Beams at Gardermoen Airport.” *Environmental Science and Policy* 5 (2): 169–82. https://doi.org/10.1016/S1462-9011(01)00044-2.

Potuzak, Megan, Kadir Sener, and David Roueche. 2023. “Pushout Tests on Steel-Timber Connections Using Self-Tapping Screws.” In .

Purnell, P. 2012. “Material Nature versus Structural Nurture: The Embodied Carbon of Fundamental Structural Elements.” *Environmental Science & Technology* 46 (1): 454–61. https://doi.org/10.1021/es202190r.

Ritchie, Hannah, Max Roser, and Pablo Rosado. 2020. "CO_2 and Greenhouse Gas Emissions." *Our World in Data*, May. https://ourworldindata.org/co2-emissions.

Schuirmann, A, C Loss, A Iqbal, and T Tannert. 2019. "STRUCTURAL AND ENVIRONMENTAL ANALYSES OF TALL WOOD- CONCRETE HYBRID SYSTEM," June, 8.

Scouse, Adam, Stephen S. Kelley, Shaboo Liang, and Richard Bergman. 2020. "Regional and Net Economic Impacts of High-Rise Mass Timber Construction in Oregon | Elsevier Enhanced Reader." https://doi.org/10.1016/j.scs.2020.102154.

Segui, William T. 2018. *Steel Design*. 6th ed. Boston, MA: Cengage Learning.

Skidmore, Owings, and Merrill. 2017. "AISC Steel & Timber Research for High-Rise Residential Buildings." Chicago, IL: Skidmore, Owings, and Merrill LLP.

Solomon, Susan, Dahe Qin, Martin Manning, Melinda Marquis, Kristen Averyt, Melinda Tignor, Henry Miller, and Zhenlin Chen, eds. 2007. *Climate Change 2007: The Physical Science Basis. Contribution of Working Group I to the Fourth Assessment Report of the Intergovernmental Panel on Climate Change*. Cambridge, UK and New York, NY, USA: Cambridge University Press.

SOM. 2017. "AISC Steel & Timber Research for High Rise Residential Buildings: Final Report." Chicago, IL: © Skidmore, Owings, and Merrill, LLP.

———. 2022. "When to Include Biogenic Carbon in an LCA." WoodWorks. https://www.woodworks.org/resources/when-to-include-biogenic-carbon-in-an-lca/.

Steel Deck Institute. 2017. *SDI-C 2017*. American National Standards Institute/Steel Deck Institute.

Steffen, Will, Jacques Grinevald, Paul Crutzen, and John McNeill. 2011. “The Anthropocene: Conceptual and Historical Perspectives.” *Philosophical Transactions of the Royal Society*. https://doi.org/10.1098/rsta.2010.0327.

StructureCraft Inc. 2022. “Engineered Wood: Glulam.” 2022. https://structurecraft.com/materials/engineered-wood/glulam.

Suh, Sangwon, and Gjalt Huppes. 2005. “Methods for Life Cycle Inventory of a Product.” *Journal of Cleaner Production* 13: 687–97. https://doi.org/10.1016/j.jclepro.2003.04.001.

United Nations Environment Programme. 2020. *2020 Global Status Report for Buildings and Construction: Towards a Zero-Emission, Efficient and Resilient Buildings and Construction Sector*. Nairobi: United Nations Environment Programme.

———. 2021. *2021 Global Status Report for Buildings and Construction: Towards a Zero-Emission, Efficient and Resilient Buildings and Construction Sector*. Nairobi: United Nations Environment Programme.

USCS. 2022. “Construction Spending.” United States Census Bureau. March 2022. https://www.census.gov/construction/c30/historical_data.html.

Vulcraft. 2022. “Composite Deck Slab Strength.” Vulcraft.Com/DesignTools. 2022. https://vulcraft.com/DesignTools/CompositeDeckSlabStrength.

WoodWorks. 2016. “Case Study: Candlewood Suites, Construction Advantages Sell Hotel Developer on CLT.” WoodWorks.

Woodworks. 2022 “U.S. Mass Timber Projects.” June 2022. https://www.woodworks.org/resources/u-s-mass-timber-projects/.

Yang, Frances, ed. 2018. *Whole Building Life Cycle Assessment*. American Society of Civil Engineers. https://doi.org/10.1061/9780784415054.

Zuo, Jian, Stephen Pullen, Raufdeen Rameezdeen, Helen Bennetts, Yuan Wang, Guozhu Mao, Zhihua Zhou, Huibin Du, and Huabo Duan. 2017. “Green Building Evaluation from a Life-Cycle Perspective in Australia: A Critical Review.” *Renewable and Sustainable Energy Reviews* 70 (April): 358–68. https://doi.org/10.1016/j.rser.2016.11.251.

Appendix A: Steel Timber Composite Design

A.1 Example of STC Vibration Calculations

Example Calculation: Steel Timber Composite Design Check

Design Scenario

Check the vibration utilization of a steel-timber composite floor system. The system is comprised of W18x40 beams at 15'-0" O.C. framing into W24x55 girders spaced at 30'-0" O.C. The floor assembly is comprised of 5-ply Southern Pine CLT topped with 1.5" NWC. Assume the acoustic mat and any necessary gypsum is accounted for within superimposed dead loads.

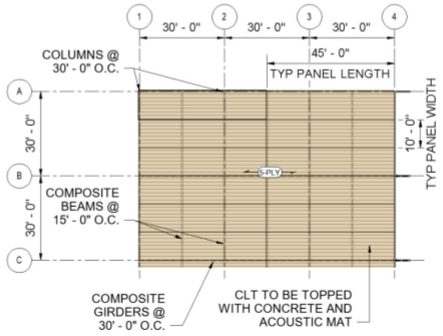

Guidance from AISC Design Guide 11

Superimposed Loads in Vibration Analysis

3.3 SUPERIMPOSED LOADS FOR VIBRATION ANALYSES

The response of a floor due to human activity is typically greatest when the floor is lightly loaded. Therefore, strength design dead and live loads should not be used for vibration analysis. Instead, estimates of actual or expected day-to-day dead and live loads should be used.

To estimate actual dead loads, it is recommended that for normal mechanical and ceiling installations, 4 psf be added to the structural system weight. For special cases, this value should be adjusted up or down as necessary.

Recommended live loads for vibration analysis are shown

Table 3-1. Recommended Superimposed Live Loads for Walking Vibration Analyses

Occupancy	Recommended Live Load, psf
Paper office	11
Electronic office	6–8
Residence	6
Assembly area	0
Shopping mall	0

Damping Coefficients

Table 4-2. Recommended Component Damping Values for Use in Equation 4-1

Component	Ratio of Actual Damping-to-Critical Damping, β_i
Structural system	0.01
Ceiling and ductwork	0.01
Electronic office fit-out	0.005
Paper office fit-out	0.01
Churches, schools and malls	0.0
Full-height dry wall partitions in bay	0.02 to 0.05*

*Depending on the number of partitions in the bay and their location; nearer the center of the bay provides more damping.

Acceleration Limit

Table 4-1. Recommended Tolerance Limits for Building Floors

Occupancy	Acceleration Limit $a_o/g \times 100\%$
Offices, residences, churches, schools and quiet areas	0.5%
Shopping malls	1.5%

Summary of service level loads and self weight:

$\rho_{CLT} := 39$ *(pcf)* *(Density of Southern Pine CLT)*

$\rho_{top} := 145$ *(psf)* *(Density of plain concrete topping)*

$DL_{super} := 4$ *(psf)* *(DG 11 Section 3.3: Superimposed DL)*

$LL := 11$ *(psf)* *(DG 11 Table 3 - 1: Expected LL)*

$W_{super} := DL_{super} + LL - 15$ *(psf)* *(Superimposed pressure)*

Beam and Girder Material Properties

$E_s := 29000$ *(ksi)*

$F_y := 50$ *(ksi)*

Concrete Topping Material Properties

$f'_c := 4000$ *(psi)* *(Compressive strength of concrete topping)*

(psi) *(Compressive strength of concrete topping)*

$E_c := \frac{\rho_{top}^{\frac{3}{2}} \cdot 33 \cdot \sqrt{f'_c}}{1000} = 3644.1$ *(ksi)* *(Modulus of elasticity of concrete topping)*

CLT Material Properties:
No. 2 Southern Pine Adjusted Design Values

$E := 1400$ *(ksi)*

$f_{cpara} := 1.450$ *(ksi)*

$f_{cperp} := 0.565$ *(ksi)*

$E'_{para} := E \cdot 1.0 \cdot 1.0 \cdot 1.0 - 1400$ *(ksi)* *(Effective E of laminations parallel to beam span)*

$E'_{perp} := 0.03 \cdot E'_{para} - 42$ *(ksi)* *(Effective E of laminations perpindicular to beam span)*

$f'_{cpara} := f_{cpara} \cdot 1.0 \cdot 1.0 \cdot 1.0 \cdot 1.0 \cdot 2.4 \cdot .9 \cdot .8 = 2.51$ *(ksi)*

$f'_{cperp} := f_{cperp} \cdot 1.0 \cdot 1.0 \cdot 1.0 \cdot 1.0 \cdot 1.67 \cdot .9 = 0.85$ *(ksi)* *(Reference NDS 2018 for adjustment factors)*

Beam Layout and Properties

Section: W18x40

$A_{sb} := 11.80$ *(in^2)* *(Cross sectional area)*

$I_b := 612$ *(in^4)* *(Moment of inertia about x-axis)*

$d_b := 17.9$ *(in)* *(Section depth)*

$w_b := 40$ *(lb/ft)* *(Section self weight)*

$L_{nb} := 30$ *(ft)* *(Beam span length)*

$S_b := 15$ *(ft)* *(Beam spacing)*

$$f_{cb} := \begin{bmatrix} f'_{cperp} \\ f'_{cpara} \\ f'_{cperp} \\ f'_{cpara} \\ f'_{cperp} \end{bmatrix} = \begin{bmatrix} 0.85 \\ 2.51 \\ 0.85 \\ 2.51 \\ 0.85 \end{bmatrix}$$ (ksi) *(Relative to BEAM: Compressive strength of CLT laminations from top to bottom)*

Girder Layout and Properties

Section: W24x55

$A_{sg} := 16.2$ (in^2) *(Cross sectional area)*

$I_g := 1350$ (in^4) *(Moment of inertia about x-axis)*

$d_g := 23.6$ (in) *(Section depth)*

$w_g := 55$ (lb/ft) *(Section self weight)*

$L_{ng} := 30$ (ft) *(Girder span length)*

$d_c := 14$ (in) *(Estimated column depth)*

$L_{clearg} := L_{ng} - \frac{d_c}{12} = 28.8$ (ft) *(Girder clear span length)*

$$f_{cg} := \begin{bmatrix} f'_{cpara} \\ f'_{cperp} \\ f'_{cpara} \\ f'_{cperp} \\ f'_{cpara} \end{bmatrix} - \begin{bmatrix} 2.51 \\ 0.85 \\ 2.51 \\ 0.85 \\ 2.51 \end{bmatrix}$$ (ksi) *(Relative to GIRDER: Compressive strength of CLT laminations from top to bottom)*

Deck and Slab Geometry

$d_{top} := 1.5$ (in) *(Concrete topping depth)*

$d_{CLT} := 6.875$ (in) *(CLT panel depth)*

$$t := \begin{bmatrix} 1.375 \\ 1.375 \\ 1.375 \\ 1.375 \\ 1.375 \end{bmatrix}$$ (in) *(Depth of CLT laminations from top to bottom)*

$W_{deck} := \rho_{top} \cdot \frac{d_{top}}{12} + \rho_{CLT} \cdot \frac{d_{CLT}}{12} - 40.5$ (psf) *(Weight of floor deck)*

Geometric Layout

$W_{floor} := 7 \cdot 30 - 210$ (ft) *(Total building width)*

$L_{floor} := 7 \cdot 30 = 210$ (ft) *(Total building length)*

Damping Ratio

$\beta := 0.03$

Acceleration Limit

$accel_{max} := 0.005$

Composite Steel Timber Beam Properties

$$n := \begin{bmatrix} \frac{E_s}{E'_{para}} \\ \frac{E_s}{E'_{perp}} \end{bmatrix} = \begin{bmatrix} 20.7 \\ 690.5 \end{bmatrix}$$ *(Modular ratio of timber laminations parallel to beam)* *(Modular ratio of timber laminations perpindicular to beam)*

$$b_{effposs} := \begin{bmatrix} 0.4 \cdot L_{nb} \cdot 12 \\ S_b \cdot 12 \end{bmatrix} = \begin{bmatrix} 144 \\ 180 \end{bmatrix}$$

$$b_{eff} := \min\left(b_{effposs}\right) = 144$$ *(in)* *(Effective flange width in vibration calculations)*

$$b_{transf} := \begin{bmatrix} \frac{b_{eff}}{n_1} \\ \frac{b_{eff}}{n_2} \end{bmatrix} = \begin{bmatrix} 6.95 \\ 0.21 \end{bmatrix}$$ *(in)* *(Transformed flange width of laminations parallel to beam)* *(Transformed flange width of lams perpindicular to beam)*

$$b_{transf} := \begin{bmatrix} b_{transf_2} \\ b_{transf_1} \\ b_{transf_2} \\ b_{transf_1} \\ b_{transf_2} \end{bmatrix} = \begin{bmatrix} 0.21 \\ 6.95 \\ 0.21 \\ 6.95 \\ 0.21 \end{bmatrix}$$ *(in)* *(Corresponds to panel orientation relative to beam span)*

$$A_{transf} := \begin{bmatrix} b_{transf_1} \cdot t_1 \\ b_{transf_2} \cdot t_2 \\ b_{transf_3} \cdot t_3 \\ b_{transf_4} \cdot t_4 \\ b_{transf_5} \cdot t_5 \end{bmatrix} = \begin{bmatrix} 0.29 \\ 9.56 \\ 0.29 \\ 9.56 \\ 0.29 \end{bmatrix}$$ *(in^2)* *(Transformed area of laminations from top to bottom)*

$$y_T := \begin{bmatrix} 0.5 \cdot d_b - 4 \cdot t_1 + 0.5 \cdot t_1 \\ 0.5 \cdot d_b - 3 \cdot t_1 + 0.5 \cdot t_2 \\ 0.5 \cdot d_b - 2 \cdot t_1 + 0.5 \cdot t_3 \\ 0.5 \cdot d_b + t_5 + 0.5 \cdot t_4 \\ 0.5 \cdot d_b + 0.5 \cdot t_5 \end{bmatrix} = \begin{bmatrix} 15.1 \\ 13.8 \\ 12.4 \\ 11 \\ 9.6 \end{bmatrix}$$ *(in)* *(Distance of each lam's neutral axis from steel neutral axis)* (Thickness of lam 1 utilized where necesseary for simplifications)

$$y_{section} := \frac{A_{transf} \cdot y_T + A_{sb} \cdot 0}{A_{transf_1} + A_{transf_2} + A_{transf_3} + A_{transf_4} + A_{transf_5} + A_{sb}} - 7.79$$ *(in)* *(Composite section neutral axis)*

$$I_T := \begin{bmatrix} \frac{1}{12}\cdot b_{transf_1}\cdot\left(t_1\right)^3 \\ \frac{1}{12}\cdot b_{transf_2}\cdot\left(t_2\right)^3 \\ \frac{1}{12}\cdot b_{transf_3}\cdot\left(t_3\right)^3 \\ \frac{1}{12}\cdot b_{transf_4}\cdot\left(t_4\right)^3 \\ \frac{1}{12}\cdot b_{transf_5}\cdot\left(t_5\right)^3 \end{bmatrix} = \begin{bmatrix} 0.045 \\ 1.506 \\ 0.045 \\ 1.506 \\ 0.045 \end{bmatrix}$$ *(in^4)* *(Moment of inertia of each lamination about it's own axis)*

$$m_1 := A_{transf_1}\cdot\left(y_{T_1} - y_{section}\right)^2$$

$$m_2 := A_{transf_2}\cdot\left(y_{T_2} - y_{section}\right)^2$$

$$m_3 := A_{transf_3}\cdot\left(y_{T_3} - y_{section}\right)^2$$ *(in^4)* *(Moment of inertia transformation)*

$$m_4 := A_{transf_4}\cdot\left(y_{T_4} - y_{section}\right)^2$$

$$m_5 := A_{transf_5}\cdot\left(y_{T_5} - y_{section}\right)^2$$ *(Moment of inertia of the steel timber section, assuming full composite action)*

$$I_{compb} := I_{T_1} + m_1 + I_{T_2} - m_2 + I_{T_3} + m_3 + I_{T_4} + m_4 + I_{T_5} + m_5 + I_b + A_{sb}\cdot y_{section}^2 - 1794$$ *(in^4)*

Deck Transformed Section Properties

$$y_{lam} := \begin{bmatrix} 4\cdot t_1 - \frac{t_4}{2} \\ 3\cdot t_1 - \frac{t_4}{2} \\ 2\cdot t_1 - \frac{t_3}{2} \\ t_1 + \frac{t_3}{2} \\ \frac{t_1}{2} \end{bmatrix} = \begin{bmatrix} 6.2 \\ 4.8 \\ 3.4 \\ 2.1 \\ 0.7 \end{bmatrix}$$ *(in)* *(Distance of each lam's center of gravity from bottom face of the panel)*

(Thickness of lam 1 utilized where necesseary for simplifications)

$$y_{CLT} := \frac{d_{CLT}}{2} = 3.44$$ *(in)* *(CLT center of gravity, relative to its bottom face; only accurate if layup is symmetric)*

$$m_{T1} := A_{transf_1}\cdot\left(y_{lam_1} - y_{CLT}\right)^2 - 2.2$$

$$m_{T2} := A_{transf_2}\cdot\left(y_{lam_2} - y_{CLT}\right)^2 = 18.1$$

$m_{T3} := A_{transf_3} \cdot \left(Y_{lam_3} - Y_{CLT} \right)^2 = 0$ *(in^4)* *(Moment of inertia transformation)*

$m_{T4} := A_{transf_4} \cdot \left(Y_{lam_4} - Y_{CLT} \right)^2 - 18.1$

$m_{T5} := A_{transf_5} \cdot \left(Y_{lam_5} - Y_{CLT} \right)^2 = 2.2$

$I_{transfCLT} := I_{T_1} \mid m_{T1} \quad I_{T_2} \mid m_{T2} \mid I_{T_3} \quad m_{T3} \mid I_{T_4} \mid m_{T4} \mid I_{T_5} \mid m_{T5} = 43.6$ *(in^4)*

Beam Mode Properties

$w_b := S_b \cdot \left(W_{super} + W_{deck} \right) + w_b - 872$ *(plf)* *(Vibration service loads)*

$\Delta_b := \dfrac{5 \cdot \left(\dfrac{w_b}{12} \right) \cdot \left(L_{nb} \cdot 12 \right)^4}{384 \cdot E_s \cdot 1000 \cdot I_{compb}} - 0.305$ *(in)* *(Beam deflection under vibration service loads)*

$f_{nb} := 0.18 \cdot \sqrt{\dfrac{386}{\Delta_b}} - 6.4$ *(Hz)* *(Natural frequency of beam)*

$D_s := \dfrac{I_{transfCLT}}{b_{eff}} \cdot 12 = 3.64$ *(in^4/ft)* *(Deck moment of inertia per unit width)*

$D_b := \dfrac{I_{compb}}{S_b} - 120$ *(in^4/ft)* *(Beam moment of inertia per unit width)*

$B_b := 2 \cdot \left(\dfrac{D_s}{D_b} \right)^{\frac{1}{4}} \cdot L_{nb} = 25.1$ *(ft)* *(Beam panel mode effective width)*

$B_b :=$ if $B_b < \dfrac{2}{3} \cdot W_{floor}$
B_b
else
$\dfrac{2}{3} \cdot W_{floor}$

$B_b = 25.1$ *(ft)* *(Controlling beam panel mode effective width)*

$W_b := 1.5 \cdot \left(\dfrac{w_b}{S_b} \right) \cdot B_b \cdot L_{nb} = 65542.1$ *(lb)* *(Effective panel weight)*

Composite Steel Timber Girder Properties

$$n := \begin{bmatrix} \frac{E_s}{E'_{para}} \\ \frac{E_s}{E'_{perp}} \end{bmatrix} = \begin{bmatrix} 20.7 \\ 690.5 \end{bmatrix}$$

(Modular ratio of timber laminations parallel to girder)
(Modular ratio of timber laminations perpindicular to girder)

$$b_{effposs} := \begin{bmatrix} 0.4 \cdot L_{ng} \cdot 12 \\ L_{nb} \cdot 12 \end{bmatrix} - \begin{bmatrix} 144 \\ 360 \end{bmatrix}$$

$b_{eff} := \min\left(b_{effposs}\right) = 144$ *(in)* *(Effective flange width in vibration calculations)*

$$b_{transf} := \begin{bmatrix} \frac{b_{eff}}{n_1} \\ \frac{b_{eff}}{n_2} \end{bmatrix} - \begin{bmatrix} 6.95 \\ 0.21 \end{bmatrix}$$

(in)

(Transformed flange width of laminations parallel to girder)
(Transformed flange width of lams perpindicular to girder)

$$b_{transf} := \begin{bmatrix} b_{transf_1} \\ b_{transf_2} \\ b_{transf_1} \\ b_{transf_2} \\ b_{transf_1} \end{bmatrix} = \begin{bmatrix} 6.95 \\ 0.21 \\ 6.95 \\ 0.21 \\ 6.95 \end{bmatrix}$$

(Corresponds to panel orientation relative to girder span)

$$A_{transf} := \begin{bmatrix} b_{transf_1} \cdot t_1 \\ b_{transf_2} \cdot t_2 \\ b_{transf_3} \cdot t_3 \\ b_{transf_4} \cdot t_4 \\ b_{transf_5} \cdot t_5 \end{bmatrix} = \begin{bmatrix} 9.56 \\ 0.29 \\ 9.56 \\ 0.29 \\ 9.56 \end{bmatrix}$$

(in^2) *(Transformed area of laminations from top to bottom)*

$$y_T := \begin{bmatrix} 0.5 \cdot d_g \quad 4 \cdot t_1 \mid 0.5 \cdot t_1 \\ 0.5 \cdot d_g - 3 \cdot t_1 + 0.5 \cdot t_2 \\ 0.5 \cdot d_g - 2 \cdot t_1 + 0.5 \cdot t_3 \\ 0.5 \cdot d_g + t_5 + 0.5 \cdot t_4 \\ 0.5 \cdot d_g + 0.5 \cdot t_5 \end{bmatrix} = \begin{bmatrix} 18 \\ 16.6 \\ 15.2 \\ 13.9 \\ 12.5 \end{bmatrix}$$

(in)

(Distance of each lam's neutral axis from steel neutral axis)
(Thickness of lam 1 utilized where necesseary for simplifications)

$$y_{section} := \frac{A_{transf} \cdot y_T + A_{sg} \cdot 0}{A_{transf_1} + A_{transf_2} + A_{transf_3} + A_{transf_4} + A_{transf_5} + A_{sg}} - 9.81$$

(in) *(Composite section neutral axis)*

$$I_T := \begin{bmatrix} \frac{1}{12}\cdot b_{transf_1}\cdot\left(t_1\right)^3 \\ \frac{1}{12}\cdot b_{transf_2}\cdot\left(t_2\right)^3 \\ \frac{1}{12}\cdot b_{transf_3}\cdot\left(t_3\right)^3 \\ \frac{1}{12}\cdot b_{transf_4}\cdot\left(t_4\right)^3 \\ \frac{1}{12}\cdot b_{transf_5}\cdot\left(t_5\right)^3 \end{bmatrix} = \begin{bmatrix} 1.506 \\ 0.045 \\ 1.506 \\ 0.045 \\ 1.506 \end{bmatrix} \quad \text{(in^4)} \quad \text{(Moment of inertia of each lamination about it's own axis)}$$

$$m_1 := A_{transf_1}\cdot\left(y_{T_1} - y_{section}\right)^2$$

$$m_2 := A_{transf_2}\cdot\left(y_{T_2} - y_{section}\right)^2$$

$$m_3 := A_{transf_3}\cdot\left(y_{T_3} - y_{section}\right)^2 \quad \text{(in^4)} \quad \text{(Moment of inertia transformation)}$$

$$m_4 := A_{transf_4}\cdot\left(y_{T_4} \quad y_{section}\right)^2$$

$$m_5 := A_{transf_5}\cdot\left(y_{T_5} \quad y_{section}\right)^2$$

(Moment of inertia of the steel timber section, assuming full composite action)

$$I_{compg} := I_{T_1} + m_1 + I_{T_2} - m_2 + I_{T_3} + m_3 + I_{T_4} + m_4 + I_{T_5} + m_5 + I_g + A_{sg}\cdot y_{section}^2 - 3920.9 \quad \text{(in^4)}$$

Girder Mode Properties

$P_g :\ \ 0.5\cdot w_b\cdot L_{nb} = 13080$ (lb) (Load transferred to girder from beam)

$w_{totalg} := 2\cdot P_g + L_{clearg}\cdot w_g - 27747$ (lb) (Total load on girder)

$W_{panelg} := \frac{w_{totalg}}{L_{nb}\cdot S_b} - 61.7$ (psf) (Equivalent pressure load)

$a := S_b \quad 0.5\cdot\frac{d_c}{12} = 14.4$ (ft) (Distance from beam bearing to column face)

$$\Delta_g := \frac{5\cdot\frac{w_g}{12}\cdot\left(L_{clearg}\cdot 12\right)^4}{384\cdot\left(E_s\cdot 1000\right)\cdot I_{compg}} + \frac{2\cdot P_g\cdot\left(L_{clearg}\cdot 12\right)^3}{48\cdot\left(E_s\cdot 1000\right)\cdot I_{compg}} = 0.206 \quad \text{(in)} \quad \text{(Deflections under vibration service loads)}$$

$$f_{ng} := 0.18\cdot\sqrt{\frac{386}{\Delta_g}} = 7.79 \quad \text{(Hz)} \quad \text{(Natural frequency of girder)}$$

$D_g := \frac{I_{compg}}{L_{nb}} - 131$ *(in^4/ft)* *(Girder moment of inertia per unit width)*

(Beam length is the girder spacing)

$B_g := -1.8 \cdot \left(\frac{D_b}{D_g}\right)^{\frac{1}{4}} \cdot L_{ng} = 52.8$ *(ft)* *(Girder panel mode effective width)*

$B_g := \text{if } B_g < \frac{2}{3} \cdot W_{floor}$
$\quad B_g$
else
$\quad \frac{2}{3} \cdot W_{floor}$

$B_g = 52.8$ *(ft)* *(Controlling girder panel mode effective width)*

$W_g := -W_{panelg} \cdot B_g \cdot L_{ng} = 97697$ *(lb)* *(Effective panel weight)*

Combined Mode Properties

$f_n := 0.18 \cdot \sqrt{\frac{386}{\Delta_b - \Delta_g}} = 4.94$ *(Hz)* *(Natural frequency of beam)*

$r := \frac{L_{ng}}{B_b} = 1.2$

$\text{if } L_{ng} < B_b$
$\quad \Delta'_g := r \cdot \Delta_g$
else
$\quad \Delta'_g := \Delta_g$

$\Delta'_g = 0.206$ *(in)* *(Reduced girder deflection)*

$W := \frac{\Delta_b}{\Delta_b + \Delta'_g} \cdot W_b + \frac{\Delta'_g}{\Delta_b + \Delta'_g} \cdot W_g - 78495$ *(lb)* *(Combined panel weight)*

$accel := \frac{65 \cdot \mathbf{e}^{0.35 \cdot f_n}}{\beta \cdot W} = 0.0049$ *(Peak acceleration due to walking excitation as a fraction of gravity)*

Acceleration limit is 0.005 -- OKAY, Design Sufficient

A.2 Example of STC Strength and Deflection Calculations

Example Calculation: Steel Timber Composite Design Check

Design Scenario

Check the strength and deflection of a steel-timber composite beam. The beam is a W18x40 spaced at 15'-0" O.C. framing into W24x55 girders spaced at 30'-0" O.C. The floor assembly is comprised of 5-ply Southern Pine CLT topped with 1.5" NWC. Assume the acoustic mat and any necessary gypsum is accounted for within superimposed dead loads.

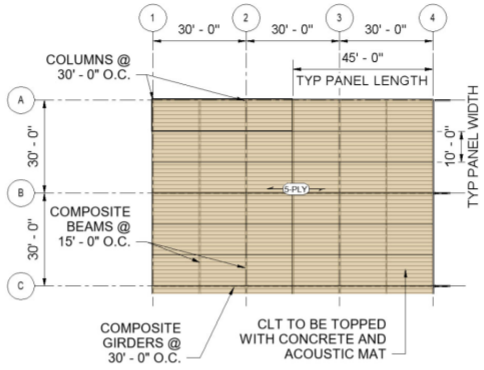

Summary of applied loads:

$w_{CLT} := 39 \cdot \frac{6.875}{12} = 22.34$ *(psf)* *(Weight of 5-ply Southern Pine CLT, 6.875" thick and 39 pcf)*

$w_{top} := 145 \cdot \frac{1.5}{12} = 18.12$ *(psf)* *(Weight of 1.5" thick plain concrete topping)*

$DL_{super} := 10$ *(psf)* *(Superimposed dead load)*

$LL := 65$ *(psf)* *(Office live load)*

$w_{beam} := 40$ *(plf)* *(W18x40 self weight)*

Beam Strength Check

Layout:

$S := 15$ *(ft)* *(Beam spacing)*

$L_n := 30$ *(ft)* *(Beam span length)*

$b_{fgirder} := 7.01$ *(in)* *(Girder flange width)*

$L_s := L_n - \frac{b_{fgirder}}{12} = 29.42$ *(ft)* *(Beam span length)*

Member demands:

$q_{self} := w_{CLT} + w_{top} = 40.47$ *(psf)*

$w_{self} := S \cdot q_{self} + w_{beam} = 647.03$ *(plf)*

$w_{Dsuper} := DL_{super} \cdot S = 150$ *(plf)*

$w_L := LL \cdot S = 975$ *(plf)*

$w_u := 1.2 \cdot \left(w_{self} + w_{Dsuper} \right) + 1.6 \cdot w_L = 2516.44$ *(plf)*

$M_u := \frac{\frac{w_u \cdot L_s^{\,2}}{8}}{1000} = 272.18$ *(k-ft)*

Steel Section Properties:

$d := 17.9$ *(in)*

$b_f := 6.02$ *(in)*

$t_f := 0.525$ *(in)*

$t_w := 0.315$ *(in)*

$h_w := 16.85$ *(in)*

$A_s := 11.80$ *(in^2)*

$I := 612$ *(in^4)*

$E_s := 29000$ *(ksi)*

$F_y := 50$ *(ksi)*

CLT Material Properties:
No. 2 Southern Pine Adjusted Design Values

$E := 1400$ *(ksi)*

$f_{cpara} := 1.450$ *(ksi)*

$f_{cperp} := 0.565$ *(ksi)*

$E'_{para} := E \cdot 1.0 \cdot 1.0 \cdot 1.0 = 1400$ *(ksi)* (Effective E of laminations parallel to beam span)

$E'_{perp} := 0.03 \cdot E'_{para} - 42$ *(ksi)* (Effective E of laminations perpindicular to beam span)

$f'_{cpara} := f_{cpara} \cdot 1.0 \cdot 1.0 \cdot 1.0 \cdot 1.0 \cdot 2.4 \cdot .9 \cdot .8 = 2.51$ *(ksi)*

$f'_{cperp} := f_{cperp} \cdot 1.0 \cdot 1.0 \cdot 1.0 \cdot 1.0 \cdot 1.67 \cdot .9 = 0.85$ *(ksi)*

(Reference NDS 2018 for adjustment factors)

CLT Section Properties:

$b_{CLTposs} := \begin{bmatrix} \frac{L_n \cdot 12}{4} \\ S \cdot 12 \end{bmatrix} = \begin{bmatrix} 90 \\ 180 \end{bmatrix}$ *(in)*

$b_{CLT} := \min\left(b_{CLTposs} \right) = 90$ *(in)*

$t := \begin{bmatrix} 1.375 \\ 1.375 \\ 1.375 \\ 1.375 \\ 1.375 \end{bmatrix}$ *(in)* *(Thickness of CLT laminations from top to bottom)*

$t_{total} := t_1 + t_2 - t_3 + t_4 + t_5 - 6.88$ *(in)*

$$f_c := \begin{bmatrix} f'_{cperp} \\ f'_{cpara} \\ f'_{cperp} \\ f'_{cpara} \\ f'_{cperp} \end{bmatrix} - \begin{bmatrix} 0.85 \\ 2.51 \\ 0.85 \\ 2.51 \\ 0.85 \end{bmatrix}$$ (ksi) *(Compressive strength of CLT laminations from top to bottom)*

Composite Strength Properties:

Composite Action assumed to be 25%

$CA := \frac{25}{100} = 0.25$

$A_s \cdot F_y = 590$ (kips) *(Maximum tension force of steel section*

$\Sigma fA := f_c \cdot b_{CLT} \cdot t = 935.4$ (kips) *(Maximum compression force of CLT section*

$C_{poss} := \begin{bmatrix} A_s \cdot F_y \\ \Sigma fA \end{bmatrix} = \begin{bmatrix} 590 \\ 935.4 \end{bmatrix}$ (kips)

$C_f := \min\left(C_{poss}\right) - 590$ (kips) *(Compressive force in flange)*

$\Sigma Q_n := CA \cdot C_f - 147.5$ (kips)

Determine depth of compression block in each lamination

$$a_1 := \text{if } \frac{\Sigma Q_n}{f_{c_1} \cdot b_{CLT}} > t_1 \quad t_1 \quad \text{else} \quad \frac{\Sigma Q_n}{f_{c_1} \cdot b_{CLT}}$$

$a_1 = 1.375$ (in) *(Depth of compression block in first lamination)*

$$a_2 := \text{if } a_1 = t_1 \quad \text{if } \frac{\left(\Sigma Q_n \quad a_1 \cdot b_{CLT} \cdot f_{c_1}\right)}{b_{CLT} \cdot f_{c_2}} > t_2 \quad t_2 \quad \text{else} \quad \frac{\left(\Sigma Q_n - a_1 \cdot b_{CLT} \cdot f_{c_1}\right)}{b_{CLT} \cdot f_{c_2}} \quad \text{else} \quad 0$$

$a_2 = 0.188$ (in) *(Depth of compression block in second lamination)*

(Example will end this proccess here as the compression block ends in the second lamination)

$a_3 := 0$ (in) *(Depth of compression block in third lamination)*

$a_4 := 0$ (in) *(Depth of compression block in fourth lamination)*

$a_5 := 0$ (in) *(Depth of compression block in fifth lamination)*

$A_{sc} := \frac{F_y \cdot A_s - \Sigma Q_n}{2 \cdot F_y} = 4.42$ (in^2) *(Area of steel required to balance compression block)*

$\frac{A_{sc}}{b_f} = 0.74$ (in)

Determine if the plastic neutral axis is in the web or flange:

$$PNA := \text{if } \frac{A_{sc}}{b_f} < t_f \text{ "flange" else "web"}$$

$PNA = \text{"web"}$

$$h_{sPNA} := \text{if } PNA = \text{"web"} \; t_f + \frac{A_{sc} - t_f \cdot b_f}{t_w} \text{ else } \frac{A_{sc}}{b_f}$$

$h_{sPNA} = 4.54$ (in)

$$y_{comp} := \text{if } PNA = \text{"web"} \; \frac{0.5 \cdot {t_f}^2 \cdot b_f + \left(0.5 \cdot \left(h_{sPNA} - t_f\right) + t_f\right) \cdot t_w \cdot \left(h_{sPNA} - t_f\right)}{A_{sc}} \text{ else } 0.5 \cdot h_{sPNA}$$

$y_{comp} = 0.911$ (in) *(Neutral axis of composite section)*

$$M_n := \frac{F_y \cdot A_s \cdot \left(\frac{d}{2}\right) - \left(2 \cdot A_{sc} \cdot F_y \cdot y_{comp}\right) + a_1 \cdot b_{CLT} \cdot {f_c}_1 \cdot \left(t_{total} - \frac{a_1}{2}\right) + a_2 \cdot b_{CLT} \cdot {f_c}_2 \cdot \left(t_{total} - a_1 - \frac{a_2}{2}\right)}{12}$$

$M_n = 479.7$ (kip-ft) *(Nominal capacity of the steel-timber beam)*

$\phi M_n := 0.9 \cdot M_n = 431.8$ (kip-ft)

$\frac{M_u}{\phi M_n} = 0.63$ ***OKAY - Cross section strength is sufficient***

Beam Deflection Check

Composite Steel Timber Section Properties:

$$n := \begin{bmatrix} \frac{E_s}{E'_{para}} \\ \frac{E_s}{E'_{perp}} \end{bmatrix} = \begin{bmatrix} 20.7 \\ 690.5 \end{bmatrix}$$

(Modular ratio of timber laminations parallel to beam)
(Modular ratio of timber laminations perpindicular to beam)

$$b_{effposs} := \begin{bmatrix} 0.4 \cdot L_n \cdot 12 \\ S \cdot 12 \end{bmatrix} = \begin{bmatrix} 144 \\ 180 \end{bmatrix}$$

$b_{eff} := \min\left(b_{effposs}\right) = 144$ *(in)* *(Effective flange width in vibration calculations)*

$$b_{transf} := \begin{bmatrix} \frac{b_{eff}}{n_1} \\ \frac{b_{eff}}{n_2} \end{bmatrix} = \begin{bmatrix} 6.95 \\ 0.21 \end{bmatrix}$$ *(in)*

(Transformed flange width of laminations parallel to beam)
(Transformed flange width of lams perpindicular to beam)

$$b_{transf} := \begin{bmatrix} b_{transf_2} \\ b_{transf_1} \\ b_{transf_2} \\ b_{transf_1} \\ b_{transf_2} \end{bmatrix}$$

(Corresponds to panel orientation relative to beam span)

$$A_{transf} := \begin{bmatrix} b_{transf_1} \cdot t_1 \\ b_{transf_2} \cdot t_2 \\ b_{transf_3} \cdot t_3 \\ b_{transf_4} \cdot t_4 \\ b_{transf_5} \cdot t_5 \end{bmatrix} = \begin{bmatrix} 0.29 \\ 9.56 \\ 0.29 \\ 9.56 \\ 0.29 \end{bmatrix}$$ *(in^2)*

(Transformed area of laminations from top to bottom)

$$y_T := \begin{bmatrix} 0.5 \cdot d \mid 4 \cdot t_1 \mid 0.5 \cdot t_1 \\ 0.5 \cdot d + 3 \cdot t_1 + 0.5 \cdot t_2 \\ 0.5 \cdot d + 2 \cdot t_1 + 0.5 \cdot t_3 \\ 0.5 \cdot d + t_5 + 0.5 \cdot t_4 \\ 0.5 \cdot d + 0.5 \cdot t_5 \end{bmatrix} = \begin{bmatrix} 15.1 \\ 13.8 \\ 12.4 \\ 11 \\ 9.6 \end{bmatrix}$$ *(in)*

(Distance of each lam's neutral axis from steel neutral axis)

(Thickness of lam 1 utilized where necesseary for simplifications)

$$y_{section} := \frac{A_{transf} \cdot y_T + A_s \cdot 0}{A_{transf_1} + A_{transf_2} + A_{transf_3} + A_{transf_4} + A_{transf_5} + A_s} = 7.79$$ *(in)*

(Composite section neutral axis)

$$I_T := \begin{bmatrix} \frac{1}{12}\cdot b_{transf\,1}\cdot\left(t_1\right)^3 \\ \frac{1}{12}\cdot b_{transf\,2}\cdot\left(t_2\right)^3 \\ \frac{1}{12}\cdot b_{transf\,3}\cdot\left(t_3\right)^3 \\ \frac{1}{12}\cdot b_{transf\,4}\cdot\left(t_4\right)^3 \\ \frac{1}{12}\cdot b_{transf\,5}\cdot\left(t_5\right)^3 \end{bmatrix} = \begin{bmatrix} 0.045 \\ 1.506 \\ 0.045 \\ 1.506 \\ 0.045 \end{bmatrix} \quad \textit{(in\^4)}$$

$$m_1 := A_{transf\,1}\cdot\left(Y_{T\,1} - y_{section}\right)^2$$

$$m_2 := A_{transf\,2}\cdot\left(Y_{T\,2} - y_{section}\right)^2$$

$$m_3 := A_{transf\,3}\cdot\left(Y_{T\,3} - y_{section}\right)^2$$

$$m_4 := A_{transf\,4}\cdot\left(Y_{T\,4} - y_{section}\right)^2$$

$$m_5 := A_{transf\,5}\cdot\left(Y_{T\,5} - y_{section}\right)^2$$

(Moment of inertia of the steel timber section, assuming full composite action)

$$I_{comp} := I_{T\,1} + m_1 - I_{T\,2} + m_2 + I_{T\,3} + m_3 + I_{T\,4} + m_4 + I_{T\,5} + m_5 + I + A_s\cdot y_{section}^2 = 1794 \quad \textit{(in\^4)}$$

Partial composite deflection:

$$I_{partialcomp} := I + \left(I_{comp} - I\right)\cdot\sqrt{\frac{\Sigma Q_n}{C_f}} = 1203 \quad \textit{(in\^4)}$$

$$\Delta_{LL} := \frac{5\cdot\frac{w_L}{12}\cdot\left(L_s\cdot 12\right)^4}{384\cdot\left(E_s\cdot 1000\right)\cdot I_{partialcomp}} = 0.471 \quad \textit{(in)}$$

$$\Delta_{limitT} := \frac{12\cdot L_n}{240} = 1.5 \quad \textit{(in)}$$

$$\Delta_{limitLL} := \frac{12\cdot L_n}{360} - 1 \quad \textit{(in)}$$

$$\Delta_T := \frac{5\cdot\frac{w_L + w_{Dsuper} + w_{self}}{12}\cdot\left(L_s\cdot 12\right)^4}{384\cdot\left(E_s\cdot 1000\right)\cdot I_{partialcomp}} = 0.856 \quad \textit{(in)}$$

$$\Delta_{super} := \frac{5\cdot\frac{w_L \mid w_{Dsuper}}{12}\cdot\left(L_s\cdot 12\right)^4}{384\cdot\left(E_s\cdot 1000\right)\cdot I_{partialcomp}} = 0.543 \quad \textit{(in)}$$

$$\frac{\Delta_{LL}}{\Delta_{limitLL}} - 0.47$$

$$\frac{\Delta_T}{\Delta_{limitT}} = 0.57$$

OKAY - Cross section deflection is sufficient

Appendix B: LCA—Tally Adjustments

B.1 Example of CLT Adjustment

28 Oct 2022 15:08:16 - 7 Story STC CLT Adjustment.sm

Author: Emma Rohde - Graduate Research Assistant, Auburn University

Date: October 2022

Life Cycle Analysis of CLT in Tally

Objective:

SmartLam, Dothan has published an EPD for its CLT products. However, Tally is currently unable to alter its databases. Preliminary analyses indicate the material defintions of "General CLT" (proxied by glulam) and European CLT EPDs do not accurately reflect the SmartLam EPD or material properties. Resulting in extreme variances in mass, embodied energy, and embodied carbon values. As a result, it has become necessary to manipulate Tally in such a way that CLT outputs reflect SmartLam Dothan CLT EPD values.

Methodology:

1. Determine "correct" values (Smartlam CLT EPD)

Table 8. *Life Cycle Impact contribution analysis for the SmartLam CLT products. Results are shown per cubic meter of product.*

Impact Indicator	Unit	A1	A2	A3	Total
Global warming potential	kg CO_2 eq	72.3	33.9	19.9	126
	%	57%	27%	16%	100%
Ozone depletion potential	kg CFC-11 eq	4.04×10^{-6}	7.93×10^{-6}	2.98×10^{-6}	1.49×10^{-5}
	%	27%	53%	20%	100%
Acidification potential	kg SO_2 eq	0.498	0.156	8.33×10^{-2}	0.737
	%	68%	21%	11%	100%
Eutrophication potential	kg N eq	0.459	3.97×10^{-2}	0.472	0.971
	%	47%	4.1%	49%	100%
Smog formation potential	kg O_3 eq	16.6	3.72	1.02	21.3
	%	78%	17%	4.8%	100%
Resource depletion potential - fossil fuels	MJ surplus	86.3	67.4	34.9	189
	%	46%	36%	18%	100%

6.2 CRADLE-TO-GRAVE CARBON SEQUESTRATION

The scope of the product system is cradle-to-gate, including the information modules: A1 - Extraction and upstream production; A2 - Transport to factory; and A3 - Manufacturing. As per ISO 21930, the net biogenic carbon emissions across the reported modules is zero (carbon neutral). This conservative assumption excludes the permanent sequestration of biogenic carbon if the LCA were to consider the typical end-of-life treatment for wood products, landfilling.

UL Environment published an addendum to the reference PCR that estimates the emissions from landfilling of wood products. The carbon sequestration addendum is based on the United States EPA WARM model and aligns with the biogenic accounting rules in ISO 21930 §7.2.7 and §7.2.12. Lacking specific data, the products are assumed disposed in a landfill at end-of-life. The following results apply the UL PCR addendum methodology to the biogenic carbon present in the SmartLam products as they leave the manufacturer in Module A3.

1 m^3 Glulam/CLT = 493.68 oven dry kg = 246.84 kg carbon = 905.08 kg CO_2eq

Carbon sequestered in product at manufacturing gate: 905.08 kg CO_2eq = -905.08 kg CO_2eq emission

Methane emitted from fugitive landfill gas: 1.74 kg CH_4= 43.57 kg CO_2eq emission

Carbon dioxide emitted from fugitive landfill gas and the combustion captured landfill gas: 101.9 kg CO_2eq emission

Permanent carbon sequestration, net of biogenic carbon emissions: 759.61 kg CO_2eq = -759.61 kg CO_2eq emission

$GWP_{EPD} := 126$	*Global warming potential [kg CO2-eq/m^3]*
$EE_{EPD} := 189$	*Embodied energy/resource depletion potential [MJ/m^3]*
$Sequ := -759.61$	*Net carbon sequestration [kg CO2-eq/m^3]*

1 / 3

$t_{5ply} := 174.625$ *CLT thickness [mm]*

$GWP_{net} := \frac{t_{5ply}}{1000} \cdot \left(GWP_{EPD} + Sequ \right) = -110.6441$ *Net GWP, accounting for carbon sequestration [kg CO2-eq/m2]*

$EE := \frac{t_{5ply}}{1000} \cdot EE_{EPD} = 33.0041$

EPD Environmental Values per Area:

$EE = 33.0041$ [MJ/m^]2

$GWP_{net} = -110.6441$ [kg CO2-eq/m^2]

Total Mass:

$w_{imperial} := 22.34$ *5-ply Southern Pine CLT weight lbs/ft^2*

$w := w_{imperial} \cdot 4.88243 = 109.0735$ *5-ply Southern Pine CLT weight kg/m^2*

$A_{CLT} := 28802$ [m^2] *CLT area, as determined by Tally & as modeled in Revit*

$M_{CLT} := w \cdot A_{CLT} = 3.1415 \cdot 10^{6}$ [kg] Total mass of 5-Ply Southern Pine CLT

2. Determine unadjusted outputs

This analysis defined the engineered wood product as "CLT (Cross Laminated Timber) , generic"

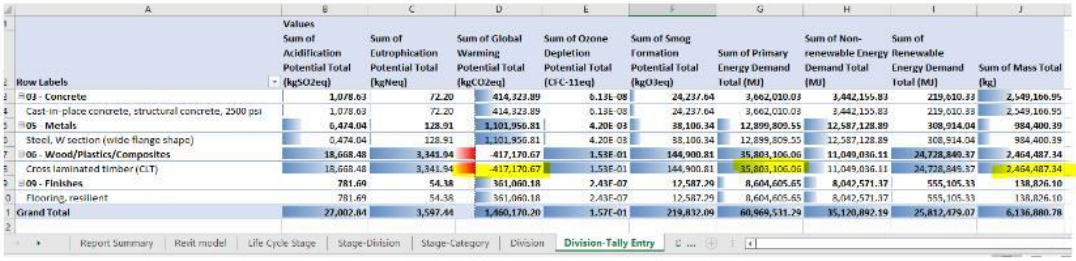

Row Labels	Values Sum of Acidification Potential Total (kgSO2eq)	Sum of Eutrophication Potential Total (kgNeq)	Sum of Global Warming Potential Total (kgCO2eq)	Sum of Ozone Depletion Potential Total (CFC-11eq)	Sum of Smog Formation Potential Total (kgO3eq)	Sum of Primary Energy Demand Total (MJ)	Sum of Non-renewable Energy Demand Total (MJ)	Sum of Renewable Energy Demand Total (MJ)	Sum of Mass Total (kg)
03 - Concrete	1,078.03	72.20	414,323.89	0.13E-03	24,237.64	3,662,010.03	3,442,155.83	219,010.33	2,549,169.95
Cast-in-place concrete, structural concrete, 2500 psi	1,078.03	72.20	414,323.89	0.13E-03	24,237.64	3,662,010.03	3,442,155.83	219,010.33	2,549,169.95
05 - Metals	6,474.04	128.91	3,101,956.81	4.20E-03	88,106.34	12,899,809.55	12,587,128.89	308,914.04	984,400.39
Steel, W section (wide flange shape)	6,474.04	128.91	3,101,956.81	4.20E-03	88,106.34	12,899,809.55	12,587,128.89	308,914.04	984,400.39
06 - Wood/Plastics/Composites	18,668.48	3,341.94	-417,170.67	1.53E-01	144,900.81	35,803,106.06	11,049,036.11	24,728,849.37	2,464,487.34
Cross laminated timber (CLT)	18,668.48	3,341.94	-417,170.67	1.53E-01	144,900.81	35,803,106.06	11,049,036.11	24,728,849.37	2,464,487.34
09 - Finishes	781.69	54.38	361,060.18	2.43E-07	12,587.29	8,604,605.65	8,047,571.37	555,105.33	138,826.10
Flooring, resilient	781.69	54.38	361,060.18	2.43E-07	12,587.29	8,604,605.65	8,047,571.37	555,105.33	138,826.10
Grand Total	27,002.84	3,597.44	3,460,170.20	1.57E-01	219,832.09	60,969,531.29	35,120,892.19	25,812,479.07	6,136,880.78

Report Summary | Revit model | Life Cycle Stage | Stage-Division | Stage-Category | Division | Division-Tally Entry

$GWP_{product} := -3548861.78$ Unadjusted CLT GWP attributed to stages [A1-A3], kg CO2-eq

$GWP_{unadjusted} := \frac{GWP_{product}}{A_{CLT}} = -123.2158$ [kg CO2-eq/m^2]

$EE_{product} := 44853669.67$ Unadjusted CLT Energy attributed to stages [A1-A3], MJ

$EE_{unadj} := \frac{EE_{product}}{A_{CLT}} = 1557.3109$ [MJ/m^2]

$M_{unadj} := 2464487.34$ [kg]

3. Determine adjustment factors

$$\psi_{GWP} := \frac{GWP_{net}}{GWP_{unadjusted}} \cdot 100 = 89.797$$

$$\psi_{EE} := \frac{EE}{EE_{unadj}} \cdot 100 = 2.1193$$

$$\psi_{M} := \frac{M_{CLT}}{M_{unadj}} \cdot 100 = 127.4721$$

4. Run analyses for each adjustment parameter

As the adjustment factors vary for each parameter, separate analyses must be run and combined to account for the adjustments. The adjustment factors above are applied by manually specificing take off method by volume and inserting the % by volume to be accounted for.

Analysis #1 - Apply adjustment for carbon:

Analysis #2 - Apply adjustment for energy:

Analysis #3 - Apply adjustment for mass:

Results:

Values obtained in analysis with NO modifications:

$GWP_{unadjusted} = -123.2158$

$error_{GWP} := \frac{\left(GWP_{unadjusted} - GWP_{net}\right)}{GWP_{net}} \cdot 100 = 11.3622 \ \%$

$EE_{unadj} = 1557.3109$

$error_{EE} := \frac{\left(EE_{unadj} - EE\right)}{EE} \cdot 100 = 4618.5342\%$

$M_{unadj} = 2.4645 \cdot 10^{6}$

$error_{M} := \frac{\left(M_{unadj} - M_{CLT}\right)}{M_{CLT}} \cdot 100 = -21.5515\ \%$

Adjusted Values, calculated from outputs of analyses 1, 2, and 3:

$GWP_{observed} := -110.64$

$error_{GWPadju} := \frac{\left(GWP_{observed} - GWP_{net}\right)}{GWP_{net}} \cdot 100 = -0.0037 \ \%$

$EE_{obsv} := 32.9999$

$error_{EEadju} := \frac{\left(EE_{obsv} - EE\right)}{EE} \cdot 100 = -0.0128\ \%$

$M_{obsv} := 3141482.02$

$error_{Madju} := \frac{\left(M_{obsv} - M_{CLT}\right)}{M_{CLT}} \cdot 100 = -0.0017\%$

SmartLam Values:

$GWP_{net} = -110.6441$

$EE = 33.0041$

$M_{CLT} = 3.1415 \cdot 10^{6}$

B.2 Example of Rubber Mat Adjustment

Author: Emma Rohde - Graduate Research Assistant, Auburn University

Date: October 2022

Life Cycle Analysis of CLT in Tally

Objective:

The current rubber mat material in Tally's database appears to be more applicable as commercial flooring, intended to withstand high traffic environments. This material has considerably higher environmental impacts than an acoustic mat underlay. This document will determine the adjustment factors necessary to equate "SBS Rubber" to U.S. Rubber's 13mm QuietSound Underlayment, utilizing the Type III EPD published by U.S. Rubber.

Methodology:

1. Determine "correct" values (US Rubber Type III EPD)

Note: Blue text indicates an input

Results (A1-A3) for 1 m² of flooring covering manufactured from post-consumer recycled tire rubber in varying thicknesses (TRACI)

	Acidification	Eutrophication	Global Warming	Ozone Depletion	Photochemical ozone formation
Product	kg SO2 eq	kg N eq	kg CO2 eq	kg CFC-11 eq	kg O3 eq
Underlayment, 2mm	2.66E-03	1.15E-03	1.26E+00	7.46E-08	3.83E-02
Underlayment, 3mm	3.99E-03	1.74E-03	1.90E+00	1.12E-07	5.77E-02
Underlayment, 5mm	6.64E-03	2.89E-03	3.15E+00	1.87E-07	9.59E-02
Underlayment, 6mm	7.98E-03	3.47E-03	3.79E+00	2.24E-07	1.15E-01
Underlayment, 9mm	1.20E-02	5.20E-03	5.68E+00	3.36E-07	1.73E-01
Underlayment, 10mm	1.33E-02	5.78E-03	6.31E+00	3.74E-07	1.92E-01
Underlayment, 12mm	1.60E-02	6.94E-03	7.58E+00	4.48E-07	2.30E-01
Underlayment, 4mm	5.32E-03	2.31E-03	2.53E+00	1.49E-07	7.68E-02
Underlayment, 7mm	9.32E-03	4.05E-03	4.42E+00	2.62E-07	1.34E-01
Underlayment, 8mm	1.06E-02	4.63E-03	5.05E+00	2.99E-07	1.54E-01
Underlayment, 11mm	1.46E-02	6.36E-03	6.95E+00	4.11E-07	2.11E-01
Underlayment, 13mm	1.73E-02	7.52E-03	8.21E+00	4.86E-07	2.50E-01

16

Table 7: LCI Impact results using CML-IA Baseline in Open LCIA Methods

Results (A1-A3) for 1 m² of flooring covering manufactured from post-consumer recycled tire rubber in varying thicknesses (CML IA-Baseline)

	Abiotic depletion potential for fossil resources	Abiotic depletion potential for non-fossil resources
Product	MJ	kg Sb eq.
Underlayment, 2mm	1.49E+01	1.18E-06
Underlayment, 3mm	2.24E+01	1.78E-06
Underlayment, 5mm	3.72E+01	2.96E-06
Underlayment, 6mm	4.47E+01	3.56E-06
Underlayment, 9mm	6.71E+01	5.33E-06
Underlayment, 10mm	7.45E+01	5.93E-06
Underlayment, 12mm	8.94E+01	7.11E-06
Underlayment, 4mm	2.98E+01	2.48E-06
Underlayment, 7mm	5.22E+01	4.35E-06
Underlayment, 8mm	5.96E+01	4.97E-06
Underlayment, 11mm	8.20E+01	6.83E-06
Underlayment, 13mm	9.69E+01	8.07E-06

`GWP := 8.21` *Global warming potential [kg CO2-eq/m^2]*

`EE := 96.9` *Embodied energy/resource depletion potential [MJ/m^2]*

`Sequ := 0` *Net carbon sequestration [kg CO2-eq/m^3]*

$t_{mat} := 13$ *Mat thickness [mm]*

$GWP_{net} := Sequ \cdot \frac{t_{mat}}{1000} + GWP = 8.21$ *Net GWP, accounting for carbon sequestration [kg CO2-eq/m2]*

EPD Environmental Values per Area:

$EE = 96.9$ [MJ/m^2]

$GWP_{net} = 8.21$ [kg CO2-eq/m^2]

Total Mass:

$\rho_{mat} := 45$ Density of acousitc QuietSound Acousitcal Underlayment [lb/ft^3]

$w := \frac{t_{mat}}{1000} \cdot \rho_{mat} \cdot 16.0185 = 9.3708$ *13 mm QuietSound Mat weight kg/m^2*

1/2" ACOUSTIC MAT
Default Floor

Assembly Code :	B1010
Total Instance Count :	7
Total Floor Area :	28,802 m²
Total Floor Perimeter :	1,797 m
Layer Thickness :	12.7 mm

$A_{mat} := 28802$ *[m^2]* *Mat area, as determined by Tally & as modeled in Revit*

$M_{mat} := w \cdot A_{mat} = 2.699 \cdot 10^{5}$ *[kg]* *Total mass of acoustic mat*

2. Determine unadjusted outputs

This analysis defined the engineered wood product as "CLT (Cross Laminated Timber) , generic"

Steel-Timber Composite

Row Labels	Values Sum of Acidification Potential Total (kgSO2eq)	Sum of Eutrophication Potential Total (kgNeq)	Sum of Global Warming Potential Total (kgCO2eq)	Sum of Ozone Depletion Potential Total (CFC-11eq)	Sum of Smog Formation Potential Total (kgO3eq)	Sum of Primary Energy Demand Total (MJ)	Sum of Non-renewable Energy Demand Total (MJ)	Sum of Renewable Energy Demand Total (MJ)	Sum of Mass Total (kg)
Floors	20,528.80	3,468.52	358,213.39	1.53E-01	181,725.75	48,069,721.74	22,533,763.31	25,503,565.04	5,152,480.39
1.5 NWC PLAIN	1,078.63	72.20	414,323.89	6.13E-08	24,237.64	3,662,010.03	3,442,155.83	219,610.33	2,549,166.95
1/2 ACOUSTIC MAT	781.69	54.38	361,060.18	2.43E-07	12,587.29	8,604,605.65	8,042,571.37	555,105.33	138,826.10

$GWP_{total\_unadjusted} := 361060.18$

$GWP_{unadjusted} := \frac{GWP_{total\_unadjusted}}{A_{mat}} = 12.5359$ *[kg CO2-eq/m^2]*

$EE_{total\_unadj} := 8604605.65$

$EE_{unadj} := \frac{EE_{total\_unadj}}{A_{mat}} = 298.7503$ *[MJ/m^2]*

$M_{unadj} := 138826.10$ *[kg]*

$w_{unadj} := \frac{M_{unadj}}{A_{mat}} = 4.82$ *[kg/m^2]*

3. Determine adjustment factors

$$\psi_{GWP} := \frac{GWP_{net}}{GWP_{unadjusted}} = 0.6549$$

$$A_{GWPperfloor} := \frac{A_{mat} \cdot \psi_{GWP}}{7} = 2694.7024 \qquad L := 3.28084 \cdot \sqrt{A_{GWPperfloor}} = 170.3101$$

$$\psi_{EE} := \frac{EE}{EE_{unadj}} = 0.3244$$

$$A_{EEperfloor} := \frac{A_{mat} \cdot \psi_{EE}}{7} = 1334.566 \qquad L := 3.28084 \cdot \sqrt{A_{EEperfloor}} = 119.8547$$

$$\psi_{M} := \frac{w}{w_{unadj}} = 1.9441 \qquad X := A_{EEperfloor} \cdot 7 = 9341.962$$

$$A_{Mperfloor} := \frac{A_{mat} \cdot \psi_{M}}{7} = 7999.3342 \qquad L := 3.28084 \cdot \sqrt{A_{Mperfloor}} = 293.435$$

4. Run analyses for each adjustment parameter

As the adjustment factors vary for each parameter, separate analyses must be run and combined to account for the adjustments. The adjustment factors above are applied by manually specificing take off method by volume and inserting the % by volume to be accounted for.

Results:

Values obtained in analysis with NO modifications:

$$GWP_{unadjusted} = 12.5359 \qquad error_{GWP} := \frac{\left(GWP_{unadjusted} - GWP_{net}\right)}{GWP_{net}} \cdot 100 = 52.6911 \ \%$$

$$EE_{unadj} = 298.7503 \qquad error_{EE} := \frac{\left(EE_{unadj} - EE\right)}{EE} \cdot 100 = 208.3078 \ \%$$

$$M_{unadj} = 1.3883 \cdot 10^{5} \qquad error_{M} := \frac{\left(M_{unadj} - M_{mat}\right)}{M_{mat}} \cdot 100 = -48.5636 \ \%$$

Adjusted Values, calculated from outputs of analyses 1, 2, and 3:

$GWP_{observed} := 8.261$ *[kg CO2-eq/m^2]*

$$error_{GWPadju} := \frac{\left(GWP_{observed} - GWP_{net}\right)}{GWP_{net}} \cdot 100 = 0.6212 \ \%$$

$EE_{obsv} := 97.23$ *[MJ/m^2]*

$$error_{EEadju} := \frac{\left(EE_{obsv} - EE\right)}{EE} \cdot 100 = 0.3406 \ \%$$

$M_{obsv} := 269713.34$ *[kg]*

$$error_{Madju} := \frac{\left(M_{obsv} - M_{mat}\right)}{M_{mat}} \cdot 100 = -0.0686 \%$$

Errors in EE and GWP are due to transportation distance; in unadjusted values the transportation distance was 455 km; with EPD the transportation distance is 805 km

Since errors are less than 1% no correction will be made

U.S. Rubber Values:

$$GWP_{net} = 8.21$$

$$EE = 96.9$$

$$M_{mat} = 2.699 \cdot 10^{5}$$

Appendix C: Preliminary Designs

C.1 CLT Floor Panel Strength Check

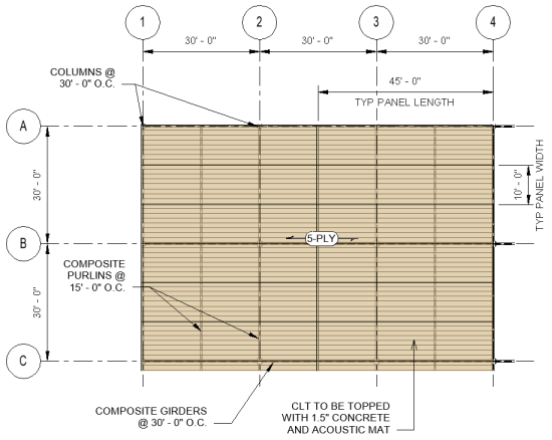

CLT Floor Deck

CLT Panel Properties			
Grade	V3		*(Ref. ANSI/APA PRG 320)*
t_{lams}	1.375	in	*(Lamination thickness)*
No. Plys	5		
t_{panel}	6.875	in	*(Total panel thickness)*
$\boldsymbol{\rho}$	0.55		*(Specific gravity)*

Major Strength Direction Properties		
$(F_bS)_{eff,f,0}$	4000	lb-ft/ft
$(EI)_{eff,f,0}$	363	10^6 lb-in^2/ft
$(GA)_{eff,f,0}$	0.98	10^6 lb/ft
$V_{s,0}$	3025	lb/ft

Floor System Geometry			
L_{panel}	45	ft	*(Total panel length)*
W_{panel}	10	ft	*(Panel width)*
S	15	ft	*(Panel span length)*
$t_{concrete}$	1.5	in	

Applied Loads

DL_{super}	10	psf	
LL	65	psf	
w_{CLT}	39	pcf	
$w_{concrete}$	145	pcf	
q_{CLT}	22.34	psf	
$q_{concrete}$	18.13	psf	
DL_{total}	50.47	psf	
w_D	50	plf	*(One foot strip of panel)*
w_L	65	plf	*(One foot strip of panel)*

Moment Demands

	Exterior Span [lb-ft/ft]		Interior Span [lb-ft/ft]	
	M+	**M-**	**M+**	**M-**
Equation	$0.08w_u l_n^2$	$0.1w_u l_n^2$	$0.025w_u l_n^2$	$0.1w_u l_n^2$
Dead	908.4	1136	283.9	1136
Live	1170	1463	365.6	1463
Load Combinations				
1.4D	1272	1590	397.4	1590
1.2D + 1.6L	2962	3703	925.7	3703
Controlling	**3703**			

Shear Demands

	Exterior Span [k/ft]	Interior Span [k/ft]
Equation	$0.6w_u l_n$	$0.5w_u l_n$
Dead	454.2	378.5
Live	585.0	487.5
Load Combinations		
1.4D	635.9	529.9
1.2D + 1.6L	1481	1234
Controlling	**1481**	

Panel Capacity

	Bending	Shear
C_M	1	1
C_t	1	1
C_L	1	1
K_f	2.4	2.0
ϕ	0.85	0.75
ƛ	0.8	0.8

$(F_bS)_{eff}'$	6528	lb-ft/ft	*(Adjusted Design Value; NDS Table 10.3.1)*
$F_s(Ib/Q)_{eff}'$	3630	lb/ft	*(Adjusted Design Value; NDS Table 10.3.1)*
$M_u/\Phi M_n$	0.57		
$V_u/\Phi V_n$	0.41		

Panel Strength Sufficient

Deflection

$$\Delta_{max} = \frac{0.0069wl^4}{EI'_{app}} = \frac{0.0069wl^4}{C_M C_t EI_{app}}$$

(Max deflection- continuous beam, three equal spans, uniform load)

K_s	11.5		*(NDS Tbale 10.4.1.1 - uniformly distributed, pinned)*
$(EI)_{app}$	320821009.6	lb-in^2/ft	*(NDS Eq. 10.4-1)*
$\Delta_{max,DL}$	0.095	in	*(Maximum DL Deflection)*
$\Delta_{max,LL}$	0.122	in	*(Maximum LL Deflection)*
K_{cr}	2.0		
Δ_T	0.312	in	*(Long Term Deflection; NDS Eq. 3.5-1)*
L/	577		

Panel Deflection Sufficient

C.2 Steel-Concrete Composite Floor Slab Design

Composite Metal Decking

Floor System Geometry			
S	10	ft	*(Slab span length)*
$t_{concrete}$	5	in	*(Total concrete thickness)*
d_{deck}	2	in	*(Depth of metal deck)*

Applied Loads		
DL_{super}	10	psf
LL	65	psf
$w_{concrete}$	145	pcf
w_{deck}	1.9	psf
$q_{concrete}$	50.23	psf
DL_{total}	60.23	psf
w_U	176.28	psf

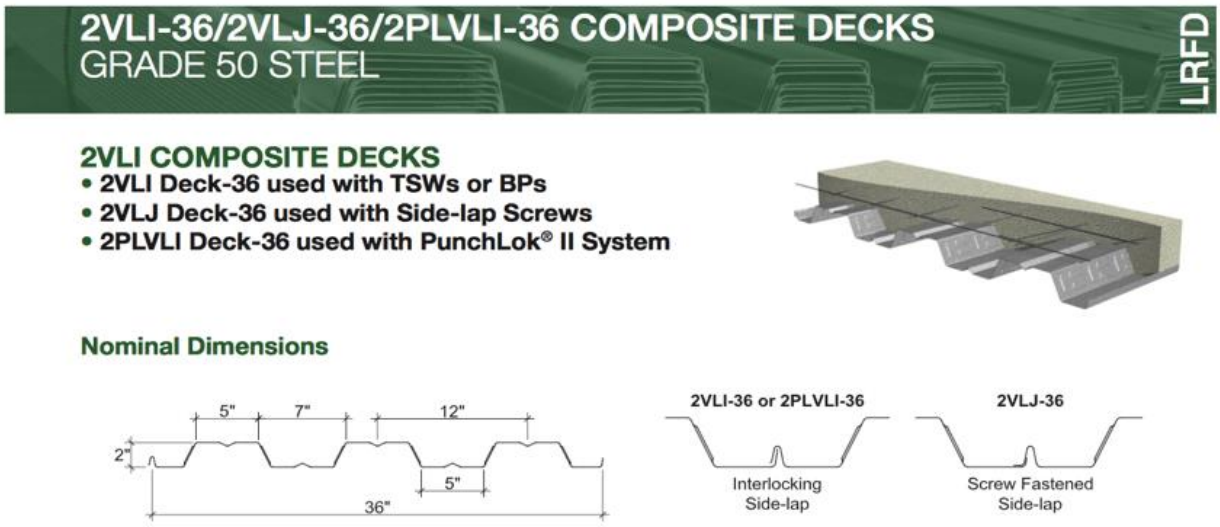

2VLI-36 Composite Steel Deck-Slab (LRFD)
with 5 in. 145 pcf 4000 psi NWC

NUCOR VULCRAFT

Superimposed Design Load, ϕWn, / Deflection at L/360 ,psf[1]

Gage	8'-0"	9'-0"	10'-0"	11'-0"	12'-0"	13'-0"	14'-0"	15'-0"	16'-0"
22	524/737	401/518	314/377	249/283	199/218	161/171	130/137	106/111	86/92
20	634/784	488/550	384/401	307/301	248/232	202/182	166/146	137/118	113/98
19	736/826	569/580	449/423	361/317	293/244	241/192	199/154	166/125	138/103
18	829/863	642/606	509/442	410/332	334/255	276/201	229/161	192/131	161/107
16	1028/940	799/660	635/481	514/361	422/278	351/219	294/175	248/142	210/117

Notes: [1] For high loads, commonly in excess of 325 psf, dynamic or impact loading, and long term concrete creep should be considered. Contact Vulcraft for further assistance.

Maximum Unshored Span

Gage	1 Span	2 Span	3 Span	
22	7'-2"	8'-2"	8'-5"	
20	8'-7"	9'-5"	9'-9"	CONTROLLING
19	9'-9"	10'-6"	10'-10"	
18	10'-1"	11'-5"	11'-9"	
16	10'-7"	13'-0"	12'-5"	

Maximum Unshored Span based on:

Uniform Construction Load	20.00	psf	Minimum End Bearing	2.00	in.
Concentrated Construction Load	150.00	plf	Minimum Interior Bearing	4.00	in.
Concrete Ponding Allowance	3.00	psf	Maximum Deflection L/	90	≤ 0.75 in.
Concrete Volume	1.23	yd^3 / 100 ft^2 (Note: Does not include allowance for ponding)			

Composite Steel Deck-Slab Properties							Min. Temperature & Shrinkage	
Gage	w_1 psf	Ic $in.^4/ft$	Iu $in.^4/ft$	Id [1] $in.^4/ft$	ϕMno kip-ft/ft	ϕVno kip/ft	As min [2] $in.^2/ft$	or Dramix® Steel Fiber 4D 65/60BG, lbs/cy
22	49.9	4.71	12.58	8.64	4.68	5.79	0.028	15
20	50.2	5.45	12.93	9.19	5.56	6.85	0.028	15
19	50.5	6.11	13.25	9.68	6.38	7.12	0.028	15
18	50.8	6.69	13.55	10.12	7.13	7.12	0.028	15
16	51.5	7.87	14.18	11.02	8.72	7.12	0.028	15

Notes: [1] Id = (Ic + Iu)/2

[2] Minimum area of steel for temperature and shrinkage

FLOOR DECKS: Vulcraft Composite Decking Design

Superimposed Loads

DL	10	psf	
LL	65	psf	
L	10	ft	*(Span length)*

Design

Deck	20 gauge 2VLI-36		
d	2	in	*(Deck depth)*
t	5	in	*(Concrete total thickness; deck + topping)*
$A_{s,min}$	0.028	in^2/ft	*(.00075Ag concrete above deck, or 6x6 - W1.4xW1.4)*
$A_{s,prov}$	0.028	in^2/ft	*(6x6-W1.4xW1.4 WWR)*
ϕq_u	314	psf	
$q_{u,\ L/360}$	377	psf	

Equivalent of 6x6-W1.4x1.4WWR

$A_{\#3}$	0.11	in^2
s_{reqd}	47.1	in

Deck Properties

Gauge	w_{self} [psf]	I_c [in^4/ft]	I_u [in^4/ft]	I_d [in^4/ft]	ϕM_{no} [k-ft/ft]	ϕV_{no} [k/ft]
22	50.23	4.71	12.58	8.65	4.68	5.79

(weight includes deck + slab)

(See 20 Ga. 2VLI-36 Deck Design *document for further calculations)*

t_{deck}	0.0358	in
wdeck [psf]	1.9	psf